Coordination Chemistry Reviews 556 (2026) 217514

Contents lists available at ScienceDirect

Coordination Chemistry Reviews

journal homepage: www.elsevier.com/locate/ccr

Computational approaches to the study of chalcogen bonding interactions☆

Massimiliano Arca [a], Vito Lippolis [a], M. Carla Aragoni [a], Enrico Podda [a,b], Gianluca Ciancaleoni [c,*], Anna Pintus [a,*]

[a] Dipartimento di Scienze Chimiche e Geologiche, Università degli Studi di Cagliari, S.S. 554 bivio per Sestu, 09042 Monserrato, Cagliari, Italy
[b] Centro Servizi di Ateneo per la Ricerca (CeSAR), Università degli Studi di Cagliari, S.S. 554 bivio per Sestu, 09042 Monserrato, Cagliari, Italy
[c] Dipartimento di Chimica e Chimica Industriale (DCCI), Università di Pisa, Via Giuseppe Moruzzi, 13, 56124 Pisa, Italy

ARTICLE INFO

Dedicated to Professor Resnati, celebrating a career in chemical bonds on the occasion of his 70th birthday.

Keywords:
Chalcogen bonding
ChB
Sigma-hole
Quantum mechanical modelling
Theoretical calculations
Cooperativity
Competition
Crystallography
Spectroscopy
Catalysis

ABSTRACT

The chalcogen bond (ChB) is acknowledged as a significant noncovalent interaction that occurs between an electron-deficient chalcogen atom (donor) and a Lewis base (acceptor). The deep understanding of this interaction remains a subject of debate, with interpretations ranging from a charge-transfer (CT) model, which suggests a polarized covalent character, to the so-called σ-hole model, which implies a predominantly electrostatic interaction. Over the past decades, various computational approaches and theoretical models have been employed to elucidate the nature of ChBs, often aiming at quantifying the different contributions - such as orbital, electrostatic, and dispersion forces - to the overall interaction energy.

In this review, we present a comparative analysis of the computational approaches used to describe chalcogen bonding interactions, their consistency with experimental evidence, and an overview of the model systems investigated.

1. Introduction

According to the IUPAC definition [1], a chalcogen bond (ChB) is a net attractive interaction of the type R–Ch···A, occurring between an electron-rich donor site (A) and an electron-poor chalcogen atom (Ch) that is part of a molecule or ion of the type R–Ch (R = organic framework) or a X_4Ch system (X = halogen; Scheme 1). Although chalcogen atoms can also act as electron-rich species, the term chalcogen bond is reserved exclusively for the former case.

The definition does not imply any specific model for the ChB, and the nature of this type of interaction remains a subject of ongoing debate. The ChB is commonly regarded as a noncovalent yet directional interaction, analogous to other such interactions, including the hydrogen bond (HB), pnictogen bond (PnB), halogen bond (HaB), and others [2]. In this context, the ChB is often described as an interaction between an electrophilic site (the Ch atom in R–Ch) and a nucleophile (A). Alternatively, it can be viewed as a Charge-Transfer (CT) interaction between a Lewis base (donor) A and a Lewis acid (acceptor) R–Ch. In terms of molecular orbitals (MOs), the interaction can be seen as a CT from a lone pair of electrons (LP) on the Lewis base A to a virtual σ*-MO localized on a R–Ch bond. In the case of double-bonded sp^2-hybridized or hypercoordinate chalcogen species, a slightly different CT scheme is considered. Here, the charge is transferred from the LP on A to a π*-MO, which is reflected in the formation of significantly bent ChB adducts in the case of hypercoordinated species (Scheme 1) [3].

Along with the increasing use of this model in the analysis of ChBs, the anisotropy of the charge distribution at the chalcogen atoms has been investigated in detail, leading to the widespread adoption of the so-called σ-hole concept in publications on chalcogen-bonded systems. This approach stems from the recognition that even negatively charged atoms can exhibit one or more regions of positive molecular electrostatic potential (MEP) [4] on their surfaces, known as σ-holes, that can interact with negatively charged bond acceptors [5–8]. σ-Holes are typically oriented along the extensions of covalent bonds involving the ChB donor

☆ This article is part of a Special issue entitled: 'Chemical Bonds' published in Coordination Chemistry Reviews.

* Corresponding authors.
E-mail addresses: gianluca.ciancaleoni@unipi.it (G. Ciancaleoni), apintus@unica.it (A. Pintus).

https://doi.org/10.1016/j.ccr.2025.217514
Received 29 October 2025; Received in revised form 5 December 2025; Accepted 18 December 2025
Available online 6 February 2026

atoms. One, two or three σ-holes can be present, depending on the oxidation state and charge of the chalcogen atom (Fig. 1). In the case of chalcogenones (>=Ch), for example, the terminal chalcogen atom involved in a double bond with an adjacent carbon atom displays a single σ-hole opposite the double bond. In contrast, in chalcogenethers donors (R_1–Ch–R_2), where the chalcogen atom forms two single bonds, two σ-holes are available, each located opposite to one of the R_1–Ch and R_2–Ch bonds (Fig. 1). Typically, σ-holes tend to become deeper when the backbone of the chalcogen-containing molecule includes electron-withdrawing substituents, and shallower in the presence of electron-donating groups. Their positive potential value also generally increases with the size of the Ch atom [9].

In some cases, a π-hole, i.e. a region of positive molecular electrostatic potential located above the molecular plane [10,11], rather than a σ-hole, can be involved in the interaction (Fig. 2).

ChBs have attracted growing interest over the past few decades, as evidenced by several reviews dedicated to this type of non-covalent interaction [12–22], as well as those included in the special issue the present paper is also part of. A key role in understanding ChBs has been played by theoretical quantum-mechanical (QM) calculations, which, over the past two decades, have been systematically employed as a computational tool to interpret and predict the nature of these interactions, as reflected in the steadily increasing number of QM studies on ChBs. A variety of theoretical approaches have been adopted, ranging from Molecular Mechanics (MM), *ab initio* Hartree-Fock (HF), and post-HF methods (most commonly according to the second order Møller-Plesset (MP) perturbation theory) [23], to calculations based on the Density Functional Theory (DFT) [24] and more computationally demanding methods such as Coupled Cluster Singles and Doubles (CCSD, including the version augmented by the perturbative treatment of triple excitations ,CCSD(T)), [25] and Complete Active Space Self-Consistent Field (CASSCF) [26] techniques.

One of the approaches often adopted in theoretical studies to interpret the nature of ChB involves the analysis of the different possible contributions to this type of interaction (e.g. orbital, electrostatic, dispersion). The relative contribution of these terms remains a matter of debate and depends strongly on both the theoretical method employed and the chemical nature of the interacting tectons. An in-depth theoretical investigation into the nature of ChB has been carried out by Kraka and coworkers, who classified ChB adducts as weakly (bond order $n <$ 0.1), normally ($0.2 < n < 0.1$), or strongly ($n > 0.2$) bonded. They demonstrated that the degree of the CT term increases with the bond order *n*, so that strong complexes exhibit a remarkable three center, four electrons (3c–4e) character in the R–Ch···A three-body system [3,27–29].

Several studies have focused on rationalizing ChBs as σ-hole interactions. A recent study, for instance, analyzed almost a thousand donor-acceptor complexes, including chalcogen-bonded systems, by correlating the electron density at bond critical points (BCP, see below) with binding energies. The resulting slope was used to distinguish between noncovalent closed-shell and shared-shell systems [30]. Politzer and coworkers have also extensively investigated correlations between the strength of σ-hole [31,32] or π-hole [33] interactions and electrostatic features – such as maximum positive/negative potentials in the molecular electrostatic potential (MEP) – as well as polarization descriptors such as polarizability and polarizing electric fields. These

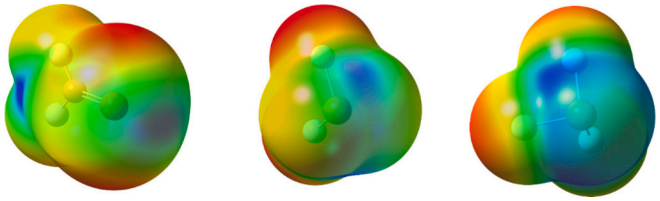

Fig. 1. Molecular electrostatic potential (MEP) mapped on density surface at the MP2/aug-cc-pVDZ level for: neutral species F_2C=Te (left), featuring a sp^2-hybridized Te atom and a single σ-hole opposite the C=Te double bond; neutral species F_2Te (center), featuring a sp^3-hybridized Te atom and two σ-holes located opposite each F–Ch bond; and cationic species F_3Te^+ (right), featuring a sp^3-hybridized Te atom and three σ-holes located opposite each F–Ch bonds. σ-holes on the chalcogen atom are mapped in blue.

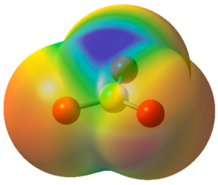

Fig. 2. Molecular electrostatic potential (MEP) mapped on density surface for SO_3 at the MP2/aug-cc-pVDZ level. The π-hole above the sulphur atom is mapped in a blue color.

studies support the interpretation of these interactions as being Coulombic in nature. However, the noncovalent and electrostatic interpretation has been increasingly contested [34–36]. Some researchers argue that the σ-hole model is a physically oversimplified representation, incorrectly assuming that the bond donor can be described as an electrostatic potential on a molecular surface and the bond acceptor as a point charge, whereas both are 3D charge density distributions. They also point out the importance of covalent components arising from molecular-orbital mixing interactions and suggest that terms like “σ-hole interaction” and “noncovalent interactions” may be inadequate. Instead, they propose the term “intermolecular covalent interactions” to more accurately describe ChBs [37]. Some authors have also recently suggested that the group-by-group nomenclature developed for the different σ-hole interactions (e.g. HaB, PnB, ChB, etc.) might represent an unnecessary overcomplication inconsistent with the naming style of most covalent and noncovalent interactions, so that alternative descriptions should be considered [38,39].

Despite a growing body of literature on the computational modelling of ChB interactions, and some reviews that touch upon these aspects [40–45], no comprehensive review has been published yet. The aim of the present work is therefore to provide an extensive overview of studies explicitly referring to these interactions as ChBs or σ/π-hole interactions. The review does not include the substantial number of older studies that described inter- or intramolecular interactions involving chalcogen atoms but do not explicitly recognized them as ChBs [46,47]. The variety of molecular systems featuring ChB interactions is indeed extremely vast. Hence, two main approaches have been adopted over the years to study them. On one hand, an in-depth investigation into the nature of ChB has been theoretically pursued by investigating simplified

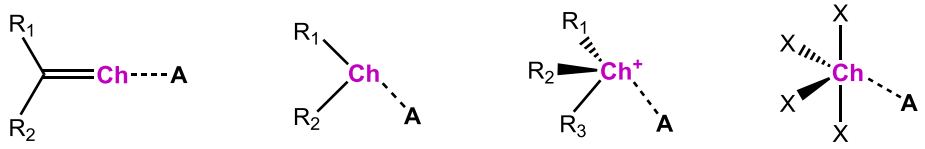

Scheme 1. Common ChB motifs; from left to right: interaction between a ChB acceptor and a ChB donor of general formula R_1R_2C=Ch, featuring a sp^2-hybridized chalcogen atom; ChB formation featuring a ChB donor of general formula R_1R_2Ch, featuring a sp^3-hybridized chalcogen atom; ChB involving a cationic ChB donor of general formula $R_1R_2R_3Ch^+$; interaction between a ChB acceptor and a ChB donor of general formula X_4Ch; (A = ChB acceptor; X = halogen; $R_{1,2,3}$ = substituent).

model systems. On the other, real systems, often structurally characterized, have been studied to assess specific effects of ChB interactions on the structural, optical, or reactivity features of compounds of interest. This review will first summarize the most popular computational methods for studying ChBs, followed by a systematic classification of both real and model compounds reported in the literature. In the final section, specific applications of quantum mechanical methods to investigate structural features, reactivity, and optical behavior of ChB-based systems will be described.

2. Computational tools

The variety of computational methods adopted to interpret ChB interactions is well-known to theoretical chemists. Not only different levels of approximation exist, such as Hartree-Fock methods, Density Functional Theory, and others, but within each method, a wide number of choices must be made, including the selection of basis sets and functionals. It is enough to say that in the case DFT method alone, a whole "Jacob's ladder" of different approximations is available, which spans from Local Density Approximation to fully non-local methods. In addition, the choice of computational details and the size of the system to model are also influenced by the computational resources currently available. Historically, a clear trend emerges from an analysis of the literature: during the period 2002–2015, most results were based on MP2 methods [23], unless the size of the system made this choice impractical. This was because, traditionally, DFT methods have not been considered the best choice for analyzing non-covalent interactions. In fact, most of them lack a specific treatment of dispersion forces, leading to either an under- or over-estimation of the bonding in noble gas dimers [48,49], which are often used as test cases.

Anyway, starting from 2013, some benchmark studies, such as those on CHAL336 [50] and the newly developed SH250x10 [51], highlighted the superior performance of certain DFT methods, in particular M06-2X [52], in characterizing of "σ-hole" interactions [53,54]. Indeed, Kozuch and Martin demonstrated that the geometry of a family of halogen-bonded adducts optimized with the M06-2X functional showed a mean signed error (MSE) of –0.009 Å and a root mean square deviation (RMSD) of 0.028 Å, taking heavy correlated methods such as CCSD(T) [25] as a reference [53]. Similarly, the dissociation energies showed a MSE of 0.04 kJ mol^{-1} and a RMSD of 1.80 kJ mol^{-1}. Bauzá and coworkers [54] estimated that the average absolute error (AAE) for a family of chalcogen-bonded adducts optimized with the M06-2X functional was 0.046 Å, with a mean absolute percentage error (MAPE) of 1.7 %, again taking CCSD(T) results as reference. For the energy, the AAE was 3.2 kJ mol^{-1} and the MAPE 8.3 %. Only the MP2 method using the resolution-of-identity approximation (RI-MP2) [55] performed better than M06-2X, with slightly lower values of AAE and MAPE. Even better results were obtained with double-hybrid functionals such as SOS0-PBE0-2-D3 (BJ) [56–58], revDSD-PBEP86-D3(BJ) [59], and various revised DSD functionals [60], but these are computationally demanding, and their use is recommended only for small systems or if large computational resources are available. Among the hybrid functionals, ωB97M-V [61] and PW6B96-D3(BJ) [62] reportedly perform quite well [50]. It is worth mentioning that good results were recently obtained by combining an interpolation along the Møller-Plesset adiabatic connection with a regularization and spin-scaling strategy applied to MP2 correlation energies [63]. As for the basis set, zeta quality plays a fundamental role, and generally, a triple-zeta basis set provides enough confidence and reliability to make the basis set superimposition error (BSSE) [64] not very significant. This has also been verified for other theoretical methods by Hamlin, Bickelhaupt, and coworkers [65]. Several studies have also tested atom-centered potentials (ACPs) [66] as corrections for different basis sets in combination with HF and DFT methods, showing contradictory results [67,68]. Importantly, according to various studies on σ-hole interactions, the widely adopted Grimme's correction for the dispersion correction (D3, D3BJ, D4) [57,58,69] tends to worsen the results and its use is not recommended [53]. This occurs due to several factors: first, some DFT functionals already overestimate the binding energy, and adding another stabilizing contribution exacerbates this overestimation. More specifically, when halide or chalcogen atoms are involved, the main cause of error does not stem from the functional itself, but rather from the self-consistent density [70]. When this happens, the errors can reach up to 20 kJ mol^{-1}. This can be partially addressed by evaluating the functional on the HF density, which reduces the error to 4–8 kJ mol^{-1}, a range that is chemically acceptable. However, geometry and dissociation energies are not the only useful parameters for ChB adducts. As mentioned in the Introduction, the nature of ChB has been thoroughly explored in recent years. This debate is common for all σ-hole interactions, and in the case of the widely explored halogen bond (HaB) many studies have attempted to support the electrostatic/polarization-only model [71–74]. In many cases, the primary evidence is a linear correlation between the electrostatic properties of the system (such as the value of the MEP at the σ-hole) and the formation energy of the adduct [75]. However, as mentioned above, most recent studies also acknowledge the significance of charge transfer, criticizing the definition of noncovalent interaction itself [76].

Among the computational tools, the most popular are certainly the various decomposition schemes, which start from the interaction energy between the two fragments of the adduct (arbitrarily chosen) to isolate the different components of the bond (such as electrostatic interaction, orbital mixing, exchange/repulsion and others). The most used methods are the canonical Energy Decomposition Analysis (EDA) [77] and the Symmetry-Adapted Perturbation Theory (SAPT) [78], which generally estimate comparable interaction energies and provide similar insights into the nature of the bond [79]. According to these analyses [65,80], it is quite clear that when the interaction is very weak, the most significant contributions are electrostatics and dispersion, whereas for normal and strong ChB interactions the relative weight of induction/orbital mixing is larger [81–83]. The latter arises from the mixing of the np-type LPs of the Lewis base with the R–Ch σ* antibonding MO of the ChB donor, as confirmed by Natural Bond Orbitals results [84].

Another useful tool is the Quantum Theory of Atoms in Molecules (QTAIM), a topological study of the electron density developed by Bader [85]. This analysis is based on partitioning the molecular electron density using zero-flux surfaces. As a result, a "bond path" is obtained, which is "a single line of maximum electron density linking the nuclei of two chemically bonded atoms" [86]. However, the "bond path" concept does not represent the chemical bond, as bond paths can also appear where bonding is not present [87]. The maximum value along the bond path is called bond critical point (BCP), and each BCP is characterized by parameters that help in the characterization of the interaction. In particular, the local kinetic energy $G(\mathbf{r})$ and the local potential energy density $V(\mathbf{r})$ are generally examined, and their sum is the energy density $H(\mathbf{r})$. From this analysis, the ChB emerges as a relatively strong interaction with some covalent character [80]. Interestingly, a correlation exists between the interaction energy of a ChB adduct and the values of $V(\mathbf{r})$ and $G(\boldsymbol{r})$ at the BCP [72,88–92]. When applied to adducts held together by multiple interactions, QTAIM also allows the evaluation of the different contributions.

The ChB can also influence regions of the adduct far from the chalcogen atom, and these effects can be evaluated through density deformation maps, which subtract the electron density of the non-interacting units from that of the adduct. These maps describe all the electronic effects due to the formation of the ChB, both on the atoms involved in the interaction (the chalcogen and the electron-rich atom) and on the rest of the molecule. For a quantitative analysis, density deformation functions can be integrated along a selected axis to derive the amount of charge displacement at the chosen point upon the formation of the ChB (Charge Displacement, CD, analysis) [93]. CD results can be used to predict the experimental formation Gibbs energy of ChB adducts [94] or to rationalize the Lewis Base activation of a Lewis Acid [95]. Regarding the latter, the method has been applied to a phenylchalcogeniranium-

olefin complex ($PhSe^+$···olefin) where the selenium atom may or may not be involved in a ChB with a Lewis base (Scheme 2). The integration of the CD method with the Natural Orbitals for Chemical Valence (NOCV) [96] analysis allowed for the isolation and quantification of the Se ← olefin σ donation, the Se → olefin π back-donation, the olefin's propensity for nucleophilic attack, and the impact of ChB on all these factors [95].

The intrinsic strength of ChB has been measured with the Konkoli-Cremer local stretching force constant [97,98], which measures the curvature of the potential energy surface between two atoms through an infinitesimal perturbation to the bond length. It is free from mode-mode coupling and, therefore, much more accurate than the standard vibration frequency. In this case also, the results are consistent with recent literature: weak ChBs are driven by electrostatics and dispersion, while the stronger ones show a partially covalent character. Some recent studies employed the periodic 3D *ab initio* calculations to determine crystal lattice energies from crystal structures, in order to evaluate the role of ChB interactions in molecular packing [99–101]. A very recent study also tested neural network potentials (NNPs) trained on DFT data as an alternative to traditional *ab initio* molecular dynamics simulations, to describe competing ChB interactions in solution [102].

3. Chalcogen bond models

In this paragraph, we discuss a selection of model ChB-interacting compounds reported in the literature so far. These compounds generally consist of two, or more rarely three or more, simple tectons featuring ChB interactions. Tectons are generally closed-shell neutral species, although examples of charged and/or radical species have also been reported. To provide a systematic classification of the adducts, model systems are categorized based on the interacting groups.

3.1. Chalcogen···chalcogen interactions

Several papers have dealt with ChB interactions involving two chalcogen atoms (Ch···Ch′; Ch, Ch′ = O, S, Se, and Te), where the most electrophilic atom behaves as the ChB donor [3]. Most studies focus on intermolecular interactions, although intramolecular ones have also been investigated.

A first question arises regarding whether oxygen can be included among chalcogen species capable of forming ChB interactions. In fact, several papers have demonstrated that chalcogen bonds could originate only from σ-holes of S, Se, or Te species, and that oxygen would not behave as a ChB donor [103–108]. On the other hand, Varadwaj and coworkers theoretically explored at DFT M06-2X and *ab initio* MP2 level the capability of the oxygen atom in the OF_2 molecule to behave as a ChB donor with a variety of interacting species (CH_3F, CH_3Cl, CH_3Br, H_2CO, HFCO, HF, SO, CH_3CN, PN, HSCN, and HCN). They concluded that "oxygen is indeed capable of forming a chalcogen bond" [109]. Notably the authors also highlighted the inadequacy of the ESP model in describing ChB interactions in the analyzed complexes. The capability of oxygen to behave not only as a ChB acceptor but also as a ChB donor was further confirmed by subsequent papers, also supported by structural data [110–114].

Moving on to the most commonly encountered systems featuring

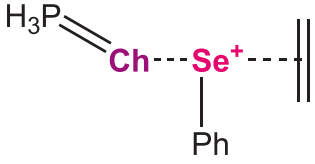

Scheme 2. $PhSe^+$···olefin models featuring a ChB with PH_3Ch (Ch = O, S, Se) studied through a combination of Charge Displacement (CD) and Natural Orbitals for Chemical Valence (NOCV) analysis [95].

ChB donor atoms heavier than oxygen, the nature of the interaction depends on the bond environment at the Ch atom. In a previously mentioned paper by Kraka and coworkers [3], a set of 100 chalcogen bonded dimeric adducts formed by variously substituted neutral and cationic sulfur, selenium, and tellurium donors with N-acceptors and Cl^- ions was described and interpreted at DFT level (Scheme 3). The authors concluded that the degree of the CT term increases with the strength of the interaction.

In addition to such wide-ranging studies, a large number of papers have been published featuring a limited number of model systems, which can be classified based on the nature of the Ch atom involved. When the chalcogen atom shows a sp^2 hybridization, it features a single σ-hole oriented along the bond axis (Fig. 1) [3,115,116]. A popular model for this type of ChB donor is represented by Ch=C=Ch′ molecules (Ch, Ch′ = O, S, Se, Te), whose interaction with a variety of acceptors, including H_2S and H_2O (Scheme 4), was investigated [3,117–119]. Due to the topology of the σ-hole, Ch=C=Ch′···Ch″H_2 adducts (Ch″ = O, S) display roughly linear C=Ch′···Ch″ moieties. This notwithstanding, the molecular geometries, optimized at MP2/aug-cc-pVTZ level, depend on the nature of Ch″. The BSSE-corrected energy of the interaction systematically decreases on passing from Ch″ = O to Ch″ = S and from Ch = O to Ch = Se [117,118].

The different types of ChB interactions formed by Ch=C=Ch′···Ch=C=Ch′ dimers (Ch, Ch′ = O, S, Se), namely type I–IV, were also investigated at MP2/aug-cc-pVTZ level (Scheme 5). It was observed that the oxygen-containing candidates failed to act as ChB donors, and the highest binding energies were found in the $(Se{=}C{=}Se)_2$ dimers. The type III interactions were observed to be the weakest, while type IV interactions the strongest, possibly due to π···π contributions [120].

Ch=C=Ch′ compounds are also capable of forming bifurcated ChBs when interacting with molecules displaying two adjacent ChB acceptor sites, such as $Ph_2N_2O_2$ [116], 1,2-dihydroxybenzene or 1,2-dimethoxybenzene (Scheme 6) [115]. M06-2X/def2-TZVPPD [121] QTAIM calculations [85] showed that bifurcated interactions are closed-shell in nature and that their strength increases with the atomic number of the interacting atom Ch′ (i.e. along the series S < Se < Te), with a corresponding increase in CT along the series, as demonstrated at natural bond orbital (NBO) [122] level [115]. The nature of the non-interacting atom Ch also affects the strength of the ChB, with interactions being strongest when Ch = O. Notably, in the case of $Ph_2N_2O_2$···Ch′=C=Ch, Ziegler-Rauk EDA [123] showed that the largest contribution is electrostatic in nature (43%–55%) [116].

The competition between chalcogen, halogen, and hydrogen bonds was also studied. As already mentioned, ChB is in fact a member of the growing "σ-hole" family, the progenitor of which is the halogen bond. While computational studies have not evidenced a substantial difference in their nature, significant dissimilarities do exist, the most important being the steric factor. In the case of halogen bonds (HaBs), the approaching Lewis base (LB) lies on the prolongation of the only R–X bond, minimizing the steric hindrance between the LB and R. In contrast, for R_1–Ch–R_2 molecules, there will be some steric hindrance between the LB interacting with the σ-holes originated by R_1 and R_2. Clearly, sp^2 hybridized species do not face this issue, as they possess only a single σ-hole. Generally, hydrogen bonds (HBs) are stronger than other σ-hole interactions. For example, in differently bound Ch=C=Ch···OHX adducts (Ch = S, Se; X = Cl, Br), while HBs and HaBs are similar in strength, both are stronger than ChBs (Scheme 7) [124].

On increasing the structural complexity of the tectons, the competition between different interactions also becomes possible. In general, when more than one weak interaction is possible, either cooperativity or anti-cooperativity can occur. This aspect is not always straightforward, as it depends on many factors: the geometry of the adducts, the nature of the species involved, and the thermodynamic parameters of the different interactions. Del Bene and coworkers, for instance, investigated the interaction of differently substituted methanimidothionic acid

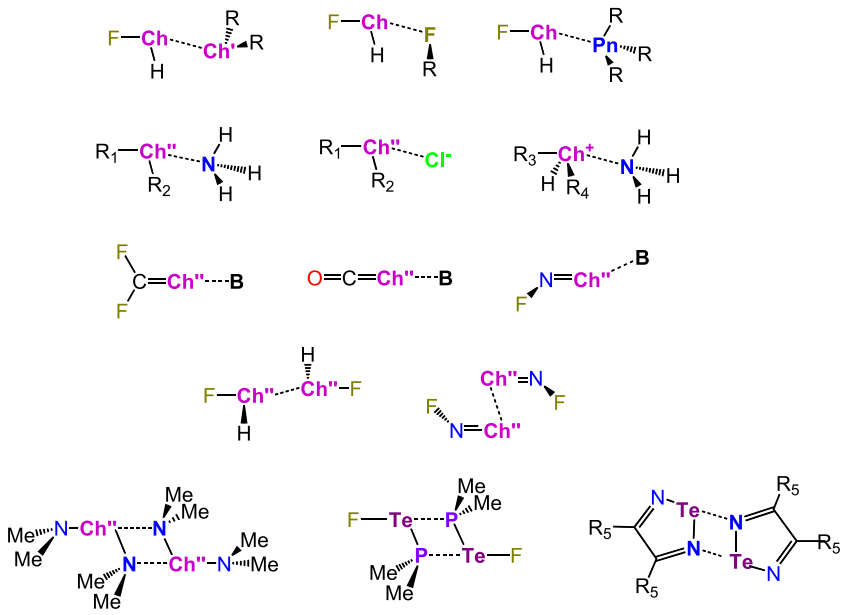

Scheme 3. Chalcogen bonded dimeric adducts investigated by Kraka and coworkers (Ch = S, Se, Te; Ch′ = O, S, Se, Te; Ch″ = Se, Te; R = H, CH_3; Pn = N, P, As; R_1 = CF_3, NF_2, OF, F; R_2 = H, CH_3, CF_2H, CF_3, F, CN; R_3 = H, F; R_4 = H, CN; R_5 = F, CH_3; B = NH_3, Cl^-) [3].

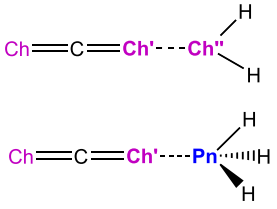

Scheme 4. Different models of Ch=C=Ch′ systems: interaction of Ch=C=Ch′ (Ch = O, S, Se; Ch′ = S, Se) with H_2Ch'' or PnH_3 (Ch″ = O, S; Pn = N, P) [117,118].

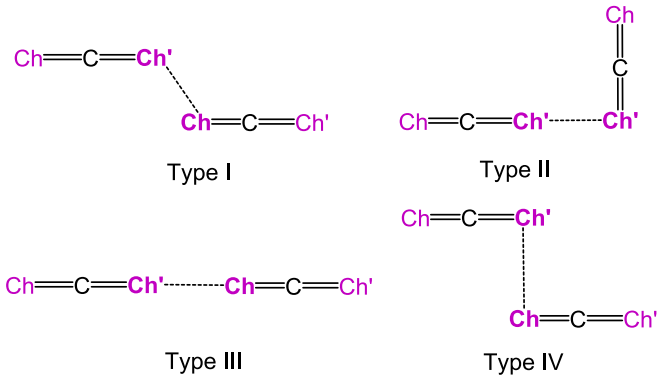

Scheme 5. Different types of ChB interactions in Ch=C=Ch′···Ch=C=Ch′ dimers (Ch, Ch′ = O, S, Se) [120].

derivatives HN=CH–S–R (R = F, NC, Cl, CN, –C≡CH, and H) with Ch′=C=Ch systems (Ch, Ch' = O, S) [125,126]. In the optimized adducts, the sulphur atom of the former synthon acts as ChB donor. However, in addition to O···S [125] or S···S [125,126] ChB interactions, N···C tetrel bond interactions can also occur (Scheme 8). All the synthons considered form stable adducts, mainly due to intermolecular CT, as demonstrated at MP2/aug-cc-pVTZ level. In the case of R = F, the tetrel interaction leads to an authentic chemical reaction between the synthons, resulting in the formation of S=C(O)–N=C–SF [125].

Another popular model for ChB donors featuring Ch atoms in a sp^2 hybridization is represented by X_2C=Ch systems. In this context,

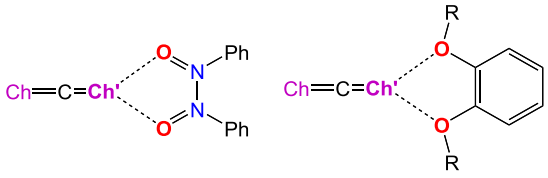

Scheme 6. Models for bifurcated ChB interactions in Ch=C=Ch′ compounds (Ch′ = S, Se, Te): adducts with $Ph_2N_2O_2$ [116] (left; Ch = S, Se) and with 1,2-dihydroxybenzene or 1,2-dimethoxybenzene (right; Ch = O, S; R = H, CH_3) [115].

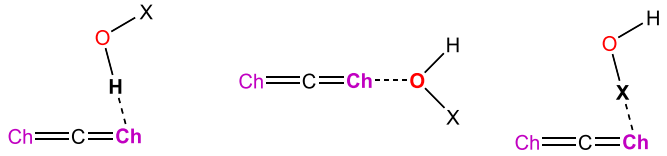

Scheme 7. Competition between HB (left), ChB (center), and HaB interactions (right) in the adducts between Ch=C=Ch (Ch = S, Se) and OHX molecules (X = Cl, Br) [124].

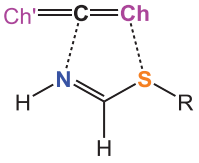

Scheme 8. Cooperative tetrel and chalcogen bonding interactions in the adducts between Ch′=C=Ch (Ch, Ch′ = O, S) and HN=CH–S–R derivatives (R = F, Cl, NC, –C≡CH, H, CN) [125,126].

different dimers of X_2C=Ch molecules (X = F, Cl; Ch = O, S) were investigated at MP2/aug-cc-pVTZ level (Scheme 9) [127]. The results showed the inability of the oxygen-containing compounds to act as ChB donors; also in this case, a preference for tetrel-bonding, as compared to ChB and HaB interactions, was observed. The most dominant contributions to ChB interactions were calculated to be the dispersion forces, as determined through SAPT-EDA.

A comparison of ChB with other σ-holes interactions was also

performed in F_2C=Se···HXO (X = F, Cl, Br, I) systems, where Se···O ChBs compete with Se···H HBs, Se···X HaBs, and C···O tetrel bonds (Scheme 10) [128]. ChB interactions were found to be the least stable. The electrostatic energy is dominant in the H-bonded (Se···H–O) and X-bonded (Se···X–O) complexes, although the polarization and dispersion contributions are also significant. In tetrel- (featuring C···O short contacts) and ChB-bonded (C=Se···O) complexes, the dispersion energy is comparable to the electrostatic contribution.

In a series of *β*-chalcogenovinylaldehydes HC(Ch)–CH=CH–Ch′H (Ch = O, S; Ch′ = Se, Te), the competition between Ch···Ch′ and intramolecular Ch···H–Ch′/Ch′···H–Ch HB interactions was analyzed using MP2 and B3LYP/6-311+G(3df,2p) [129,130] calculations (Scheme 11) [131,132]. The ChB interactions, further investigated by means of QTAIM and NBO approaches, exhibit significant differences depending on the specific Ch/Ch′ combination. In particular, the strength of the interaction increases on passing from Ch′ = Se to Ch′ = Te. The electrostatic and dative contributions decrease with the atomic number of the chalcogen species. In the case of ChB involving oxygen (Ch = O), the electrostatic term dominates, while the orbital-mixing contribution is the most significant for Ch = S, especially in S···Te–H interactions [131]. A correlation was also found between the charge density at the ring critical point and the strength of ChB interactions [132]. A related study on 3-mercapto-propenal and 3-mercapto-propenthial showed that S···O interactions are stronger than S···S ones, with both types being primarily governed by electrostatics and relatively unaffected by the nature of the solvent [133]. Another study extended this analysis to the saturated chalcogenoaldehyde analogues HC(Ch)–CH_2–CH_2–Ch′H (Ch, Ch′ = O, S, Se, Te), revealing significantly weaker noncovalent interactions compared to the unsaturated compounds, despite the potential for resonance-assisted stabilization arising from tautomeric forms [134].

A peculiar example of ChB donors featuring the Ch atom in a sp^2 hybridization state is SO_2, whose interaction with a variety of R–C(O)–CH_3 carbonyl-containing donors (Scheme 12) was investigated [90]. As expected, the presence of electron-withdrawing substituents on the CO-containing Lewis donors reduces the binding energy, whereas in amide-containing systems the interaction is strengthened. According to the authors, the ChB interaction is primarily attributed to a CT orbital-mixing interaction between the LPs on the carbonyl oxygen atoms and the antibonding π*-MOs on SO_2 (π-type ChB). Binding energies as high as 36.0 kJ mol^{-1} were reported.

Adducts between ChO_2 and $(CH_3)_2$Ch′ molecules (Ch = S, Se, Te; Ch′ = O, S, Se, Te) were also investigated, revealing that the strength of the Ch···Ch′ interactions increases with the size of Ch and decreases with the size of Ch′. Binding energies between –21.6 and –61.4 kJ mol^{-1} were calculated, indicating strong interactions primarily dominated by the electrostatic forces, although QTAIM and SAPT analysis suggest a non-negligible covalent character [135].

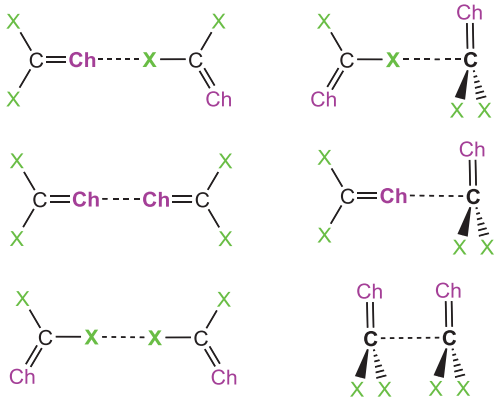

Scheme 9. Different interaction modes in X_2C=Ch dimers (X = F, Cl; Ch = O, S) [127].

On the other hand, ChB donors featuring a sp^3-hybridized chalcogen atom display two σ-holes (Fig. 1) [136], the magnitude of which depends not only on the nature of substituents, but also on the overall molecular charge. Several model compounds belonging to this class have been reported in the literature.

In a pair of studies, an extensive set of ChB donors and acceptors was investigated, resulting in the definition of 32 different 'dimeric' model systems composed of a dimethylchalcogenoether, $(CH_3)_2$Ch, interacting with a CH_3Ch′R acceptor (Ch, Ch′ = O, S, Se, and Te; R = CH_3, CN; Scheme 13) [81]. Using different computational approaches, the authors concluded that Te-containing species exhibit the strongest interactions (with interaction energies in the range 12.5–25.0 kJ mol^{-1}), while O- and S-containing species show lower ChB energies (8.4–12.5 kJ mol^{-1}). The strength of the interaction increases along the Ch′ series Te > Se > S > O, a trend largely attributable to dispersion forces, while electrostatic attractive or repulsive interactions dominate only when at least one of the interacting atoms is oxygen or sulfur. The dative contribution p → σ* was found to be insufficient to fully account for the observed trends and details of the examined structures [81,137].

In a related study, homodimers of chalcogenocyanic acid HChCN (Ch = S, Se, Te) proved capable of stably interacting in a variety of relative orientations, optimized at MP2/aug-cc-pVTZ level, depending on the type of interactions established [138]. A QTAIM analysis showed that some of the orientations are supported by ChB Ch···Ch interactions, with the electron density ρ at the bond critical points (BCPs) increasing with the size of the chalcogen atom Ch, as also reflected by the NBO analysis, which shows a regular decrease of the orbital interaction along the series Te > Se > S. The corresponding binding energies, evaluated at CCSD(T)/CBS level, fall in the range between –20 and –44 kJ mol^{-1}, depending on the nature of the chalcogen atom Ch and the optimized dimer conformation.

Homodimers of HTe–ChH molecules (Ch = O, S, Se, Te) were also studied, showing a plethora of possible conformations in which chiral discrimination was also investigated, revealing small energy differences between the homo- and heterochiral adducts. In all cases, the most stable minima correspond to hydrogen-bonded complexes, except for HTe–TeH, and the strength of Te···Ch interactions increases with the difference in electronegativity between Te and Ch. Dispersion was observed to be the most important attractive force [139].

The adducts between CH_3SR molecules (R = CH_3, H, NH_2, SCH_3, CF_3, OH, CN, NO_2, F, Cl) and several Lewis bases, including H_2O, H_2CO, NH_3, $(CH_3)_2O$, and $(CH_3)_3N$, were studied, and a strong substituent effect was observed on the strength of S···O/N interactions, with more electron withdrawing groups resulting in more stable ChBs as a consequence of deeper σ-holes on sulphur. As a result, in the case where R = CH_3, H, SCH_3, and NH_2, the concurrent hydrogen-bonded interactions were stronger than ChBs (Scheme 14). In order to rationalize the directionality of the interaction, the study was also extended to nucleophiles featuring carbonyl groups [140].

The ability of *sp*- sp^2- and sp^3-hybridized ChB donors (C≡Ch, Ch=C=Ch, and F_2Ch, respectively; Ch = O, S, Se) to engage in type I ChBs in homo-and heterodimers was also comparatively investigated at the MP2/aug-cc-pVTZ level, showing the sequence $sp^2 > sp > sp^3$ for the computed binding energies [141].

As for competition studies, CH_3SH and CH_3SF have been adopted by Scheiner to model the interactions with *N*-methylacetamide, which can involve ChB, HB, and tetrel bonds (Scheme 15). The introduction of the electron-withdrawing F-substituent increases the strength of the ChB interaction (O···S–F: 26.8 kJ mol^{-1}). When cationic sulfured compounds, $CH_3SH_2^+$ and CH_3SHF^+, were considered, the interactions were dramatically enhanced, the counterpoise-corrected binding energies reaching as much as 163 kJ mol^{-1} in the case of the O···S–F interaction in the CH_3SHF^+·*N*-methylacetamide adduct (Scheme 15) [142]. Another recent contribution dealt with the competition between HB and ChB in the homodimers of chalcogen hydrides H_2Ch (Ch = O, S, Se, Te), showing that while H_2O is solely hydrogen bonded, ChB emerges in H_2S

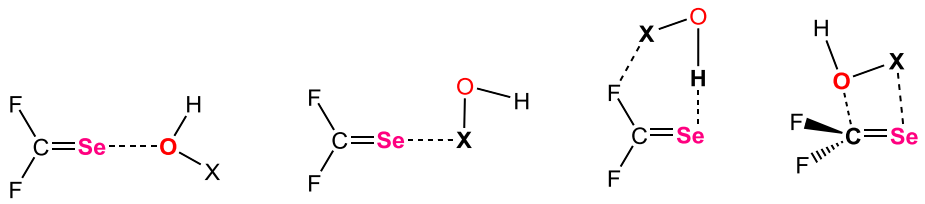

Scheme 10. Different interaction modes between F_2C=Se and HXO systems (X = F, Cl, Br, I) [128].

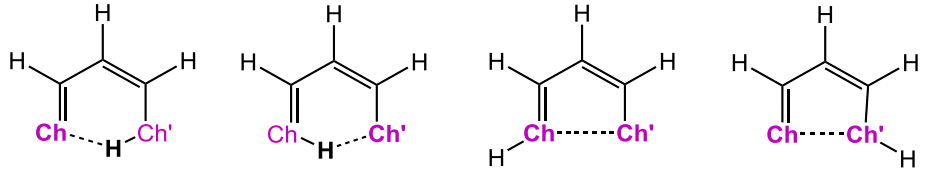

Scheme 11. Competing intramolecular interactions in β-chalcogenovinylaldehydes HC(Ch)–CH=CH–Ch′H (Ch = O, S; Ch′ = Se, Te) [131,132].

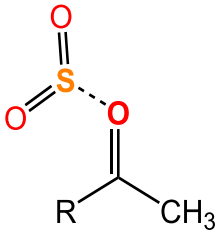

Scheme 12. ChB interaction between SO_2 and different carbonyl donors (R = H, CH_3, C_2H_5, OH, OCH_3, NH_2, $N(CH_3)_2$, F, Cl, Br, $COOCH_3$, $NHCOCH_3$) [90].

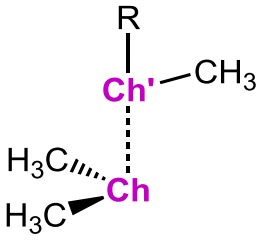

Scheme 13. Dimeric model systems composed of a dimethylchalcogenoether $(CH_3)_2$Ch and a CH_3Ch′R acceptor (Ch, Ch′ = O, S, Se, and Te; R = CH_3, CN) [81].

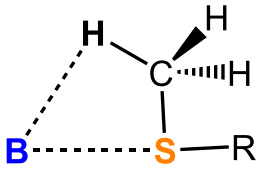

Scheme 14. Concurrent ChB and HB interactions between CH_3SR molecules (R = CH_3, H, NH_2, SCH_3, CF_3, OH, CN, NO_2, F, Cl) and different Lewis bases (B = H_2O, H_2C=O, NH_3, $(CH_3)_2O$, $(CH_3)_3N$, *N*,*N*′-dimethylurea, *N*-methylacetamide, methylethylketone) [140].

and eventually dominates in H_2Se and H_2Te [143].

When the chalcogen atom carries a positive charge in trivalent sulfonium, selenonium, and telluronium cations of the type $(CH_3)_3Ch^+$ [3], three σ-holes are present on the Ch atom, located along the extension of the C–Ch bonds and capable of directing an equal number of directional charge-assisted interactions (CAChB) with ChB acceptor species (Fig. 1). In this context, 21 different complexes were theoretically investigated (PBE0-D3/def2-TZVP), including 15 featuring Ch···O interactions, in the adducts formed between $(CH_3)_3Ch^+/F_3Ch^+$ (Ch = S, Se, Te) and three tripodal ChB acceptors containing terminal –CHO, –COOH, or $H_2(O)N^+$ groups (Scheme 16) [144].

Passing to the study of cooperativity effects, the interactions of 1,4-benzoquinone and its perfluoro-derivative with HSF and HSCl where analyzed comparatively (MP2/6-311++G**), both in the absence and in the presence of a halide X^- interacting perpendicular to the π-electron system of the quinone derivative (Scheme 17). Worthy of note, the anion···π interaction enhances the O···S interaction: a combined CT and QTAIM analysis indicated that the calculated CT values both in the anion···π and ChB interactions are slightly larger than in the corresponding isolated complexes, thus indicating cooperativity between the two types of interactions [145].

Heterocyclic systems were also explored; the adducts between 1,2,5-chalcogenadiazole rings and the carboxyl groups of R–COOH systems (Ch = S, Se, Te; R = NH_2, CH_3, H, CN, NO_2) are an example. Ch···O interactions coexist in the adducts with OH···N HBs (Scheme 18), and the introduction of an electron-withdrawing substituent on the carboxylic acid strengthens both the HB and ChB. There is a certain degree of cooperativity between them, with the HB being, in most cases, the stronger of the two [146].

Bifurcated ChBs between 1,2,4-dithiazolidine-3,5-dione and various Lewis bases, including water and formaldehyde, were also investigated (Scheme 19), showing binding energies of up to approximately 145 kJ mol^{-1} and a predominantly electrostatic attractive interaction [147].

The stability between pairs of model chalcogen-bonded nucleobases, in which the amino group of adenine (A), cytosine (C), and guanosine (G) was replaced by a Ch–X group (Ch = S, Se; X = F, Cl, Br), was investigated, leading to the formation of one or two ChBs (Scheme 20), in place of the hydrogen bonds present in canonical A:T and G:C pairs (T = tyrosine). The most stable pairs were those with Ch = Se and X = F, showing binding energies of the same order of magnitude as those of the corresponding canonical pairs, both in the gas phase and in water. Preliminary molecular dynamics (MD) analysis indicated that the G and C derivatives do not introduce significant distortion or destabilization in DNA oligonucleotides [148].

The ability of chalcogen-rich species to form oligomers based on ChB interactions has been occasionally investigated. Trimers of the type $(HSR)_3$ (R = F, Cl, CN, NC, –C≡CH, OH, OCH_3, and NH_2) are calculated to be held together by S···S interactions, featuring R–S···S linear moieties, with the H atoms pointing outward of the planar trigonal S_3 core (Scheme 21). ChB interactions were calculated to range approximately from –15 to –60 kJ mol^{-1}, depending on the nature of R. The Laplacian of the electron density at BCPs associated with S···S interactions shows the highest value for R = F and the lowest for R = NC and –C≡CH. The total energy density (H_{BCP}) at the S···S BCPs is positive for weakly bound trimers, but negative in the strongest case (R = F), indicating a partial degree of covalent character in the ChB for this system [149].

An alternative type of trimers consists of two HChCl molecules (Ch =

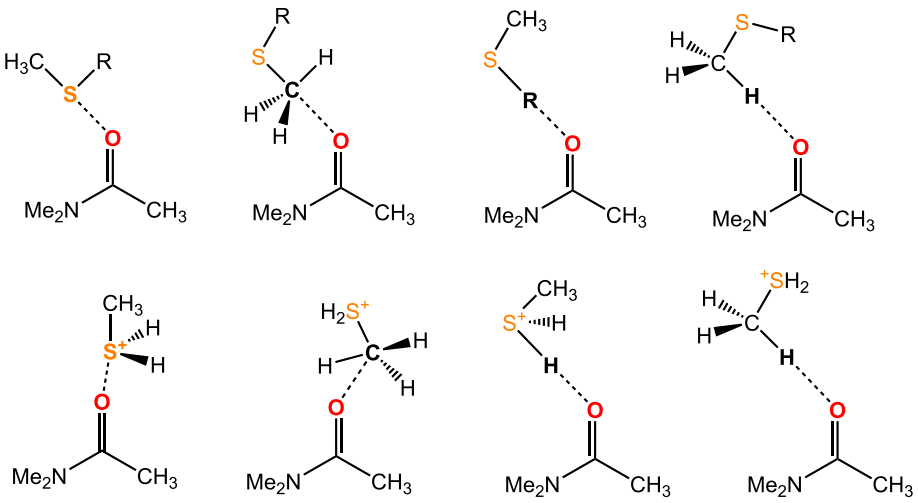

Scheme 15. Different interactions modeled for the adducts between *N*-methylacetamide and CH_3SH and CH_3SF or $CH_3SH_2^+$ and CH_3SHF^+ cations (R = H, F) [142].

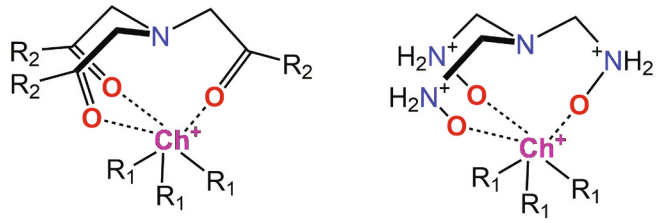

Scheme 16. Models of tripodal ChB acceptors (R_2 = H, OH) interacting with $(R_1)_3Ch^+$ ChB donors (R_1 = CH_3, F; Ch = S, Se, Te) [144].

S, Se) interacting through a Ch···Ch chalcogen bond and a PH_2Cl, HSCl, or Cl_2 synthon, forming a Ch···P PnB, Ch···S ChB, or Ch···Cl halogen bond (HaB), respectively. (Scheme 22). Shorter bond distances, higher electron densities and second-order perturbation energies, along with negative three-body interaction energies in the trimers all suggest a high degree of cooperativity between non-covalent interactions, especially in the case of PH_2Cl [150].

The cooperativity between O···Se ChB interactions and M···N spodium bonds in triads formed by carbonates MCO_3 (M = Zn^{II}, Cd^{II}), various HSeR molecules (R = F, Cl, OH, OCH_3, NH_2, and $NHCH_3$), and nitrogen-containing bases was also assessed (Scheme 23). It was observed that the ChB (along with a concurrent HB between MCO_3 and HSeR) is strengthened more than the spodium bond, as the stronger interaction exerts a greater influence on the weaker one [151].

The cooperativity between spodium and chalcogen bonds was observed also studying the interaction between model systems [(thiourea)$_2MX_2$] (M = Zn^{II}, Cd^{II}, Hg^{II}; X = Cl, I) and Lewis bases as acetonitrile, carbon monoxide and thioformaldehyde [152]. NOCV CD results showed that the interaction is generally a complex mixture of spodium, halogen, chalcogen, and hydrogen bonds. Conveniently, the NOCV tool was able to isolate and quantify each contribution, revealing that, depending on the nature of the two fragments, in some cases the spodium bond was not detectable.

Anticooperativity between Ch···Ch′ and Ch···N interactions in HCN···O_3Ch···Ch′HR trimers (Ch′ = S, Se; R = H, Cl, Br, –C≡CH, NC, OH, OCH_3) was also investigated at the MP2/aug-cc-pVTZ level [153].

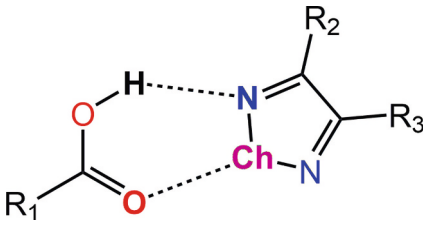

Scheme 18. Cooperative HB and ChB in the adducts between 1,2,5-chalcogenadiazole rings and the carboxyl groups of R–COOH systems (Ch = S, Se, Te; R_1 = NH_2, CH_3, H, CN, NO_2; R_2 = NH_2, H, CN, NO_2; R_3 = NH_2, H, O^-, CN, NH_3^+) [146].

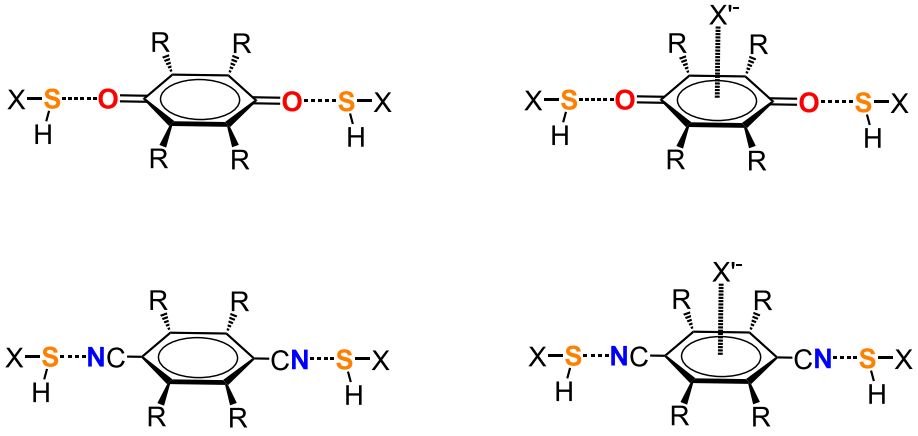

Scheme 17. ChB of 1,4-benzoquinone (top) or 1,4-dicyanobenzene (bottom) and their perfluoro-derivatives towards HSF or HSCl, with (right) and without (left) an interacting halide (X, X′ = F, Cl; R = H, F) [145].

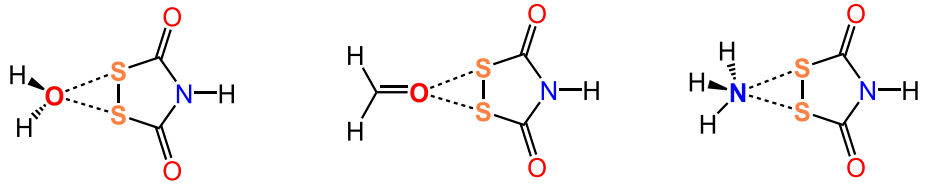

Scheme 19. Bifurcated ChB interactions between 1,2,4-dithiazolidine-3,5-dione and different electron-donors [147].

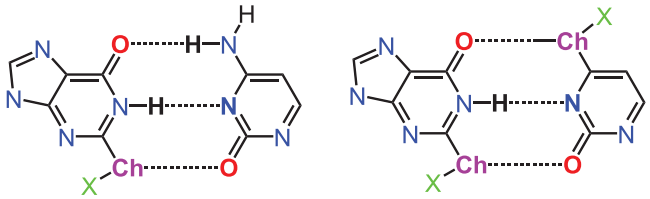

Scheme 20. Examples of modified G:C base pairs showing one or two ChB interactions (Ch = S, Se; X = F, Cl, Br) [148].

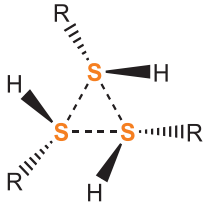

Scheme 21. Model $(HSR)_3$ trimers (R = F, Cl, CN, NC, –C≡CH, OH, OCH_3, and NH_2) [149].

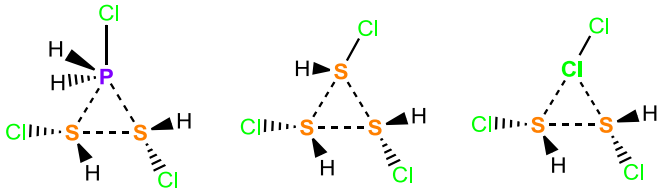

Scheme 22. Investigated HSCl···HSCl···PH_2Cl, HSCl···HSCl···HSCl, and HSCl···HSCl···ClCl trimers [150].

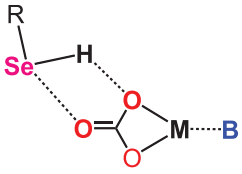

Scheme 23. O···Se ChB interactions and M···N spodium bonds in the triads formed by carbonates MCO_3 (M = Zn, Cd), HSeR molecules (R = F, Cl, OH, OCH_3, NH_2, $NHCH_3$), and nitrogen-containing bases B (B = HCN, $NHCH_2$, NH_3) [151].

Some examples of more extended aggregates were also investigated, including $(SO_2)_n$ or $(SO_2)_n{\cdot}H_2O$ clusters (n = 1–7) [154], as well as related systems involving SO_3 [155–157], and linear clusters of the type $(O{=}C{=}Ch)_n$ (Ch = S, Se; n = 2–8) [158]. In the latter case, the intermolecular Ch···O distances shorten as the length of the supramolecular chain increases. A degree of cooperativity was confirmed by QTAIM: the σ-hole on the second monomer of the chain is deeper than that on the first one, due to the polarization induced by the latter on the former.

3.2. Chalcogen···pnictogen interactions

The computational study of ChB interactions involving pnictogen-containing donors began in the early 2010s, with a series of papers by Scheiner and coworkers [159–164]. The authors initially compared at the MP2 level [23] various Y···N interactions, specifically the ChB between H_2S and ammonia and the corresponding HB and PnB interactions with HCl and PnH_3 (Pn = N, P, As). Energetics, geometries, and other properties of these complexes were found to be relatively independent on the nature of the Y atom. In contrast, the hydrogen-bonded analogues exhibited a strong dependence on the nature of Y [159]. The interactions were calculated to arise equally from induction and electrostatic components, with a minor contribution from dispersion forces [159]. The same authors also investigated the influence of substituents on the H_2S molecule in similar interactions (RHS···NH_3; R = F, Cl, Br, CH_3, NH_2, CF_3, OH, NO_2) [160,161], observing a general correlation between the interaction energy and the electron-withdrawing properties of the substituent R. Furthermore, they compared the effect of angular distortion and intermolecular separation in these systems with those in related halogen- and hydrogen-bonded complexes [162,163]. Their results highlighted a greater sensitivity of ChBs to angular distortion as compared to HBs, primarily attributed to exchange repulsion components.

In general, most studies involve S···N interactions, although works on selenium-containing ChB donors and/or phosphorus-based ChB acceptors are not lacking. Much less common are studies on tellurium ChB donors, while the only reports on oxygen concern the interactions of OF_2 with different nitrogen compounds within the already cited discussion on the possibility of oxygen to from ChBs (see above) [109], and a study on the interaction between OX_2 and NX_3 (X = F, Cl), which showed that for these systems the interaction has instead a PnB character [165].

A number of papers analyzes the cooperativity or competitivity of this type of ChBs with different non-covalent interactions. These aspects were particularly studied by Esrafili and coworkers in a series of computational investigations performed at the MP2 level of theory [145]. A particularly well-studied system is represented by trimers in which the central molecule can simultaneously act as both a Lewis acid and a Lewis base. The chalcogen bond is thus combined with H···π interactions in trimers of the type RHCh···NCH···C_6H_6 (R = F, Cl, Br, CN, NC; Ch = S, Se; Scheme 24a) [166]; with HaBs or HBs in RF_2Ch^+···NCX···NH_3 (R = H, CN, F; Ch = S, Se; X = Cl, Br; Scheme 24b) [167]; with HaBs in F_2S···NCX···NCR_1 (X = F, Cl, Br, I; R_1 = H, F, OH) [168] or R_2Cl···OCS···NH_3 (R_2 = F, OH, NC, CN, –C≡CF; Scheme 24c) [169]; with PnBs in H_3S^+···$NC(H_2)P$···PyR (R = NH_2, CH_3, H, CN, F, Cl, Br; Scheme 24d) [170] and XHS···$NC(H_2)P$···NCR (X = F, Cl; R = H, OH, NH_2, CN, NC) [171]; and even with aerogen bonds in B···SHCN···ZO_3 adducts (B = NH_3, N_2; Z = Ar, Kr, Xe; Scheme 24e) [172], alkaline-earth bonds in B···ChX_2···MCl_2 (B = NH_3, HN=CH_2, HCN; Ch = S, Se; X = F, Cl; M = Be, Mg; Scheme 24f) [173], or dihydrogen bonds in XHCh···CNH···HY (X = F, Cl, Br, I; Ch = S, Se, Te; Y = Li, Na, BeH, MgH; Scheme 24g) [174]. A positive cooperative effect is observed, arising from the mutual polarization of the interacting moieties: the formation of the additional interaction results in a loss of electron density on the chalcogen atom and a simultaneous accumulation on the pnictogen atom. The magnitude of this cooperative effect also depends on the nature of the substituent on the chalcogen-containing Lewis acid, with the more electron-withdrawing groups generally having an enhancing effect.

Dronskowski and coworkers published a paper on dimers, trimers,

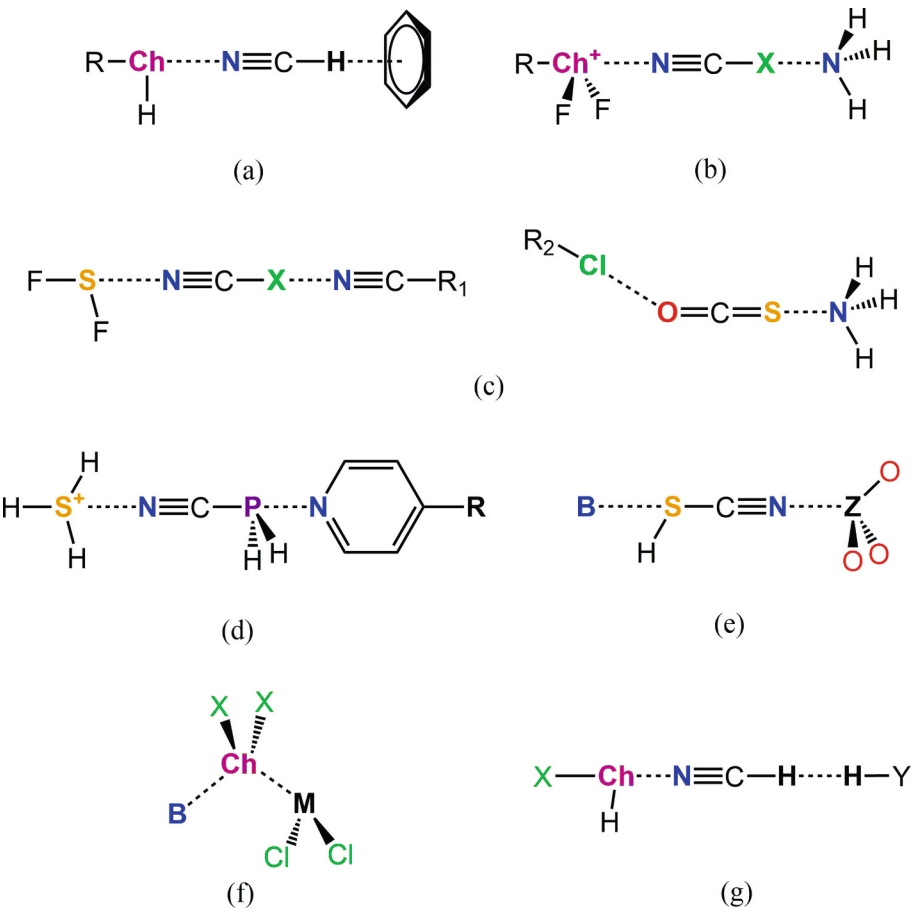

Scheme 24. Different model trimers studied for the mutual effect between ChB and (a) H···π interactions (R = F, Cl, Br, CN, NC, Ch = S, Se) [166]; (b) halogen or hydrogen bonds (R = H, CN, F; Ch = S, Se; X = Cl, Br) [167]; (c) halogen bonds (X = F, Cl, Br, I; R_1 = H, F, OH; R_2 = F, OH, NC, CN, –C≡CF) [168,169]; (d) pnictogen bonds (R = NH_2, CH_3, H, CN, F, Cl, Br) [170]; (e) aerogen bonds (B = NH_3, N_2; Z = Ar, Kr, Xe) [172]; (f) alkaline-earth bonds (B = NH_3, HN=CH_2, HCN; Ch = S, Se; X = F, Cl; M = Be, Mg) [173]; (g) dihydrogen bonds (X = F, Cl, Br, I; Ch = S, Se, Te; Y = Li, Na, BeH, MgH) [174].

and infinite chains of $(NC)_2Ch$ molecules (Ch = O, S, Se, Te) [175]. The monomers were calculated to form stable linear head-to-tail aggregates through Ch···N ChB interactions (Scheme 25), and the stability of the chain to increase as the central atom becomes heavier, in accordance with a σ-hole interpretation. Moreover, the chains become more stable as the number of interacting monomers increases, revealing a cooperative effect. In the same paper, systems showing infinite chains held together by HaBs were also analyzed, showing that the degree of cooperativity is system-dependent, and that even anti-cooperative effects can be foreseen (for example in the case of 1,4-dioxane combined with a halogen molecule).

Several authors have also studied, at the *ab initio* level, the competition between PnB and ChB interactions in RHS···PH_2R adducts (R = F, Cl, Br, H, OH, OCH_3, CH_3, C_2H_5, NH_2, –C≡CH, and COH; Scheme 26) [176–178]. These studies reported that the preferential formation of ChBs or PnBs depends on the electron-donating or-withdrawing nature of the R substituents on the two monomers. EDA indicated that electrostatic and dispersion contributions are important in the formation of these complexes, while NBO analysis suggested that CT interactions play a significant role in chalcogen-pnictogen adducts. QTAIM analysis further confirmed that the interactions are purely closed-shell in character.

A variety of papers by different authors also dealt with the comparison of ChBs to other non-covalent interactions, such as HBs [179,180], tetrel bonds [181], and HaBs [182,183]. One of these studies investigated the competition among tetrel, pnictogen, chalcogen, and halogens bonds at the MP2 level by analyzing the interaction of various H_nY, CH_3YH_n, $(CH_3)_nYF_n$, HYF_n, and FYH_n Lewis acids (n = 0–3; Y = Br, Se, As, Ge) with ammonia (Scheme 27) [184]. In the absence of H atom substitution, chalcogen bonds were found to be the strongest, followed by halogen, pnictogen, and tetrel bonds. Methyl substitution was found to weaken all interactions, while fluorine substitution showed an opposite effect, leading to a bonding strength order of tetrel > pnictogen > chalcogen. The most dramatic enhancement was predicted when the atom opposite the Lewis base was replaced by fluorine, which resulted in a different order of halogen > chalcogen > pnictogen > tetrel. A similar study was carried out on the adducts between NH_3 and YF_n molecules (Y = Si, P, S, Cl; n = 1–4), which showed in this case a tetrel > halogen > chalcogen > pnictogen bonding strength order [185].

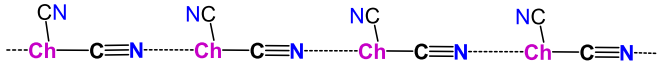

Scheme 25. Schematic representation of the infinite chains formed by $(NC)_2Ch$ molecules (Ch = O, S, Se, Te) [175].

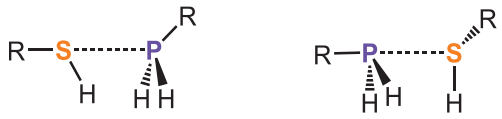

Scheme 26. Chalcogen bonded (left) and pnictogen-bonded (right) RHS···PH_2X adducts (R = F, Cl, Br, H, OH, OCH_3, CH_3, C_2H_5, NH_2, –C≡CH, COH) used to study the competition between the two types of σ-hole interactions [176,177].

Different results were obtained in a similar study conducted by Li and McDowell, also at the MP2 level, on complexes of 6-OYF$_2$-Fulvene (Y = As, Sb, Se, Te, Be, I) with nitrogen-containing bases FCN, HCN, and NH$_3$ (Scheme 28) [186]. Their findings showed that, regardless of the Lewis base involved, the interaction strength increases in the order ChB < PnB < HaB. They also suggested that both the number and the type of substituents attached to the acidic center significantly affect the interaction strength. Furthermore, the authors observed that the heavier Y atoms form stronger interactions than their lighter counterparts, and that, although the interactions are predominantly electrostatic, the polarization contribution becomes increasingly significant as the interaction strength increases.

The formation of chalcogen bonds through a π-hole rather than a σ-hole in the case of SO$_3$ was also explored in interactions with Pn-containing Lewis bases (namely, NH$_3$, H$_2$C=NH, NH$_2$F, NP, NCH, NCF, NF$_3$, and N$_2$, and their phosphorous analogues) [187]. An important structural feature of these complexes is the distortion from planarity of the SO$_3$ molecule, such that in the corresponding adducts the deformation energy represents an important contribution to the interaction energy. The latter depends, in this case, on the electron-donating ability of the P- and N-donor Lewis bases investigated, which is enhanced by the introduction of electron-donating substituents and is greater for *sp*^{3}-hybridized than for the *sp*-hybridized chalcogen bases.

A related study explores the possibility of forming ChB interactions through π-holes in the adducts of ammonia with SeO$_3$, SeO$_2$, or SeF$_2$. As expected, the introduction of LPs in SeO$_2$ and SeF$_2$ reduces the magnitude of the π-hole and the propensity to engage in the ChB interactions, although in all cases the π-holes were observed to be deeper and the resulting bonds stronger than the corresponding σ-hole interactions [188]. Also in the case of π-hole interactions, cooperativity studies were performed on triads [88,189,190], showing a mutual strengthening between the π-hole ChB and the concurrent σ-hole hydrogen/lithium/halogen/triel bonding interaction, often indicating that the cooperativity contribution is larger in the π-hole compared to the σ-hole interaction.

A study [167] on the tunability of the S···N interaction depending on the nature of the Lewis base was performed on the adducts between FR$_1$R$_2$S$^+$ cations (R$_{1,2}$ = H, F) and different *sp*- and *sp*^{3}-hybridized bases (Scheme 29a), revealing that while for the *sp*-hybridized bases the interaction energy decreases in the order H$_2$FS$^+$ > HF$_2$S$^+$ > F$_3$S$^+$, no single pattern was found for the variation of the interaction energy in complexes with *sp*^{3}-hybridized bases. Similar studies were performed on OCS in combination with different bases (Scheme 29b) [191], showing that complexes with the *sp*-hybridized nitrogen have linear chalcogen bonds whose interaction energies depend on the electron-donating or -withdrawing ability of the substituents, while in the case of *sp*^{2}-hybridized nitrogen bases, the ChBs deviate slightly from linearity. A further study on the complexes of F$_2$CSe with various nitrogen bases (Scheme 29c) showed that the chalcogen bond becomes stronger when moving form *sp*- to *sp*^{2}- and from *sp*$^{2-}$ to *sp*^{3}-hybridized systems, although some inconsistency was observed regarding the electronegativity of the hybridized N atom [192]. A similar trend was observed in the case of SOXY (X, Y = F, Cl; Scheme 29d) [193], while, contrary to expectations, the strength of the interaction varies in the order SOF$_2$ < SOFCl < SOCl$_2$, showing that is does not depend solely on the electron-withdrawing properties of the substituent and the subsequent depth of the σ-hole,

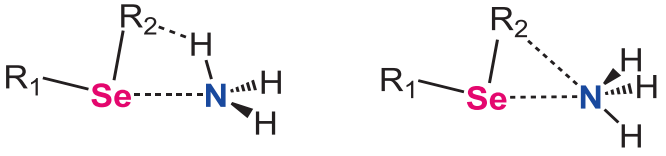

Scheme 27. Different interaction modes between R$_1$SeR$_2$ (R$_1$ = H, F, CH$_3$; R$_2$ = H, F) and ammonia [184].

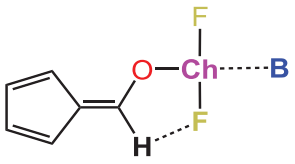

Scheme 28. Complexes between 6-OChF$_2$-Fulvene (Ch = Se, Te) and nitrogen-containing bases B (B = FCN, HCN, NH$_3$) [186].

and highlighting the fact that the interaction is not governed exclusively by electrostatic forces. The same trend in ChB strength depending on the nitrogen hybridization of the Lewis base was observed for F$_2$Se, and the bond is also strengthened by replacing hydrogen substituents on the base with methyl groups, or by substituting the N atom to which the base is attached with carbon (Scheme 29e) [194].

As for the influence of the Pn atom, a recent study on the interactions between PnR$_3$ (Pn = N, P, As, Sb; R = H, CH$_3$) and F$_2$Se or FHSe molecules, performed at the M06-2X/def2-TZVP level, showed a decrease in the strength of the ChB interaction upon moving from N to Sb [195].

On the other hand, regarding the influence of the Ch atom, the adducts between a series of Ch-containing aromatic cycles and different N- and O-containing bases (Scheme 30) showed that when Ch = S or Se, relatively weak ChB interactions are calculated (formation energies ranging from –13 to –26 kJ mol^{-1}), dominated by electrostatic and dispersion contributions. In contrast, when Ch = Te, strong interactions (up to –54 kJ mol^{-1}) were calculated, with a predominance of electrostatic and induction terms, and whose orientation is directed by steric effects [196].

The effect of substitution, backbone modification, and replacement of S with Se on intramolecular Ch···N interactions was investigated in a series of benzothiophene-based derivatives (Scheme 31). As expected, in the model system featuring a more rigid geometry that orients the LP on the N atom towards the σ-hole on the S atom, stronger interactions are established. An increase in interaction energies was also computed on moving from S to Se and upon substituting CH groups in the organic backbone with more electronegative N atoms [197].

Scheiner and coworkers [198] studied cationic systems at the MP2/aug-cc-pVDZ level, investigating the effect of charge and substituents on S···N chalcogen bonds in RHS···NH$_3$ and R(CH$_3$)S···NH$_3$ systems (R = H, CH$_3$, NH$_2$, CF$_3$, OH, Cl, F, NO$_2$), as well as in the corresponding cation dimers RH$_2$S$^+$···NH$_3$ and R(CH$_3$)$_2$S$^+$···NH$_3$ (Scheme 32). They reported the expected trend in interaction strength, which increases as the R substituent becomes more electron-withdrawing. Furthermore, the ionic complexes were found to be significantly more strongly bound than their neutral counterparts. As in the neutral systems, the primary source of the interaction is the CT from the LP on the N atom to the σ*(S–R) antibonding MO, complemented by a strong electrostatic component and a smaller contribution from dispersion forces.

The same authors studied, at the same level of theory, the S···N interactions between tetravalent SF$_4$ and different amines, including NH$_3$ and its methylated derivatives, as well as various N-containing heteroaromatic compounds [199]. They described, also in this case, the expected effect upon addition of electron-releasing substituents such as the –CH$_3$ group to NH$_3$, resulting in an enhanced interaction strength. Decomposition of the total interaction energy revealed induction as the main component; in all systems, one of the S–F bonds is oriented opposite the N atom, and the interaction mainly results from a CT from the nitrogen LP to the corresponding F–S σ* antibonding MO. Reportedly, the particularly strong complex between (CH$_3$)$_2$N and SF$_4$ suggests that the S···N bond is close to a situation where it's better described as covalent.

In a related study on different hypervalent ChF$_4$ molecules (Ch = S, Se, Te, Po), which interestingly represents one of only two computational studies reported so far where the chalcogen donor is polonium [200], the interaction of ChF$_4$ with two molecules of ammonia was

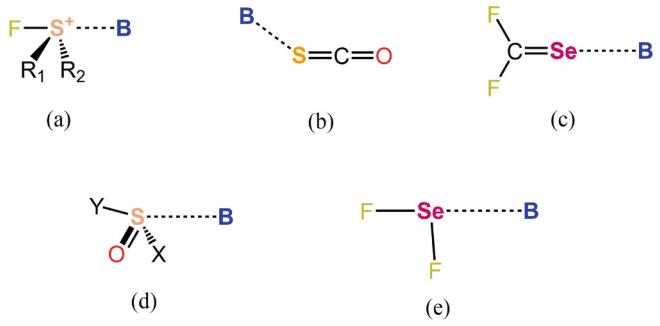

Scheme 29. Different systems studied for the effect of hybridization on N-containing Lewis bases B: (a) adducts between $FR_1R_2S^+$ cations ($R_{1,2}$ = H, F) and *sp* (NCH, NCF, NCCl, NCCN, $NCCH_3$, NCOH, N_2) or sp^3 (NH_3, NH_2F, NH_2Cl, NH_2CN, NH_2CH_3 and NH_2OH) ChB acceptors B [167]; (b) complexes between OCS and sp^2 (imidazole, pyrazole, pyridine, N_2H_2) or *sp* (NCLi, NCH, NCF, NP, N_2) bases B [191]; (c) interaction between F_2CSe and *sp* (N_2, NCH, NCLi), sp^2 ($NHCH_2$), or sp^3 (NH_3, $N(CH_3)_3$) nitrogen bases B [192]; (d) complexes between SOXY (X, Y = F, Cl) and *sp* (HCN, PN) or sp^2 ($NH{=}CH_2$) bases B [193]; (e) complexes between F_2Se and *sp* (N_2, HCN, CH_3CN), sp^2 (N_2H_2, $HN_2{=}CH_3$, $N_2(CH_3)_2$, $NH{=}CH_2$, $CH_3N{=}CH_2$, C_5H_5N), or sp^3 bases B (NH_3, $(NH_2)_2$, NH_2CH_3, $NH(CH_3)_2$, $N(CH_3)_3$) [194].

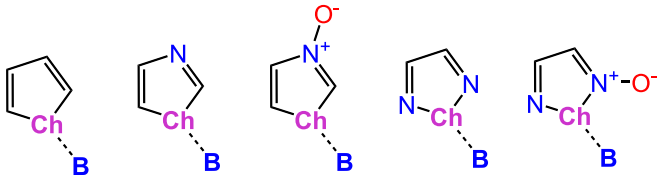

Scheme 30. Interaction between different heterocyclic aromatic systems and N- and O-containing bases (Ch = S, Se; B = $COHNH_2$, $N(CH_3)_3$, $P(CH_3)_3$, pyridine, chalcogenazole, and others) [196].

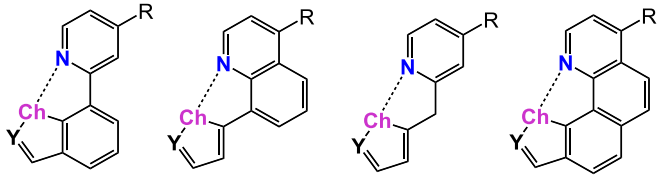

Scheme 31. Benzothiophene-based derivatives studied for their intramolecular Ch···N interactions (Ch = S, Se; R = H, OH; Y = CH, N) [197].

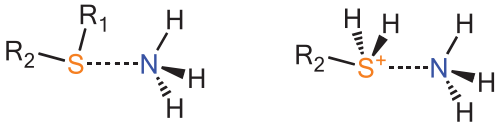

Scheme 32. $R_1R_2S{\cdots}NH_3$ and $R_2H_2S^+{\cdots}NH_3$ adducts (R_1 = H, CH_3; R_2 = H, CH_3, NH_2, CF_3, OH, Cl, F, NO_2) [198].

investigated. Two possible conformations were revealed: one where the two bases occupy adjacent positions in a modified octahedral geometry, and a second where the ChF_4 molecule is deformed from a seesaw into a nearly square-planar conformation, with one NH_3 molecule interacting with the π-hole above the ChF_4 pseudoplane and the other aligned along a σ-hole (Scheme 33). The former geometry is preferred by SF_4, while the latter is favored for TeF_4 and PoF_4; the two isomers are nearly isoenergetic in the case of SeF_4 [201].

Recent studies explored the possibility of forming ChBs through the so called lone-pair hole (LP-hole) [202] opposite to the LP on ChF_4 molecules in a seesaw geometry (Ch = S, Se; Scheme 34). Interactions established through the σ-hole on the chalcogen atom with NH_3 and HF were computed to be stronger than those involving the LP-hole. While σ-hole interactions are predominantly electrostatic and become stronger with increasing chalcogen size, LP-hole interactions are mainly driven by dispersion forces and tend to weaken with increasing chalcogen size [203].

Another paper discussed the energetics of the adducts formed between $TeOX_4$ systems and NH_3 or HCN (X = F, Cl, Br, I), showing that upon coordination of the base, the central tellurium atom passes from a trigonal bipyramidal to an octahedral geometry (Scheme 35), and revealing a significant covalent component in these strong interactions (interaction energy up to 205 kJ mol^{-1} for $H_3N{\cdots}TeOF_4$) [204].

An example of bifurcated Ch···N interactions was investigated in triads formed between R_1ChR_2 molecules (Ch = S, Se, Te; R_1, R_2 = F, Br, I, ^{t}Bu) or chalcogenazole rings and ammonia (Scheme 36). It was reported that when the σ-hole on Ch is too shallow (e.g., when moving from Te to S and Se, or upon replacing electron-withdrawing halogen substituents R_1 and R_2 groups with ^{t}Bu), the anti-cooperative effect due to the CT from ammonia to the Ch atom hinders the formation of the second ChB, sometimes even preventing it altogether [205].

A recent paper by Michalczyk and others showed that the structure of 5,6-dichloro-2,1,3-benzoselenadiazole features an uncommon binding motif: two moieties pair to establish not only two Se···N ChBs, but also a N···N PnB (N···N distance 2.812 Å), which is generally difficult to observe (Scheme 37) [206]. NBO and QTAIM analyses confirmed the existence of the PnB, which is made possible by the two ChBs that force the two N-atoms in close spatial proximity. Indeed, the NBO analysis revealed a CT from the LP on the nitrogen atom to the N–Se σ* MO, typical of ChB interactions, with an associated energy of 15.1 kJ mol^{-1}. Additionally, a minor CT from the same nitrogen LP to the C–N σ* MO (0.92 kJ mol^{-1}) indicates of the presence of the PnB. When selenium is replaced by tellurium and the geometry of the dimer optimized, the Te···N ChB becomes stronger (LP N → σ* N–Te = 31.4 kJ mol^{-1}), as expected, resulting in a further shortening of the N···N distance (2.674 Å). Consequently, the PnB is dramatically strengthened (LP N → σ* N–C = 12.5 kJ mol^{-1}).

Concluding with an example of more complex aggregates, Arfaoui and coworkers studied the interaction between Ch=C=Ch (Ch = S, Se, Te) and diazines [207] to form both binary complexes and complexes of higher stoichiometry (Scheme 38), given the ability of Ch=C=Ch molecules to simultaneously interact with multiple Lewis bases by multiple σ-holes. The supramolecular complexes exhibited stronger interactions compared to the binary ones, with a greater CT and a lower HOMO-LUMO energy gap calculated at DFT level. This study was recently extended to the aggregates formed by diazines with SO_2 and SO_3, showing the possibility of forming both σ- and π-hole interactions [208].

3.3. *Chalcogen···halogen interactions*

Interactions of chalcogen-rich species with halogen-containing ChB acceptors are frequently encountered, and several papers investigated such interactions both in model compounds and in case studies. The conceptually simplest cases involve interactions of ChB donors and halides, a field of growing interest in anion recognition [209–211] and catalysis [212]. One of the few theoretical studies exploring ChB interactions between sp^2-hybridized ChB donors (>C=Ch) and the

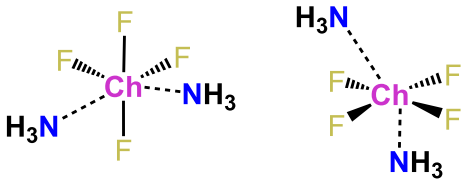

Scheme 33. Different isomers of the adducts between ChF_4 molecules (Ch = S, Se, Te, Po) and two NH_3 molecules [201].

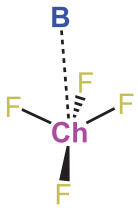

Scheme 34. Lone-pair interactions between ChF_4 and bases (B = NH_3, HF) [203].

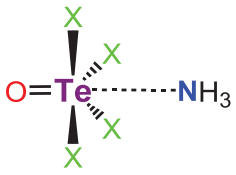

Scheme 35. Adduct between $TeOX_4$ systems and NH_3 (X = F, Cl, Br, I) [204].

chloride anion dates back to 2009 [213]. In particular, the interactions in $(R)_2C{=}S\cdots Cl^-$ (R = H, F) and $Ch{=}C{=}S\cdots Cl^-$ (Ch = O, S) were investigated in detail at MP2/aug-cc-pVTZ level (Scheme 39). For the latter compounds, a contraction of the Ch=C bond distance was observed. The studies employed a variety of approaches, including QTAIM and NBO analyses, and led to the recognition of ChB as a sister noncovalent interaction to HaB.

Much larger is the number of papers involving the interaction between sp^3-hybridized ChB donors and halides or halogen-containing acceptors. Chalcogenides featuring electron-withdrawing substituents are potentially ideal ChB donors for such purpose. In this context the interaction of $(NC)_2Ch$ and RChX (R, X = Cl, F; Ch = S, Se) with chloride and fluoride anions was investigated, and MP2 calculations correctly predicted the arrangement of sub-units in the resulting complexes, particularly when R ≠ X [89]. Notably, the charge-assisted ChB is classified as a strong interaction (BSSE-corrected binding energies as large as 230 kJ mol^{-1} for $(CN)_2Se\cdots F^-$), with negative values of total electron density at BCPs, indicating a partly covalent nature of the interaction.

An experimental and theoretical investigation by Caballero, Frontera and coworkers explored the possibility of chloride/bromide sensing by chalcogenophene (C_4H_3Ch; Ch = S, Se, and Te) derivatives, such as C_6H_5-C_4H_3Ch, C_6F_5-C_4H_3Ch, and $C_6F_4(C_4H_3Ch)_2$, potentially capable of ChB, HB, and π-interactions (Scheme 40). A MEP surface analysis (carried out on PBE0-D3/def2-TZVPP optimized geometries) showed that the anions exhibit a preference for ChB/HB rather than ChB/π-interactions. The contribution of the σ-hole interaction increases on passing from Ch = S to Ch = Te, such that in tellurophene derivatives ChB becomes more relevant than HB in stabilizing the halide adducts [209].

As expected, the introduction of a positive charge on the ChB donor increases the electrostatic contribution to the interaction with halides

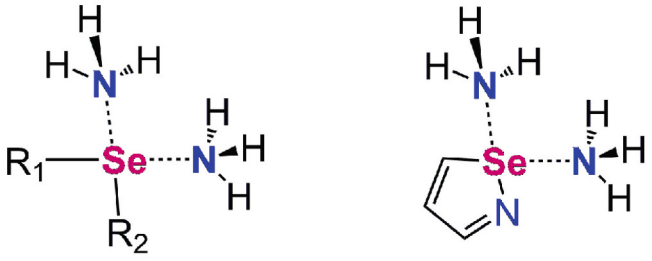

Scheme 36. Triads between R_1ChR_2 molecules (Ch = S, Se, Te; R_1, R_2 = F, Br, I, and ^{t}Bu) or chalcogenazole rings and ammonia [205].

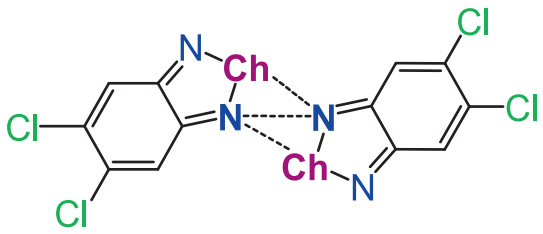

Scheme 37. Structure of 5,6-dichloro-benzochalcogendiazole homodimers (Ch = S, Se, Te) [206].

[3]. This is the case of variously substituted cyclic pyrylium cations and their thio-, seleno- and telluro-analogues, whose interaction with the chloride anion was investigated at DFT (BP86 [214], B97 [215]), MP2, and CCSD(T)/CBS levels of theory (Scheme 41) [216].

The interaction of the chloride anion with more complex, bifurcated ChB donors, such as benzo[1,2-*d*:4,3-*d*']di([1,3]selenazole)s [103] (Scheme 42a) and dithieno[3,2-*b*:2′,3′-*d*]-thiophenes [103,217] (Scheme 42b), was studied in the framework of their application to catalysis. The potential anion transport properties of dithieno[3,2-*b*;2′,3′-*d*]thiophene derivatives and their bis-isothiazole analogues (Scheme 42c), were also investigated [218], showing (i) a decrease in interaction energies with Cl^- upon solvation, (ii) an increase in interaction strength when the carbon atom in S–C was replaced with nitrogen, and (iii) a marked selectivity for F^- and NO_3^- compared to Cl^- and Br^-. The adducts between halides and *N*-methyl-1,3-bis[2(3H)-methylseleno-benzoimidazolium] benzene) [219] (Scheme 42d) and related systems (Scheme 42e) [220], were also studied and compared to their hydrogen-, tetrel-, halogen-, and pnictogen-bonding analogues, showing in all cases a distinct preference for F^-. In general, however, the chalcogen-bonded complexes were found to be the weakest ones [217,220].

Polyatomic anions were analyzed in a study on the adducts between X_2Ch ChB donors and $[MX_6]^{2-}$ (Ch = S, Se, Te; X = F, Cl, Br, I; M = Se, Pt), featuring bifurcated ChBs (Scheme 43). In this case, a combination of QTAIM, NBO, and IQA [221] analyses indicates a significant covalent contribution to the ChB [222].

The interaction of chloride with an anionic receptor, resulting in an interanion ChB (IAChB), was also investigated (Scheme 44). The results showed that energy terms are almost unchanged compared to systems where the ChB acceptor is neutral, with the exception of the electrostatic interaction, which varies non-monotonically along the ChB. This electrostatic interaction represents a dominating force in the kinetic stability of inter-anions [223].

Only a few papers explored the interactions of neutral ChB donors with neutral ChB acceptors featuring halogen atoms, including, for example, hypohalous acids [128]. In some cases, intramolecular interactions were also investigated. One example is a study examining the influence of intramolecular ChBs on the rotational dynamics of moieties such as the YF_3 group around a phenyl ring (Y = C, Sn) or the two phenyl rings bonded to a planar TeF_4 group (Scheme 45). In the first case, the introduction of a –SeH or, even more, –SeF substituent in *ortho* to the CF_3 group lowers its rotational barrier, due to the formation of a Se···F ChB that stabilizes the rotational transition state, which was studied by means of QTAIM, and NBO. On the other hand, when one or two such substituents are added to the Ar–TeF_4–Ar system, the rotation barrier of the Ar rings increases due to steric repulsive effects [224].

3.4. Chalcogen···π and chalcogen···C interactions

A peculiar type of ChB occurs when the acceptor is represented by an unsaturated bond system. In such a case, a filled molecular orbital (MO) of the π-system in the unsaturated bond overlaps with an empty σ*-MO of the chalcogen atom. Alternatively, the interaction can be interpreted as an attractive interaction between the electron-rich π-system and the σ-hole(s) located on the ChB donor. Not surprisingly, acetylene was an

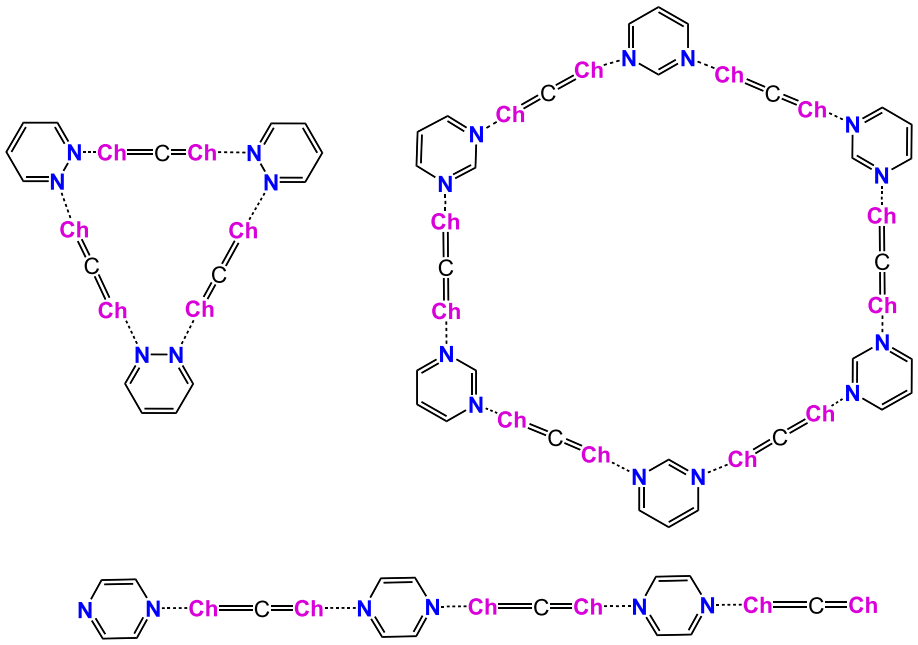

Scheme 38. Examples of supramolecular complexes between Ch=C=Ch (Ch = S, Se, Te) and diazines studied by Arfaoui and coworkers: (Pyridazine–CCh_2)$_3$ (top left); (Pyrimidine–CCh_2)$_6$ (top right); (Pyrazine–CCh_2)$_3$ (bottom) [207].

Scheme 39. Investigated $(R)_2C{=}S{\cdots}Cl^-$ (R = H, F) and $Ch{=}C{=}S{\cdots}Cl^-$ (Ch = O, S) adducts [213].

ideal model ChB acceptor when interacting with RChH donors (Ch = S, Se; R = F, Cl, Br, CN, OH, OCH_3, NH_2, CH_3) to form complexes containing the T-shaped R–Ch···C_2 moiety [225]. The CCSD(T)/aug-cc-pVTZ interaction energies were calculated in the range between –4.9 and –20.2 kcal mol^{-1}, classifying these as weak ChB interactions. It is worth noting that the stability of chalcogen···π complexes was mainly attributed to electrostatic and correlation effects.

On the contrary, the role of π→σ* charge transfer (CT) was evidenced when the interactions of SFH [226], SF_2 [226,227], and SF_4 [227] with several ChB π-acceptors, including ethene, ethyne, 1,3-butadiene, and benzene, were investigated at MP2, M06-2X-D3 and CCSD(T)/CBS levels of theory (Scheme 46). The CT-interaction, resulting in the elongation of the optimized S–F bond opposite to the S···π ChB, was evaluated to fall in the range 13.8–27.6 kJ mol^{-1}.

Calculations on the complexes between $(R)_2Se$ (R = H, F, Cl, CH_3) as well as selenophene and $C_6R'_6$ aromatic systems (R′ = H, F, CH_3; Scheme 47) showed that Se···π interaction energies increase when R is an electron-withdrawing and R′ an electron-donating group. The role of dispersion energy is not very significant, except in the weaker adducts, as stronger interaction energies result in an increase of both orbital and electrostatic contributions [228].

In the adducts between X_2Ch molecules (X = F, Cl, Be, I; Ch = O, S, Se, Te) and acetylene, ethylene, or 2-butyne, it was observed that complexes become more stable as the electronegativity difference

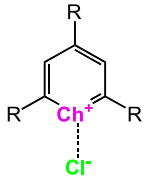

Scheme 41. Interaction of Cl^- with pyrylium cations and their thio-, seleno- and telluro- analogues (R = H, CH_3, Ph; Ch = O, S, Se, Te) [216].

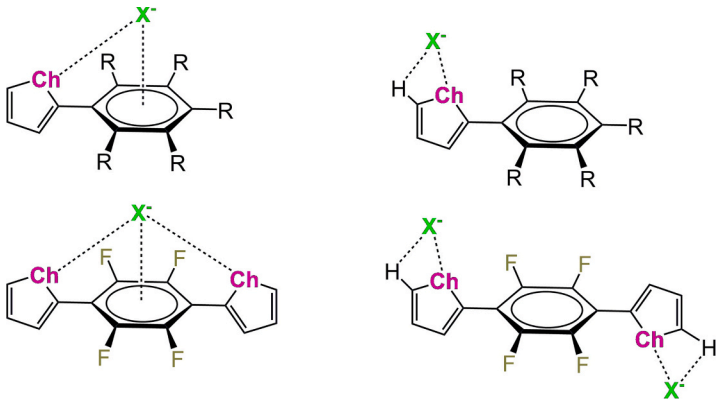

Scheme 40. Possible binding modes between C_6R_5-C_4H_3Ch or $C_6F_4(C_4H_3Ch)_2$ systems and X^- (R = H, F; Ch = S, Se, Te; X = Cl, Br): cooperative ChB and anion-π interactions (left) and ChB/HB (right) [209].

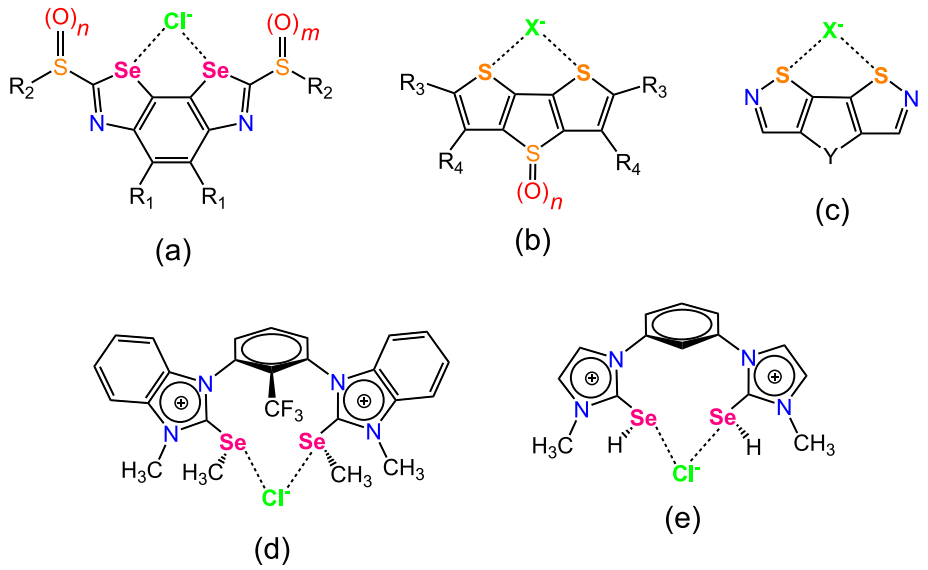

Scheme 42. Interaction of halides with: (a) benzo[1,2-*d*:4,3-*d*]di([1,3]selenazole)s (*n*, *m* = 0–2; R_1 = CN, CH_3; R_2 = *p*-methyl-phenyl) [103]; (b) dithieno[3,2-*b*:2′,3′-*d*]-thiophenes (*n* = 0–2; R_3 = CN; R_4 = ^{i}Bu; X = F, Cl, Br, I) [103,217] and (c) their bisisothiazole analogues (Y = SO_2, O, S, PCH_3, CH_2, NCH_3; X = F, Cl, Br) [218]; (d) *N*-methyl-1,3-bis[2(3H)-methylseleno-benzoimidazolium]benzene cations [219]; (e) 4,4′-(1,3-phenylene)bis[5-(tellanyl)-1H-1,2,3-triazole] cations [220].

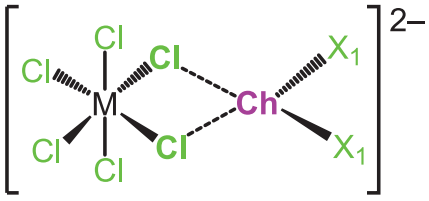

Scheme 43. Adducts between X_2Ch ChB donors and $[MX_6]^{2-}$ (Ch = S, Se, Te; X = F, Cl, Br, I; M = Se, Pt) [222].

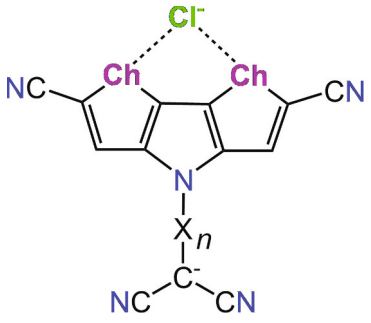

Scheme 44. Adducts between chloride and ditiheno[3,2-*b*:2′,3′-*d*]pyrrole scaffolds, featuring interanion ChBs (Ch = S, Se, Te; X = $-C_6H_4-$; *n* = 0–2) [223].

between Ch and X increases, with the strongest Ch···π bonds formed with 2-butyne. This was mainly attributed to enhanced orbital interactions [229]. The interactions of $(CF_3)_2Ch$ and F_2C=Ch model compounds (Ch = Se, Te) with the π-system of benzene were also

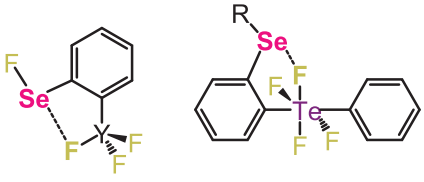

Scheme 45. ChB interactions occurring in different systems where they influence rotational dynamics (Y = C, Sn; R = H, F) [224].

investigated at DFT level (BP86-D3/def2-TZVPD). The resulting optimized complexes showed the ChB donor to be always disposed perpendicular to the benzene ring (Scheme 48), with BSSE-corrected interaction energies in the range of –14.6/–22.6 kJ mol^{-1}, systematically increasing from Ch = Se to Ch = Te [230].

One of the few examples of S···C interactions investigated theoretically is represented by the adducts between CS and SHR compounds (R = F, NO_2, NC, Cl, CN, –C≡CH, NH_2). Interestingly, complexes with traditional ChBs exist for all systems except those with R = F or Cl, where sulfur-shared ChBs are found to be more stable. The two types of structures are connected by transition structures, and the transition between them is reflected in the changes in the $^{1}J_{C,S}$ spin-spin coupling constants [231]. Another recent example is the modelling of fullerene or polyynic carbon chains featuring chalcogena-diazole/-triazole substituents, showing the role of intramolecular Ch···C ChB interactions in stabilizing the covalent N–C bond with the substituent (Scheme 49) [232,233]. Scheiner and coworkers also investigated at the M06-2X/def2-TZVPP level the possible role of strained propellane and pyramidane hydrocarbon molecules as Lewis bases towards molecules including F_2Ch (Ch = S, Se, Te), given the formation of regions of negative electrostatic potential on the bridgehead C atom as a result of the strain [234].

It is also worth mentioning a recent investigation on Se···C ChBs in Al$(CH_3)_3$·SeHCX_3 model systems (X = H, F) within a broader computational study on Al$(CH_3)_3$···Y interactions (Y = Li, Ga, Ge, As, Br) investigating the role of methyl groups as Lewis bases in noncovalent interactions [235], a survey recently extended to different systems by other authors [200,236].

3.5. ChB radical donors and acceptors

A few papers have addressed the theoretical modelling of ChB interactions involving radical species. One example is the interaction of a closed-shell ChB donor with a radical acceptor, modelled in the case of XChH donors (X = F, Cl, Br; Ch = S, Se) interacting with alkyl radicals such as •CH_3 and •C_2H_5, leading to what has been termed a "single-electron chalcogen bond interaction" [237]. An EDA of this very weak interaction (E_{int} = between –7.1 and –25.1 kJ mol^{-1} at CCSD(T)/aug-cc-pVTZ level) revealed that the dominant term is electrostatic in nature. This term increases as Ch goes from S to Se, with significant attractive polarization and dispersion components. In a subsequent paper, the

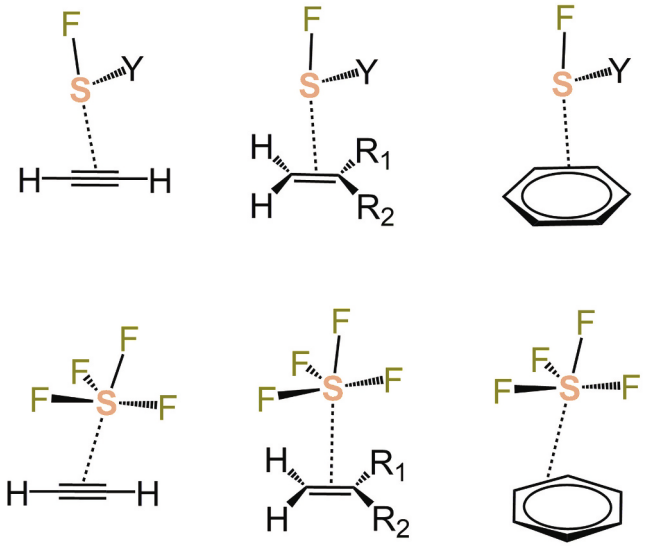

Scheme 46. Interaction between FSY (top) or SF_4 (bottom) and acetylene, ethylene, *cis*- and *trans*-butadiene, and benzene (Y = F, H; R_1, R_2 = H, –CH=CH_2) [226,227].

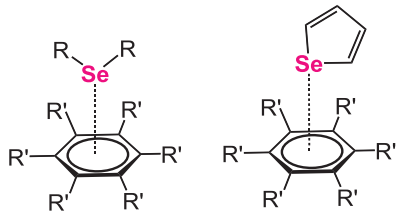

Scheme 47. Interaction between $(R)_2Se$ (R = H, F, Cl, CH_3; left) or selenophene (right) and $C_6R'_6$ aromatic systems (R′ = H, F, CH_3) [228].

radical···radical interactions between the ChB acceptor benzodithiazolyl (BDTA) and the ChB donors of dichalcogenadiazolyl species (*p*-R-C_6F_4–CN_2Ch_2; Ch = S (DTDA), Se (DSDA); R = H, F, CN, NO_2, CH_3, NH_2, $N(CH_3)_2$; Scheme 50) were investigated at the unrestricted PBE0-D3/def2-TZVP level of theory, with a further MP2/def2-TZVP validation [238]. A combined theoretical and structural approach, supported by CSD data, demonstrated that ChB radical···radical interactions represent a common supramolecular motif encountered in the solid state. In DSDA/DTDA radicals, a σ-hole was calculated in the center of the Ch–Ch bond, promoting bifurcated ChB interactions. Finally, in analogy to what described above, the interaction energy was calculated to be finely tunable depending on the nature of the R substituent.

A further significant contribution was recently presented by Puskarevsky and coworkers, who demonstrated that the dianionic trimeric units $(\mathbf{L}^1_3)^{2-}$, found in the solid state after reduction of 2,1,3-benzotelluradiazole ($\mathbf{L}^1$), afford the diamagnetic compound [K(18-crown-6)(THF)]$_2\mathbf{L}^1_3$ (Scheme 51). This compound was described as the result of the interaction between two reduced radical species $\mathbf{L}^{1-\bullet}$ and a neutral unit of $\mathbf{L}^1$, connected through N–Te···N ChB interactions. These interactions were investigated in-depth using CASSCF and unrestricted B3LYP-D3 broken-symmetry DFT calculations [239].

On the other hand, the so-called R$^\bullet$-hole interactions between $\bullet SO_2F$ and N_2, HCN, and CO_2 were investigated using QTAIM, non-covalent interaction theory via the reduced density gradient (NCI-RGD) [240], and SAPT-EDA approaches (Scheme 52). The study showed that interaction energies increased with the basicity of the Lewis base (e.g. HCN > CO_2 > N_2), with electrostatic and dispersion forces being the dominant contributions [241].

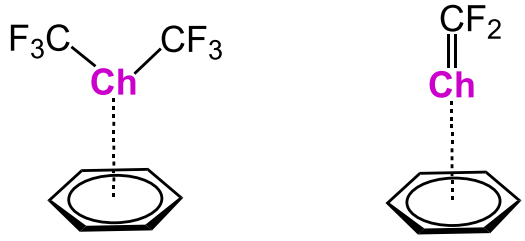

Scheme 48. Adducts between benzene and $(CF_3)_2Ch$ or F_2C=Ch model compounds (Ch = Se, Te) [230].

4. Applications of computational methods to ChB interactions

Over the past decades, computational techniques have been successfully applied to complement and clarify experiments, involving not only the synthesis, but also the modulation of reactivity, as well as the structural and spectroscopic features of various systems based on ChB interactions. In the following, a selection of these applications will be reviewed.

4.1. Crystal packing interactions

Understanding solid-state intermolecular interactions is crucial in molecular recognition, crystal engineering, and sensing [242,243]. In addition to the most commonly explored non-covalent interactions, including HB and HaB, ChB is increasingly recognized as a fundamental σ-hole interaction. ChB is particularly useful in rationalizing the nature and directionality [244] of frequent intra- and intermolecular nonbonded interactions involving chalcogen centers in the solid state [245,246]. Diffractometric data, typically deposited at the Cambridge Structural Database (CSD), are essential for identifying ChB interactions in the solid state structures [230].

An early study critically examined structural data using DFT and MP2 results for chalcogenophthalic anhydrides $C_8O_2H_4Ch$ (Ch = O, S, Se, Te), for which the electron density distribution ρ(r) around chalcogen atoms Ch and the L(r) = $-\nabla^2\rho(r)$ function were investigated to characterize the directionality and strength of Se···O and Se···Se ChB interactions [244]. A few years later, CSD data (about 120 hits) were extracted and compared to BP86-D3/def2-TZVP calculations to investigate the relative strength of ChB and PnB interactions between $(CF_3)_2Ch/F_2C$=Ch ChB donors (Ch = Se, Te) and trimethylamine and benzene as ChB acceptors (see above, Scheme 48) [230]. This investigation revealed that Ch···N contacts were less frequent in the CSD compared to relevant HaB interactions. Notably, only a few structurally characterized systems could be related to the considered computational model systems. A CSD search of C=S···S=C intermolecular interactions revealed mostly type-I ChB interactions; binding energy calculations on

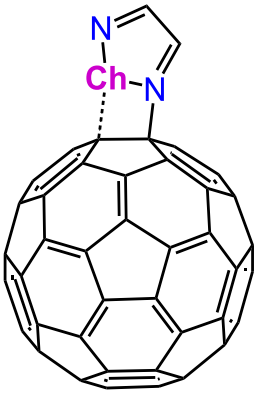

Scheme 49. Fullerene C_{60} featuring chalcogenadiazole substituents, showing the intramolecular Ch···C ChB (Ch = O, S, Se, Te) [233].

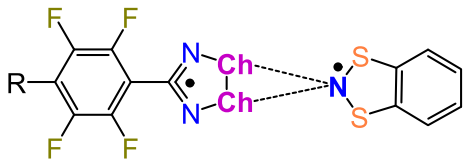

Scheme 50. ChB radical···radical interactions between the benzodithiazolyl (BDTA) and *p*-R-C_6F_4–CN_2Ch_2 species (Ch = S, Se; R = H, F, CN, NO_2, CH_3, NH_2, $N(CH_3)_2$) [238].

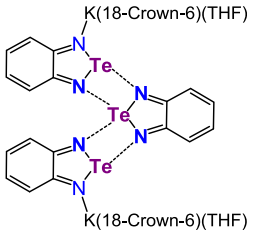

Scheme 51. Structure of $[K(18\text{-crown-6})(THF)]_2\mathbf{L}^1_3$ ($\mathbf{L}^1$ = 2,1,3-benzotelluradiazole) [239].

selected dimers extracted from the CSD revealed that most of these interactions are destabilizing and likely result from crystal packing effects [247].

A study conducted by QTAIM on a large number of crystal structures containing Se···Br and Te···Br interactions, retrieved from the CSD and mostly comprising chalcogen bonded dimers, enabled the identification of a continuous spectrum of bonding characteristics in the selected systems, ranging from weak van der Waals interactions to covalent bonds [248]. On the other hand, Ch···X interactions (Ch = Se, Te; X = Cl, I) were modelled in selected systems as part of an investigation on ChB in Pd/Pt coordination complexes, featuring Ch-coordinating ligands whose structures were also extracted from the CSD. These studies showed that coordination to the metal center enhances the σ-hole donor abilities of the Ch atoms [249]. In a related context, Aragoni et. al recently proposed a scale of strength, derived from structural data, based on the relative shortening of the Ch···A distance with respect to the sum of the relevant van der Waals radii [250].

In addition to the abovementioned broad-spectrum studies, several authors have employed theoretical calculations to investigate the structural features of more specific cases, which can be grouped according to the types of interacting atoms examined.

4.1.1. Chalcogen-chalcogen interactions

Both intra- and intermolecular interactions involving Ch···Ch contacts have been identified in the solid state, and their nature has been investigated by computational methods. Intramolecular ChB interactions often play a key role in the formation of stable ring systems. A notable example was recently observed in the case of arylhydrazones of sulfamethizole [251]. DFT calculations on structural data clearly demonstrated that π-conjugation is established through the formation of a five-membered ring, enabled by a O···S intramolecular resonance-assisted ChB interaction (RAChB; Fig. 3).

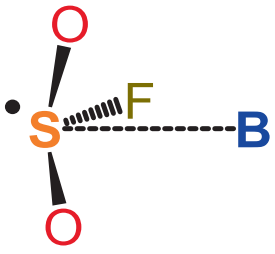

Scheme 52. R•-hole interactions between •SO_2F and B bases (B = N_2, NCH, and CO_2) [241].

Another case of resonance-assisted ChB was observed in a series of *ortho*-chalcogen benzaldehydes featuring Ch···O interactions (Ch = S, Se, Te); this interaction, whose strength increases in the order S < Se < Te and whose major contributions derive form orbital mixing and electrostatic interactions, controls the formation of the conformer observed in the crystal structure. The imine derivatives of the aldehyde were also investigated, and it was observed that the resulting Ch···N ChB decelerates the kinetics of their formation and thermodynamically stabilizes them [252]. A further example of intramolecular ChB contributing to the formation of a five-membered ring was identified in *o*-nitro-O-aryl oximes, which were structurally characterized and investigated at DFT level (M06-2X/aug-cc-pVQZ). A topology analysis, supported by EPS calculations clearly evidencing the presence of σ-hole, confirmed an O···O ChB interaction (Fig. 4) [253].

Examples of bifurcated intramolecular ChBs were also investigated, for example from the crystal structures of ion pairs containing dithienylnitrophenol anions (Fig. 5a) [254], in *N*,*N*′-diaryl thiourea derivatives [255], and in 2,5-thiophenediamides (Fig. 5b), leading to the *cis*-conformation at the base of the helical structures observed in their crystal packing [256]. In both cases, the nature of the interaction, originating from the oxygen LPs to the antibonding σ*(S–C) orbital, was confirmed through NBO [122] methods.

Moving to intermolecular interactions, and starting with those involving tellurium atoms, intermolecular Te···O interactions were observed and computationally studied (B3LYP-D3 and B2PLYP) in 1,3-benzotellurazole derivatives [257]. Analogously, Te···O ChB interactions were found to drive the reversible assembly of 3-methyl-5-phenyl-1,2-tellurazole-2-oxide into a variety of supramolecular aggregates, both in solution, as proved by NMR experiments, and in the solid state (Fig. 6) [258]. DFT-D3 calculations using the PBE [259] functional, showed that the Te atom in the tellurazole cycle displays two σ-holes, with the one opposite the N-atom being more prominent [258]. Consequently, the Te atom acts as the ChB donor, and the $^{+}$N–O^{-} group as the acceptor in the (N)Te···O–N moiety. The same authors recently reported on similar supramolecular aggregates based on *N*-phenoxide analogues [260]. This study was also extended to benzo-1,2-chalcogenazole 2-oxides [261].

Te···O, Se···O, and S···O, interactions were observed in the cocrystals of 1,2,5-chalcogenadiazoles and a few crown ethers (Fig. 7). A combination of QTAIM and NBO calculations showed that the ChB interaction, resulting from charge transfer (CT) from the crown ether to the chalcogenadiazole, was accompanied by back CT in the opposite direction, thus demonstrating the ambiphilicity of 1,2,5-chalcogenadiazoles

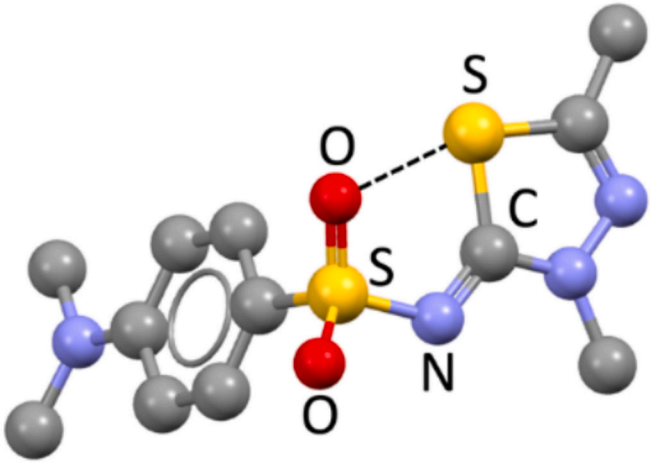

Fig. 3. Molecular structure of a sulfamethizole derivative, showing the intramolecular resonance-assisted ChB interaction. Hydrogen atoms were omitted for clarity [251].

[262].

Bifurcated Te···Ch ChB interactions (Ch = S, Se, Te) where studied using the X-ray structures of a series of cocrystals between dichalcogenides Ph_2Ch_2 (Ch = S, Se, Te) and perfluorinated ChB donors Ar^F_2Te (Ar^F = 4-$CF_3C_6F_4$, 4-NC_5F_4; Fig. 8). The interactions were studied at PBE0-D3/def2-TZVP level through QTAIM [85] and NCI, and the contribution of the heterovalent ChBs to the binding anergy was estimated to range between –19.7 and –27.2 kJ mol^{-1} [263].

On the other hand, trifurcated ChBs were observed in the crystal structures of the adducts between tris[3,5-bis(trifluoromethyl)-phenyl] telluronium tetrakis[3,5-bis(trifluoromethyl)phenyl]borate and triphenylphosphine oxide (Fig. 9), and were studied at the DFT level, confirming the dominant contribution of Coulombic forces in establishing the observed Te···O ChB interactions [264].

A series of helical structures self-assembled by planar benzotellurazole amides through Te···Ch ChB interactions (Ch = O, Te) were recently described [265]. These compounds form single helices through Te···O interactions, and in one case, a double helix is held together by Te···Te ChBs. Both interactions, studied in model systems through QTAIM and EDA, were calculated to amount to about –34/50 kJ mol^{-1} [265].

An example of homovalent Ch···Ch ChB interactions is the Te_4 rectangular motifs formed in the crystal structures of several diaryl ditellurides (Fig. 10), which were studied at DFT level, confirming the presence of BCPs through QTAIM analysis [266].

Moving to intermolecular ChBs involving Ch atoms other than Te, Frontera and coworkers analyzed a series of dimers featuring Se···O, Se···S, or S···O interactions at the PBE0-D3/def2-TZVP level, computing interaction energies ranging from –13.4 to –62.3 kJ mol^{-1} and studying the ChB also through QTAIM NCI, and NBO analysis. A dependence in the interaction strength on the depth of the σ-hole in the monomers, investigated through MEP analysis, was found, and the study was also extended to some model systems based on Protein Data Bank archive (PDB) structures [267]. The intra- and intermolecular interactions in a series of thiophene derivatives were studied at QTAIM level to establish the interplay between the σ-hole and LPs of electrons on sulphur and the strength of the electrophilic-nucleophilic interactions [268].

The ability of H-selenite anions ($HSeO_3^-$) to form supramolecular chains in the solid state through a combination of anion-anion Se···O ChB and HB interactions was also observed experimentally and confirmed theoretically using QTAIM, NCI, and NBO methods. Although in the gas phase the model dimers exhibit repulsive interaction energies, very small energy minima (about 5.0 kJ mol^{-1}) were calculated in solution [269].

Square tetravalent Ch···O ChB interactions (Ch = S, Se, Te) involving >Ch=O fragments were also investigated based on a series of crystal structures extracted from the CSD (Fig. 11) in different model dimers, revealing a correlation between the strength of ChBs and the ESP maxima and minima on the Ch and O atoms, respectively [270]. Consistently, the Te···O interactions were calculated to be the strongest, also featuring a covalent contribution, and electron-withdrawing substituents were found to increase the strength of the interaction. Electrostatic is the dominating factor, with the second contribution being the orbital term, while dispersion plays a limited role, particularly when Ch = Te.

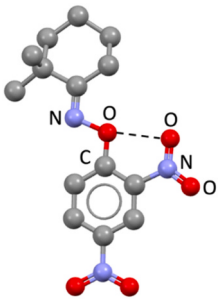

Fig. 4. Molecular structure of the *o*-nitro-O-aryl oxime featuring an intramolecular O···O ChB interaction. Hydrogen atoms were omitted for clarity [253].

Trifurcated Se···N/O ChBs between 2,1,3-benzoselenadiazole derivatives and pyridine-2,6-dicarboxylic acid were predicted based on DFT calculations at the ωB97X-D/def2-TZVPP level, and based on the theoretical calculations ChB donors featuring strong electron-withdrawing groups were selected for cocrystal synthesis experiments, which led to the formation of the anticipated trifurcated chalcogen bonds [271].

Intermolecular ChBs interactions involving coordination compounds have also been occasionally studied, as in the case of $[Cu_2(\mu_{1,3}\text{-}\mathbf{L^3})_4(DMSO)_2]$ ($\mathbf{HL^3}$ = 2-chloro-4-nitrobenzoic acid; Fig. 12), where S···O interactions involving DMSO ligands were investigated, along with the other interactions observed in the solid state (HB, S···π), at the RI-BP86-D3/def2-TZVP level [272]. Another example is $[Fe_3(\mu_3\text{-}O)(2\text{-furate})_6(H_2O)_2(NCS)]$, where a weak O···O interaction (estimated at about 13 kJ mol^{-1}) between the COO^- groups of neighboring furoic acid residues was studied using QAITM, NCI, and NBO methods [273]. A further case is the recent investigation of the Se···Se intermolecular contacts in the crystal structure of diselenophosphinate Ni^{II} complexes, leading to a supramolecular zigzag pattern; a DFT investigation combining ESP, ELF, and SAPT analyses reveled that the shortest interactions are governed primarily by dispersion forces, while the longer ones by electrostatic forces [274].

Moving to case studies involving biological systems, the possibility for the chalcogen atom in sulfinic and seleninic acid derivatives to function as a ChB donor through its three σ-holes was studied using QTAIM and MEP, based on the crystal structure of 3-selenino-L-alanine (selenocysteine seleninic acid; Fig. 13), a functional component of several enzymes, along with different analogues from the CSD [275].

The importance of an S···O ChB interaction found in the crystal structure of the adduct between the SET7/9 methyltransferase enzyme and the S-adenosylmethionine methyl (AdoMet) donor, involving the oxygen atom of an asparagine residue in the active site, was also investigated [276]. Ch···O ChB interactions (Ch = S, Se) were also studied at RI-MP2/def2-TZVP level using QTAIM, NCI, and NBO in different model systems for the interaction between uracil bases and Ch-adenosyl methionine in different RNA riboswitches, based on PDB entries. The calculated energies ranged from –23 to –60 kJ mol^{-1}, suggesting ChB interactions play an important role in the recognition and folding mechanisms of these systems [277]. On the other hand, the Se···O and Se···S ChB interactions between Se-carbohydrates and aminoacids were studied based on a series of PDB structures. Interaction energies in the corresponding model systems were found to range from –4.6 to –46.4 kJ mol^{-1} [278]. In a separate study, the role of S···O and Se···O ChB interactions in stabilizing the adducts between proteins and various ligands found in the PDB was also investigated using simplified model systems. This study showed that ChBs represent the dominant interactions, especially in the case of charged systems [279].

Intermolecular Se···O interactions were also studied in the polymorphs of the organoselenium antioxidant ebselen (2-phenyl-1,2-benzoselenazol-3(2H)-one, Fig. 14), where they represent the shortest such ChBs known for organoselenium compounds. A strong electrostatic nature was ascertained for this interaction, and the possible role of intermolecular Se···O ChBs with substrates such as water and reactive oxygen species in the cleavage of the Se–N bond, central to its antioxidant activity, was also investigated [280].

Intermolecular S···O ChB interactions were also identified in the crystal structures of various salts and cocrystals of the drug riluzole (6-(trifluoromethoxy)-1,3-benzothiazol-2-amine), where they appear bifurcated in combination with a HB. The S···O ChB motif plays only a secondary role in stabilizing the crystal packing compared to the HBs. Analysis via QTAIM, NBO, and Roby-Gould [281] bond indices showed

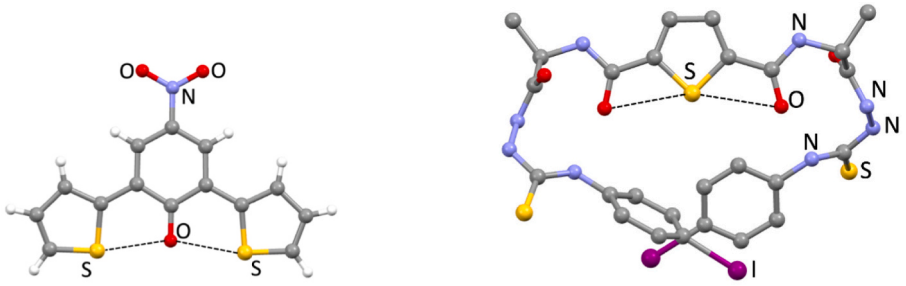

(a) (b)

Fig. 5. (a) Molecular structure of the dithienylnitrophenol anion in the crystal structure of its salt with TBA, showing bifurcated intramolecular S···O interactions [254]; (b) crystal structure of a 2,5-thiophenediamide, whose *cis*-conformation is driven by similar ChBs. Hydrogen atoms were omitted for clarity [256].

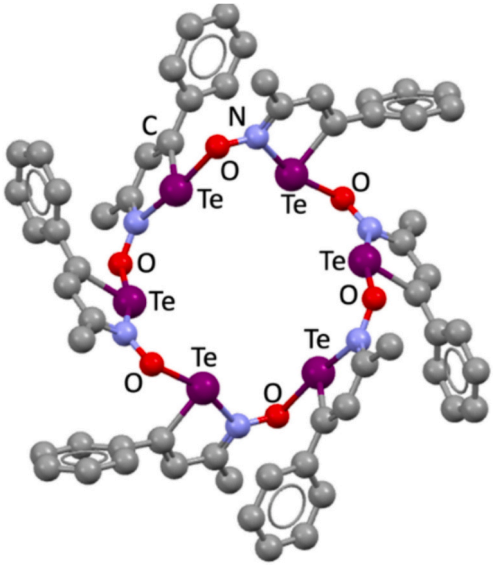

Fig. 6. Portion of the crystal packing of an hexameric assemble of 3-methyl-5-phenyl-1,2-tellurazole-2-oxide, kept together by Te···O ChB interactions. Hydrogen atoms were omitted for clarity [258].

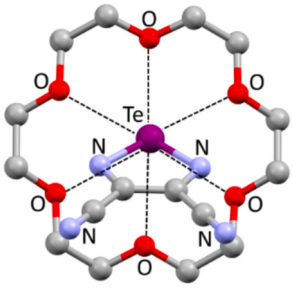

Fig. 7. Te···O ChB interactions in the cocrystals of 1,2,5-telluradiazole and 18-crown-6. Hydrogen atoms were omitted for clarity [262].

bond orders in the range 0.11–0.34 and indicated a predominantly ionic nature of the interaction [282].

S···S interactions were also examined in the crystal structure of the organic conductor 7,9-di(thiophen-2-yl)-8H-cyclopenta[a]acetaphtylen-8-one through theoretical charge density analysis, which assigned type-I and type-II characteristics to the two distinct S···S interactions. However, these interactions appear to have only a minor influence on the overall electronic structure of the conductor compared to π···π stacking interactions [283].

S···O and S···S interactions were also explored in the context of anion

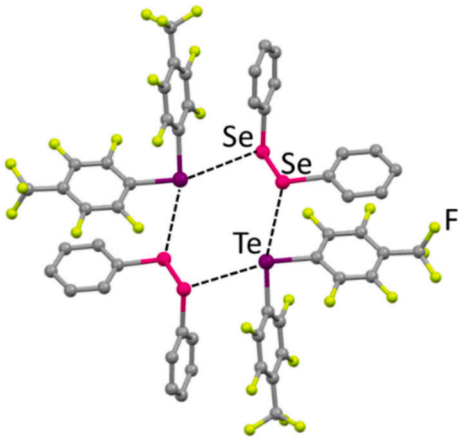

Fig. 8. Portion of the structure of the cocrystal between Ph_2Se_2 and 4-$CF_3C_6F_4Te$, kept together by Te···Se ChB interactions. Hydrogen atoms were omitted for clarity [263].

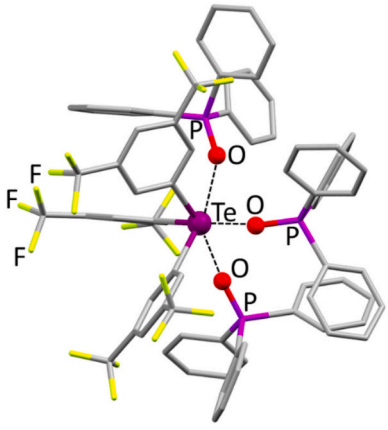

Fig. 9. Structure of the cation in $[\mathbf{L^2}(OPPh_3)_3]^+BArF^-$ ($\mathbf{L^{2+}}$ = tris[3,5-bis(trifluoromethyl)-phenyl]telluronium; $BArF^-$ = tetrakis[3,5-bis(trifluoromethyl) phenyl]borate), showing trifurcated Te···O ChB interactions. Hydrogen atoms were omitted for clarity [264].

recognition in a series of adducts between benzothienoiodolium cations and $CF_3CO_2^-$ or SCN^- anions. The formation of the observed synthons involves a combination of HaB, HB, and ChB interactions (Fig. 15). These were analyzed at crystallographic coordinates using QTAIM, ELF [284], and NBO methods at PBE0-D3/def2-TZVP level, revealing a synergic effect among the various noncovalent interactions [285].

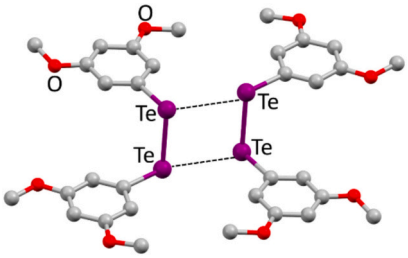

Fig. 10. Te···Te ChB interactions in the crystal structure of a ditelluride, forming rectangular Te_4 motifs. Hydrogen atoms were omitted for clarity [266].

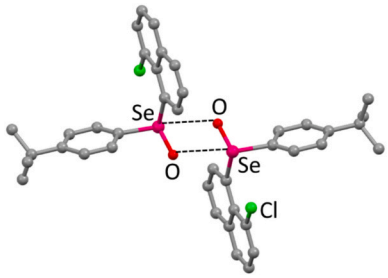

Fig. 11. Square tetravalent Ch···O ChB interactions in 8-chloro-1-(*p*-t-butylphenylseleninyl)naphthalene, whose model system was one of the many employed to investigate this type of interaction. Hydrogen atoms were omitted for clarity [270].

4.1.2. *Chalcogen-pnictogen interactions*

Among intramolecular ChBs involving chalcogen and pnictogen species, a notable case is represented by the reaction of cis-[$PdCl_2$(C,N-Xyl)$_2$] (Xyl = 2,6-$(CH_3)_2C_6H_3$) with 1,3-thiazol-2-amines and 1,3,4-thiadiazol-2-amines. These reactions yield two regioisomeric binuclear diaminocarbene Pd-complexes, with the isomeric ratio dependent on the reaction conditions. A combined experimental and QTAIM and NBO DFT-analysis on the crystallographically characterized regioisomers, revealed that the thermodynamically favored isomer features an intramolecular S···N contact, whereas the kinetically controlled one exhibits a S···Cl interaction (Fig. 16). The product distribution is governed by the relative strength of these interactions with estimated energies of 11.7–12.5 kJ mol^{-1} for S···Cl and 19.2–20.9 kJ mol^{-1} for S···N [286].

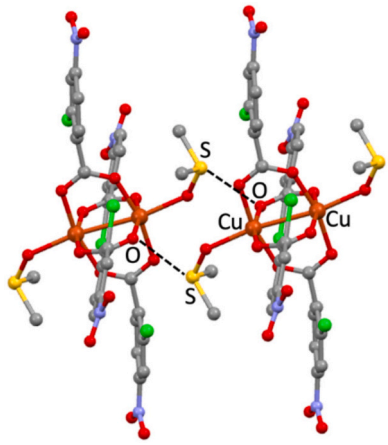

Fig. 12. Portion of the crystal packing of [$Cu_2(\mu_{1,3}$-$\mathbf{L^3})_4(DMSO)_2$] ($\mathbf{HL^3}$ = 2-chloro-4-nitrobenzoic acid), showing S···O ChB interactions. Hydrogen atoms were omitted for clarity [272].

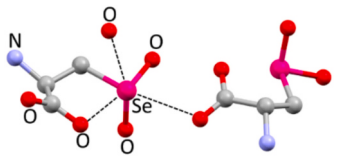

Fig. 13. Intra- and intermolecular Se···O ChB interactions formed in the solid state by the selenium atom of selenocysteine seleninic acid, also involving a co-crystallized water molecule. Hydrogen atoms were omitted for clarity [275].

Another example of intramolecular S···N interaction was analyzed at DFT level in the crystal structure of chlothianidin (CLO), a neonicotinoid insecticide whose structure was previously reported [287]. Notably, QM/QM' ONIOM calculations (M06-2X/6-311G(d)) revealed that ChB intermolecular interactions play a crucial role, undetectable at lower level of theory, in the binding of neonicotinoids, such as CLO and thiametoxam (THA), to *Aplysia californica* acetylcholine-binding protein (Ac-AChBP), whose structural and binding features closely resemble those of the insect nicotinic acetylcholine receptor (nAChR).

An intramolecular Te···N interaction was also observed in (C_6F_5)Te$(CH_2)_3$N$(CH_3)_2$, which was characterized as borderline between open and closed shell [288]. O···N intramolecular oxygen-azide interactions were studied in a series of structures (Fig. 17) and related model systems, with estimated interaction energies in the range of 6–12 kJ mol^{-1}. These results indicated that electrostatic and dispersion forces are the dominant attractive contributions, although conformational studies suggested that intermolecular packing effects may also play an important role in stabilizing the azide interaction [289].

Intermolecular ChBs between chalcogen and pnictogen species are instead capable of driving supramolecular self-assembly, often in mutual interplay with other σ-hole interactions, such as HaB. QTAIM, NCI and NBO DFT-analyses were employed to rationalize such interactions, as in the case of systems containing ditopic chalcogenazolo-pyridine modules (Fig. 18) [245].

In some cases, Pn···Ch interactions were studied to discriminate their PnB *vs* ChB nature. For example, a series of crystal structures extracted from the CSD featuring As···S intermolecular interactions were investigated at the ωB97X-D [290] or M06-2X/def2-TZVP level using a combination of QTAIM, NCI, NBO, EDA, and ELI (electron localizability indicator) [291] analyses. The study showed that the opposing electron-density distributions can be used to rationalize whether the As···S interactions behave as PnBs or ChBs in different systems [292]. Another study focused on a series of stibanyl telluranes of the type $(R)_2$Sb–TeR (R = CH_3, CF_3), based on the crystal structures of Et_2Sb–TeEt, $(CH_3)_2$Sb–Te–Sb$(CH_3)_2$, and Et_2Sb–Te–SbEt_2 (Et = C_2H_5; Fig. 19). The Sb···Te metalloid···metalloid interactions observed in the crystal structures were interpreted as ChBs based on DFT calculations. Additionally, the chalcogen- and pnictogen-bonded adducts between $(R)_2$Sb–TeR model systems and various bases were studied, showing that PnB complexes are stronger than ChB ones [293].

An investigation performed on selenadiazolium supramolecular building blocks revealed the formation of dimeric aggregates stabilized

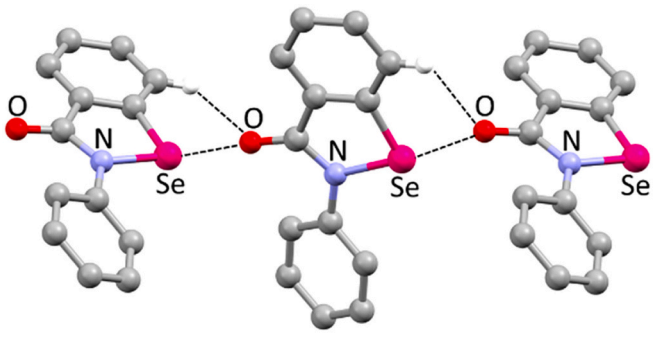

Fig. 14. Portion of the crystal packing of one of the polymorphs of ebselen, showing the intermolecular Se···O ChB interactions. Hydrogen atoms not involved in contacts were omitted for clarity [280].

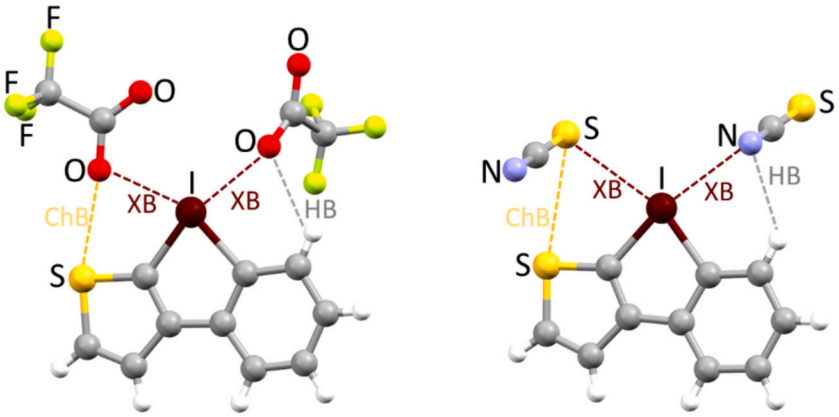

Fig. 15. Synergistic HaB, ChB, and HB interactions between 2-(3-thienyl)benziodolium and $CF_3CO_2^-$ (left) or SCN^- (right) studied through DFT calculations [285].

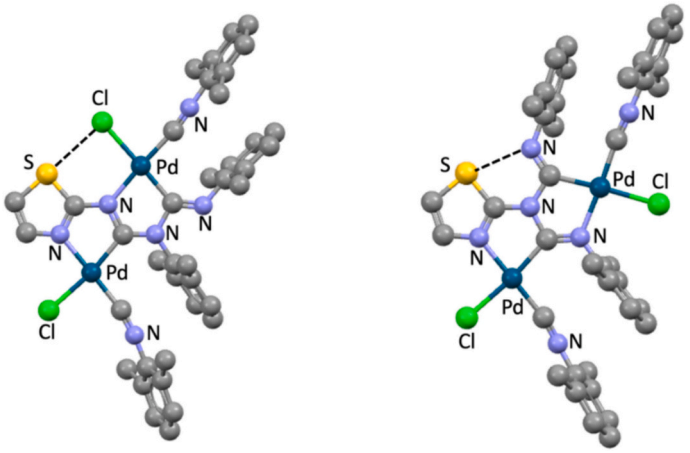

Fig. 16. Kinetically (left) and thermodynamically controlled (right) isomers of one of the investigated binuclear aninocarbene Pd complexes, showing the intramolecular S···Cl and S···N ChB interactions. Hydrogen atoms were omitted for clarity [286].

by four-center $[Ch\cdots N]_2$ ChB interactions and Se···X^- anion binding (X = Cl, Br, I; Fig. 20). The nature of these interactions was elucidated through DFT-D3 calculations employing PBE exchange and correlation functionals and the Zeroth Order Regular Approximation formalism (ZORA) with a TZP basis set [295].

The four-center $[Ch\cdots N]_2$ ChB is in fact a common supramolecular synthon. It has been investigated in a number of systems, including adducts between 1,2,4-selenadiazole cations and various anions such as halide, trifluoroacetate, $AuCl_4^-$, ReO_4^-, TcO_4^-, ClO_4^-, and BPh_4^-, as studied by Tskhovrebov and coworkers [296–299]. In these systems, ChBs were found to compete with similar rectangular $[Se\cdots X^-]_2$ motifs (X = Cl, Br),

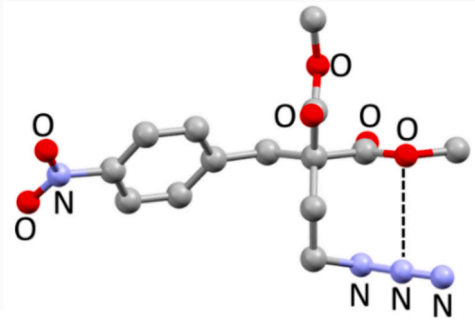

Fig. 17. O···N oxygen-azide intramolecular interaction in dimethyl(2-azidoethyl)[(4-nitrophenyl)methyl]propanedioate. Hydrogen atoms were omitted for clarity [289].

which are also involved in anion recognition processes or other types of ChB interactions [297–299]. The four-center $[Se\cdots N]_2$ ChBs in these systems were studied and compared to the other observed intermolecular interactions at the M06-2X/6-311++G** and ωB97X-D3/def2-TZVPP [300] levels of theory through QTAIM, ELF, and NBO methods, and the estimated interaction energy of each contact was between about –8 and –25 kJ mol^{-1} [296–299].

A comparative study of $[S\cdots N]_2$, $[Se\cdots N]_2$, and $[Te\cdots N]_2$ ChB interactions was performed on $(C_6N_2R_4Ch)_2$ dimers (Ch = S, Se, Te; R = H, F), based on the crystal structures of 2,1,3-benzothia-, benzoselena-, and benzotellura-thiazole. Calculations at the MP2 level using QTAIM, electron density difference (EDD), and IGM [301] methods, showed that the strength of the interaction increases in the order S < Se < Te, in agreement with the larger V_{max} values of the σ-hole on Te. Fluoro-substituents also increase the intensity of the σ-hole on Ch and thus enhance the resulting ChB strength. Electrostatic interactions were calculated to dominate in the dimer complexes. The adsorption of the dimers on Ag surfaces was also investigated, showing that adsorption energies increase in the order S < Se < Te, and the Ch···N ChB is strengthened by interaction with the silver layer [302].

The effect of substitution and metal coordination on the strength of $[Se\cdots N]_2$ interactions was also studied in a series of 5-substituted benzo[c][1,2,5]selenadiazoles and their copper complexes [303]. No clear correlation was found, in either the free ligands or complexes, between the strength of ChB interactions and the Hammet's *para*-substituted constants of the substituents. Metal coordination was found to weaken the ChB interactions in some complexes and strengthen them in others; both observations were attributed to the effect of secondary

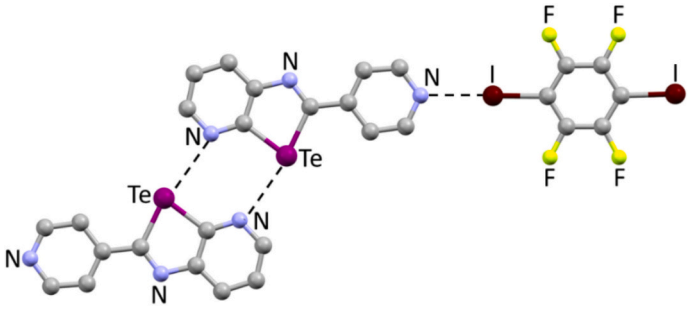

Fig. 18. Example of crystal structure based on self-associating chalcogenazolo-pyridine modules in which double ChB and HaB interactions coexist. Hydrogen atoms were omitted for clarity [245].

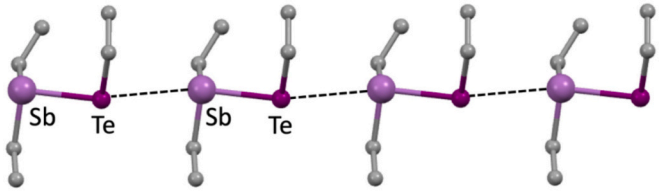

Fig. 19. Sb···Te metalloid···metalloid ChB interactions in the crystal structure of Et_2Sb–TeEt [294] (Et = C_2H_5) investigated at DFT level. Hydrogen atoms were omitted for clarity [293].

intermolecular interactions. Moreover, recent reports highlight the possibility of employing ChBs, including $[Ch\cdots N]_2$ interactions, in the construction of metal-organic frameworks (MOFs) based on 5-(benzo[*c*][1,2,5]selenadiazole-5-carboxamido)isophtalic acid [304] and coordination polymers based on 3,4-dicyano-1,2,5-telluradiazole and *N,N,N′,N′*-tetramethyl-ethane-1,2-diamine [305]; these interactions were studied at the DFT level on simplified models.

Based on a CSD research, $[Ch\cdots N]_2$ hexagonal motifs in the dimers of chalcogenazolo-pyridine and triazolo-chalcogenadiazole derivatives (Scheme 53) were examined in addition to the $[Ch\cdots N]_2$ square motifs in 2,1,3-benzochalcogenadiazole and 2,1,3-pyridocalcogenadiazole dimers (Ch = S, Se, Te) [306]. Electrostatic energy was found to be the main contribution to the attractive interactions, followed by the orbital term, which becomes particularly prominent (about 38%) for Ch = Te, supporting a partial covalent character of the $[Te\cdots N]_2$ interactions. Substituent effects were also investigated, showing electron-withdrawing substituents NO_2, CN, or CF_3 and C_6F_5 or CF_3 groups enhance the strength of the square and hexagonal motifs, respectively. A two-parameter model correlating the binding energies with the maximum positive/negative potentials in the MEP could also be established.

It is worth noting that a suitable combination of this type of $[Ch\cdots N]_2$ intermolecular interactions could also be exploited to prepare water-stable supramolecular capsules (Scheme 54), based on cavitands containing terminal 2,1,3-benzochalcogenadiazoles [307,308].

Interestingly, a series of cocrystals between 4′-substituted derivatives of ebselen and various 4-amino-substituted pyridines were prepared and evaluated for the covalency of their Se···N ChB interactions. An empirical "covalency quotient" was proposed as the negative slope of the plot correlating the Se–N bond length in ebselen with the ChB distance. The validity of this model was confirmed through SAPT and QTAIM calculations on model systems [309].

4.1.3. Chalcogen-halogen interactions

As mentioned above, ChB donors have been investigated for halide sensing and recognition.

Recent studies on Se···I interactions between bis-4-imidazoline-2-selone derivatives and I^- (Fig. 21) were conducted on model systems at the mPW1PW [310]/LanL08(d) [311] level, within the framework of the two potentially opposing models: a MO-mixing approach and the noncovalent σ-hole interpretation. Calculations showed that the two models converge to the same conclusions, with the σ-holes on Se being topologically related to the direction of the antibonding C–Se natural orbitals [312].

Ch···X interactions (Ch = Se, Te; X = Cl, Br, I) between various 1,2,5-chalcogenadiazoles and halides were instead investigated based on the crystal structures of $[\mathbf{L^4}\cdots X]^-C^+$ systems ($\mathbf{L^4}$ = 5,6-dicyano[1,2,5]selenadiazolo[3,4-*b*]pyrazine; $C^+ = Ph_4P^+$, $[K(18\text{-crown-}6)]^+$; Fig. 22), showing that the orbital contribution dominates in the Te···X bonding energy, while electrostatics and dispersion dominates in the Se···X interactions [313].

The cation-anion S···X (X = Cl, I) interactions between the $[Mo_3S_7(Et_2dtc)_3]^+$ cluster (Et_2dtc = diethylthiocarbamate) and halides were studied (along with the corresponding S···O interactions in the salts with ClO_4^- and SO_4^{2-}) based on a series of crystal structures (Fig. 23) [314,315], for which interaction energies as large as 389 kJ mol^{-1} were

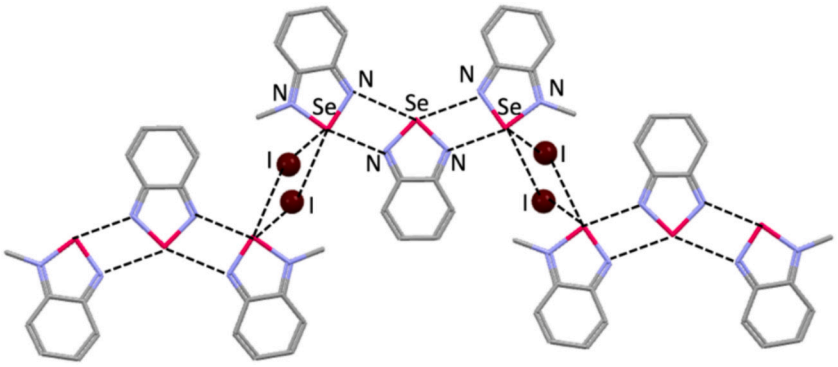

Fig. 20. Pattern of Se···N ChB interactions and Se···I^- anion binding in the crystal structure of $(C_6H_4N_2Se)[C_6H_4N(NCH_3)Se]_2[I]_2$. Hydrogen atoms were omitted for clarity [295].

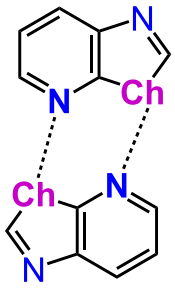

Scheme 53. Schematic representation of $[Ch\cdots N]_2$ hexagonal motifs in the dimers of chalcogenazolo-pyridine derivatives [306].

calculated, demonstrating the ability of these clusters to act as effective anion receptors [316].

Cation-anion interactions were also studied in the crystal structure of Appel's salt, consisting of chloride anions and planar 4,5-dichloro-1,2,3-dithiazolium cations $C_2Cl_2NS_2^+$. This salt was used as a model system for investigating chemical bonding through an approach based on electrostatic and kinetic force density fields. A conclusion of this study was that the three-center $Cl^-\cdots S$–S ChB interaction in the crystal structure of Appel's salt resembles the initial state of bimolecular nucleophilic substitution reactions [317].

As for ChB acceptors other than halides, an example is provided by the supramolecular self-assembled architectures recently reported for 4-(4-chlorophenyl)-3-[(4-fluorobenzyl)sulfanyl]-5-(thiophen-2-yl)-4H-1,2,4-triazole, a selective cyclooxygenase 2 (COX-2) inhibitor: the EPM revealed σ-holes on Cl, F, and S atoms. Thus, the supramolecular self-assembly is mediated by HBs, an uncommon C–S···Cl ChB, and S···C (π) and F···C(π) contacts (Fig. 24) [318].

A recent study highlighted the synergistic interplay between HaBs and ChBs in the crystal packing of the dihalogen adducts of 2,5-bis(pyridine-2-yl)tellurophene, which were investigated at the mPW1PW/Def2-SVP/LANL08(d) level [319,320]. Interestingly, Te···Cl intermolecular interactions between the anions in the crystal structure of $C_5H_5NBr^+[Te(C_6H_5)Cl_4]^-$ (Fig. 25) prompted a theoretical study of these anion···anion interactions in a series of model dimers of $[Ch(C_6H_5)X_4]^-$ species (Ch = S, Se, Te; X = Cl, Br, I) [321]. The study showed that the anions can interact with each other despite the strong Coulomb repulsion. In particular, while the optimized dimers represent metastable systems in the gas phase, the interaction energies become exothermic in aqueous solution (especially for larger halogen atoms), mostly due to an increase in the polarization term [321].

Based on a crystal structure featuring mesityltelluride (MesTe), the different interactions between Te and I in the $[MesTe(I)(I_2)(I_3)]^-$ anion were investigated by means of ELF, NBO, EDA, QTAIM, and other methods, revealing the presence of a more covalent bond with the iodide ligand, a HaB with I_2 and a ChB with triiodide [322].

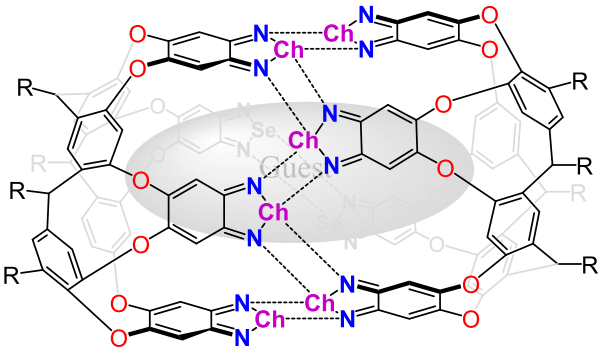

Scheme 54. Schematic representation of the capsules formed through N···Ch ChB interactions between terminal 2,1,3-benzochalcogenadiazole molecules [307,308].

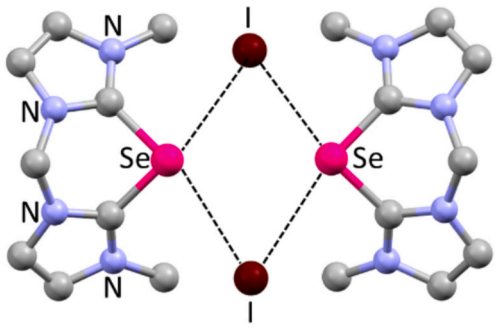

Fig. 21. Portion of the crystal packing of the salt formed by the cyclization product of a bis-4-imidazoline-2-selone derivative and iodide, showing the Se···I ChB interactions. Hydrogen atoms were omitted for clarity [312].

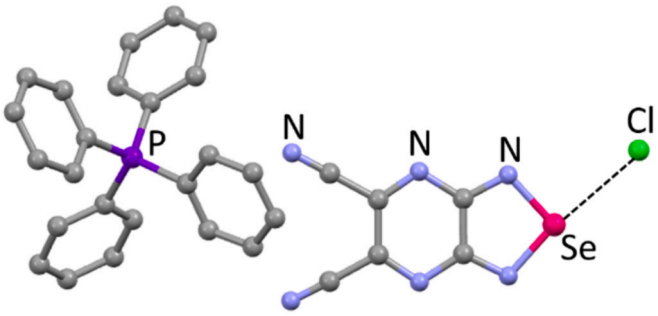

Fig. 22. Portion of the crystal packing of $[\mathbf{L^4}\cdots Cl]Ph_4P$ ($\mathbf{L^4}$ = 5,6-dicyano [1,2,5]selenadiazolo[3,4-*b*]pyrazine) showing the Se···Cl interaction between the ligand and chloride anion. Hydrogen atoms were omitted for clarity [313].

Also in the case of intermolecular Ch···X interactions, few crystal structures involving coordination compounds were investigated. Examples include the S···X interactions (X = Cl, Br, I) in a series of Hg^{II} coordination polymers, where they connect neighboring chains, and were calculated to be relatively weak (–16.3/–19.7 kJ mol^{-1}, the larger energies computed for X = Cl) in model systems [323]. Another example is the weak S···Cl interactions (4–8 kJ mol^{-1}) in the crystal packing of *trans*-$[PtCl_2(RSCN)_2]$ complexes, (R = Et, ^{n}Pr) [324]. Moreover, the enhancement in the ability of Ch atoms to establish ChB interactions upon metal coordination was confirmed for different selenated ligands and tellurium analogues [325,326]. S···F intermolecular interactions were found in the crystal structures of different iron(II) clathrochelates and investigated at the PBE-D3/def2-TZVP level [327].

4.1.4. Other types of interactions

Ch···π ChB interactions were also investigated in few cases. One example is the interaction between selenium and the aromatic rings in a

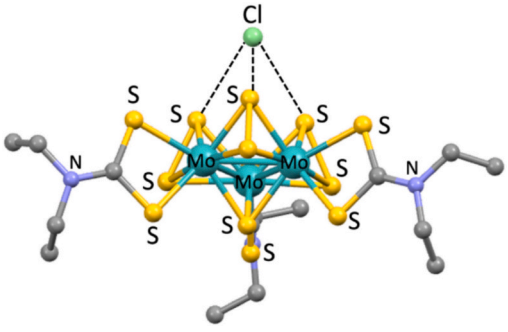

Fig. 23. Portion of the crystal packing of $[Mo_3S_7(Et_2dtc)_3]Cl$, showing the S···Cl interactions between the cluster and chloride anion. Hydrogen atoms were omitted for clarity [315,316].

series of benzylic-substituted 1,2,4-selenodiazolium salts (Fig. 26) [328]. An investigation at the PBE0-D3/def2-TZVP level showed that these Se···π interactions are stronger than the concurrent $[Se\cdots N]_2$ ones, due to the participation of a more positive σ-hole of Se and the existence of a repulsive N···N interaction in the $[Se\cdots N]_2$ motif.

Similarly, in the crystal structure of 12-Ph-*closo*-1-$SB_{11}H_{10}$ [83,329] and its derivatives, S···π ChB interactions, responsible in some cases for the formation of noncovalent organic frameworks (COFs) [329], were calculated to be stronger than the S···X ChBs (X = Cl, I) found in the halogenated analogues [83]. Bifurcated Ch···π ChB interactions were instead studied in the crystal structures of diphenylselenide and telluride, where the chalcogen atom engages in two simultaneous interactions with the phenyl rings of an adjacent molecule. The total stabilization from dispersion was found to dominate compared to the electrostatics and charge transfer contributions, and the interaction energy was calculated to be about –15 kJ mol^{-1} for both systems [330].

Few cases of Ch···C interactions were also considered. An example is the Te···C intermolecular interactions found, along with Te···N ChBs, in the crystal structures of two cyanidoaurate telluronium salts (Fig. 27), where the tellurium atom forms three charge-assisted ChBs with the adjacent anions; electrostatic and CT effects were found to be preeminent [331]. Another recent related report investigated the Te···C interactions in the cocrystals between chalcolanes and different isocyanides, finding interaction energies between –27 and –40 kJ mol^{-1} at the PBE0-D4/def2-TZVP level [332].

On the other hand, intermolecular M···Ch (M = Pd, Pt; Ch = Se, Te) ChB interactions were observed in some coordination compounds. An example is provided by a series of cocrystals between Pt^{II} complexes and ChB donors $(4\text{-}NC_5F_4)_2Ch$ (Ch = Se, Te), showing the presence of Pt···Ch interactions, which in some cases were proven to be retained in solution based on ^{195}Pt and ^{125}Te NMR titrations. Calculations at the PBE0-D3BJ level on different model systems, performed through QTAIM, ELF, independent gradient model based on Hirshfeld partition (IGMH) [333], atomic dipole moment corrected Hirshfeld population (ADCH) [334], and NOCV analyses, confirmed these interactions as ChBs involving a π-hole at the Ch atom, with an estimated interaction energy between –29.2 and –50.2 kJ mol^{-1} [335]. This investigation was recently extended by the same authors to different Pt^{II} complexes [336,337] and to chalcogenadiazole donors (ChDAs; Ch = Se, Te; Fig. 28) [338]. The donation from 5*d* atomic orbitals on Pt to the antibonding π* orbital on the Ch atom comprises more than 50% of the total orbital interaction energy, with the remaining contributions deriving from Ch → Pt back-donation and the π component of the Pt → Ch donation. The principal component of the attractive part of the Pt···Ch interactions comes from dispersion and electrostatic terms, while induction plays a secondary role.

Finally, intramolecular Si–H···Se interactions were studied in a series of silanes [339] (Fig. 29), where QTAIM, NCI, and NBO calculations described them as weak chalcogen bonds or hydride bonds (also called inverse hydrogen bonds and previously investigated theoretically by Li and coworkers) [340], rather than agostic bonds, and revealed only a small contribution of charge transfer mixing [341].

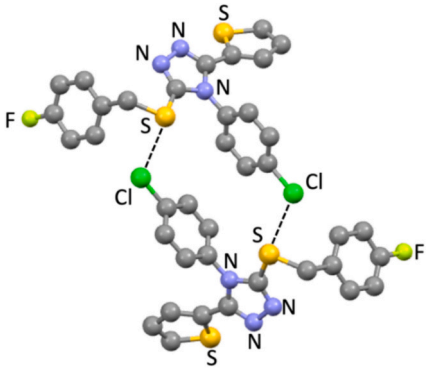

Fig. 24. Portion of the crystal packing of 4-(4-chlorophenyl)-3-[(4-fluorobenzyl)sulfanyl]-5-(thiophen-2-yl)-4H-1,2,4-triazole, showing the intermolecular C–S···Cl ChB interactions. Hydrogen atoms were omitted for clarity [318].

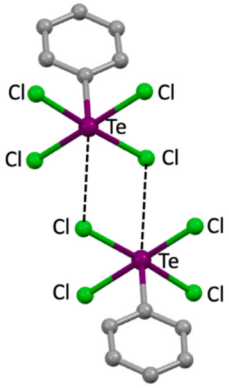

Fig. 25. Te···Cl interactions between the anions in the crystal structure of $C_5H_5NBr^+[Te(C_6H_5)Cl_4]^-$, used as a starting point for calculations on $[Ch(C_6H_5)X_4]^-$ dimers (Ch = S, Se, Te; X = Cl, Br, I). Hydrogen atoms were omitted for clarity [321].

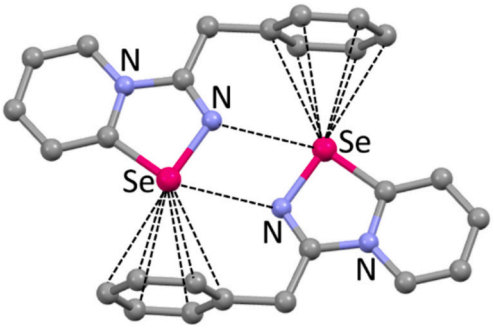

Fig. 26. Dimers in the crystal structure of the $AuCl_4^-$ salt of benzyl-1,2,4-selenodiazolium, showing both the Se···π and $[Ch\cdots N]_2$ interactions. Anions and hydrogen atoms were omitted for clarity [328].

4.2. *ChB and spectroscopy, optical properties, and sensing*

In addition to investigating the nature of ChB interactions in either discrete molecules or extended frameworks, theoretical calculations have been applied to interpret and/or predict IR and NMR spectroscopic features of bonded systems. Vibrational data for a very large (100) set of different model adducts were calculated by Kraka and coworkers with ωB97X/aug-cc-pVTZ in their analysis on ChB (Scheme 3) [3]. More specifically, in the case of the adducts formed by the interaction of HChF (Ch = S, Se, Te) ChB donors with *N*-methylacetamide, specific changes (stretching vibration frequencies and band intensification) were calculated in the IR bands attributed to H–F and F–Ch stretching vibrations in the ChB donor and the C=O in the ChB acceptor. A related study on $FHCh\cdots NH_3$ adducts (Ch = S, Se, Te) and related halogen-, pnicogen-, and tetrel-bonded systems showed in all cases a red shift in the stretching frequency of the Ch–F bond, with the magnitude being larger for second-row elements and following the order halogen > chalcogen > tetrel > pnicogen; the shielding of the σ-hole atom is increased, and those of F and N decreased, with third-row atoms undergoing the largest change [342]. Two recent reports by the same authors extended this approach to Lewis bases $(CH_3)_3PSe$ and $(CH_3)_2C{=}O$ and their interaction to different Lewis acids, including ChB donors, finding a good correlation between interaction energies, red-shift of the P=Se or C=O bond,

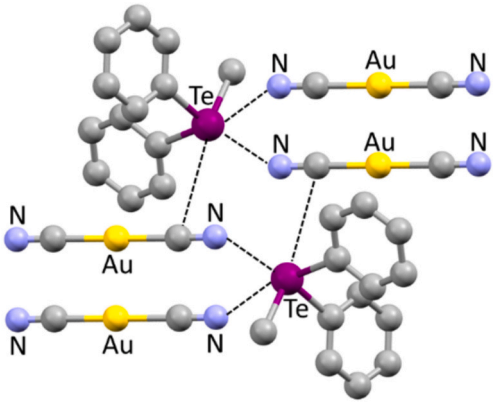

Fig. 27. Portion of the crystal packing of $[(CH_3)(Ph)_2Te][Au(CN)_2]$, showing the intermolecular Te···C and Te···N ChB interactions. Hydrogen atoms were omitted for clarity [331].

and NMR coupling constants [343,344]. Yet another paper on the adducts between HChF (Ch = S, Se, Te) and a wide range of bases showed a very good linear correlation between the interaction energies and both the red shift of the F–Ch stretching band (suggesting a shift of about 10 cm^{-1} for a rise in bond strength of about 8.0 kJ mol^{-1}) and the increase in shielding of the Ch NMR signal [345]. On the other hand, FT-IR matrix isolation spectroscopy was employed to study the complexes of SO_3 with NH_3 in NH_3/SO_3/Ar matrixes; DFT calculations allowed for the assignment of a first group of bands to the 1:1 $O_3S\cdots NH_3$ complex, while a second group of bands was assigned to the 1:2 complex $SO_3\cdots(NH_3)_2$, where the two ammonia molecules coordinate SO_3 on opposite sides with different strength (Scheme 55) [346].

In the case of the interaction between 2,2,4,4-tetrafluoro-1,3-dithietane ($C_2F_4S_2$) and dimethylether (DME; Scheme 56), a theoretical investigation supported by vibrational FT-IR and Raman measurements in liquid-krypton solutions agreed in evaluating the stability of the 1:1 complex, held by ChB F–S···O interactions (Scheme 56; $\Delta H = -13.5(1)$ kJ mol^{-1}). A Ziegler-Rauk EDA pointed to a predominant electrostatic nature of the interaction, which is nevertheless accompanied by a significant CT from the oxygen atom of DME to one of the sulfur atoms of $C_2F_4S_2$ [347]. This type of study was further extended to other Lewis bases, such as water [348] and CH_2F_2 [349].

An approach combining computed vibrational corrections with experimentally determined rotational constants of different isotopologues allowed for the structural characterization of the DMS-SO_2 complex (DMS = dimethylsulfide), revealing that it is held together by S···O ChB interactions where the electrostatic contribution plays a dominant role. A combination of NOCV/CD and NBO analyses indicated a donation from the sulphur atom of DMS to that of SO_2 [350].

A study on the ChB interactions between CS_2 and halides Cl^-, Br^-, and I^- was also performed through a combination of CCSD(T) calculations and anion photoelectron spectroscopy, revealing a $S\cdots Cl^- < S\cdots Br^- < S\cdots I^-$ trend in the strength of the ChB interaction [351].

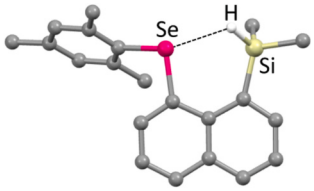

Fig. 29. Crystal structure of 1-mesitylselanyl-8-(dimethylsilyl)naphthalene, showing the intermolecular Si–H···Se chalcogen-hydride bond. Only the hydrogen atom involved in the interaction is shown for clarity [341].

On the other hand, a recent study employed DFT calculations to assist in the interpretation of solid-state ^{77}Se and ^{125}Te NMR studies performed on a series of adducts between diacyanoselena- and -telluradiazole and ChB acceptors such as halides and nitrogen bases, allowing the assignment of the different NMR peaks to the various chalcogen sites observed in the crystal structures [352]. In a recent paper, ^{125}Te magic-angle spinning solid-state NMR measurements were performed on $[K(18\text{-crown-}6)]^+$ 3,4-dicyano-1,2,5-telluradiazole-ChCN$^-$ (Ch = O, S, Se) salt cocrystals featuring Te···N/S/Se ChBs, and experimental tellurium chemical shift tensors were compared with those calculated by different computational approaches, highlighting the importance of spin-orbit relativistic effects [353]. More recent contributions include an investigation on the ability of telluronium salts to act as Lewis acids towards $OPPh_3$ through a combination of DFT and *ab initio* calculations and diffusion-ordered NMR spectroscopy [354], and a study on the role of ChB for the stabilization of the transition state in molecular rotors based on dynamic NMR and DFT calculations [355].

Passing to studies on the UV-Vis absorption and emission properties of Ch-bonded systems, the intramolecular O···S ChB interactions observed in a series of bithiazoles *N*-oxides (Scheme 57) were investigated at the B3LYP/6-311++g(d,p) level, and TD-DFT calculations were employed in order to account for the bathochromic shift in the experimental absorption and emission maxima compared to the non-oxidized, ChB-lacking analogues [356].

TD-DFT calculations were also employed to interpret the experimental changes (red-shift of absorption) observed in the UV-Vis

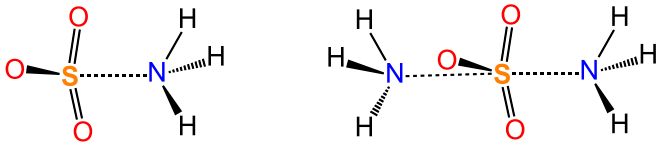

Scheme 55. $O_3S\cdots NH_3$ and $SO_3\cdots(NH_3)_2$ complexes investigated by FT-IR matrix isolation spectroscopy and DFT calculations [346].

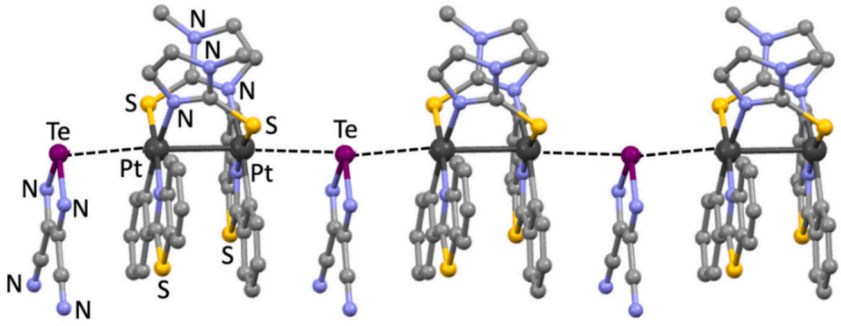

Fig. 28. Portion of the crystal packing of $[Pt_2(Pbt)_2(\mu_2\text{-}S,N\text{-Metim})_2]\cdot 3TeDA\cdot THF$ (PbtH = 2-phenylbenxothiazole; TeDA = 1,2,5-telluradiazole-3,4-dicarbonitrile; MetimH = 1-methyl-1*H*-imidazole-2-thiol), showing the intermolecular Te···Pt^{II} ChB interactions. Solvent molecules and hydrogen atoms were omitted for clarity [338].

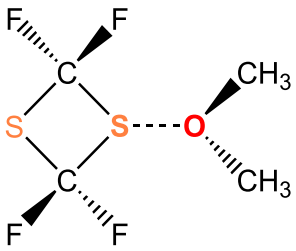

Scheme 56. ChB interaction modelled for the adduct between $C_2F_4S_2$ and dimethylether [347].

absorptions spectra of a series of benzotelluradiazoles upon complexation with different anions (Cl^-, Br^-, I^-, NO_3^-) and the neutral acceptor quinuclidine in various solvents [357]. A series of donor-π-acceptor merocyanine molecules featuring intramolecular Ch···O ChBs, with applications in photon-to-current conversion optoelectronic devices, were observed to have narrower absorption spectral widths and higher absorption coefficients than the corresponding halogen-bonded systems. These properties were rationalized by means of DFT calculations based on the difference in the dipole moment ($\Delta\mu$) between the ground and first excited states and resonance parameter c^2 [358]. The photoswitchable properties of the reduced and oxidized forms of an azobenzene containing an intramolecular N···Te ChB interaction were compared experimentally. While the oxidized form was found to undergo a *trans/cis* isomerization upon irradiation, the reduced form was not photoswitchable (Scheme 58). This behavior was attributed by DFT calculations to the higher strength of the intramolecular N···Te ChB in the reduced form, given the necessity to brake and reform this interaction during the photoisomerization process. In contrast, the reduced forms of the O, S, and Se analogues can undergo the photoswitching due to the lower strength of the corresponding N···Ch intermolecular ChBs [359]. A more recent manuscript from the same authors studied at the PBE0-D3/def2-TZVP level the ground (S_0) and excited state (S_1) in a series of model systems, including chalcogen-containing azobenzenes, by using SMD [360] as a solvation model. The authors concluded that the ChB present in these systems in S_0 convert to covalent bond in S_1, thus influencing the switching behavior of azobenzens [361].

Moving on to examples involving fluorescent sensors, the study of two different fluorophores bearing benzothiazole and benzoselenazole groups, respectively, demonstrated that the latter behave as more sensitive fluorescence sensors for the detection of trimethylarsine vapor. Computational analyses revealed that this enhanced sensitivity is due to the formation of a stronger As···Se ChB compared to the As···S interactions of the sulphured analogues [362].

DFT calculations provided insight into the differing behavior of two tripodal sensors for halide anions based on selenophene (Scheme 59). The hydrogen-substituted sensor binds the halide through trifurcated HBs, resulting in the formation of 1:1 complexes. In contrast, the fluorine-substituted receptor forms 1D polymers, due to the simultaneous establishment of Se···X^- ChBs and CH···X^- HBs. This is enabled by the activation of the σ-holes on the Se atom, induced by the electron-withdrawing fluorine substituents [363].

Beer and coworkers synthesized a 3,5-bis-triazole pyridine scaffold covalently linked to benzo-15-crown-5 ether moieties [364,365]. The remaining position on the triazoles was substituted with hydrogen, iodine or tellurium, to investigate anion binding through the formation of HB, HaB, or ChB interactions, respectively (Scheme 60) [364,365]. It was found that in all cases the interaction was scarse (anion association constants $K_a < 50\ M^{-1}$), or even null in the case of tellurium. However, after the addition of $NaPF_6$ in solution, K_a exceeded 350, 5000 and 1000 M^{-1}, for the hydrogen-, iodine- and tellurium-substituted systems, respectively. First, the binding of the sodium cation by each crown ether moiety strengthens the interaction due to the electrostatic interaction between the anion and the resulting dicationic species. Beyond this, DFT calculations demonstrated that molecular electrostatic potential (MEP) at the the σ-hole on tellurium becomes significantly more positive upon complexation. This enhances the polarization of the iodine and chalcogen atoms, thereby strengthening the ChB [364]. Recently, this study was extended to an analogue system featuring a nitro-benzene backbone featuring 3,5-bis-telluro-triazole perfluorophenyl or phenyl ChB donors, each Te atom being covalently bonded to a benzo-15-crown-5 ether, which proved selective towards KCl [365]; and to a series of mechanically interlocked[2]rotaxane molecules which are capable of acting as either multidentate Lewis acids or bases for the selective binding of halides or metal ions [366].

A combination of DFT and MD calculations was also adopted to rationalize the halide recognition properties of selenated cationic chalcogen-bonding macrocycles and rotaxanes [367]. The calculations elucidated the higher affinity of the receptors for larger halides in terms of a greater degree of covalency in the Ch···X^- interactions, as well as a lower degree of hydration of the anion binding site.

The importance of synergic ChB and PnB interactions in controlling supramolecular chirality in a series of assemblies between phosphonium-selenium conjugates and π-conjugated aminoacids was also investigated through DFT calculations [368].

Finally, the first demonstration of on-surface molecular recognition solely governed by ChBs was recently reported for a series of chalcogenazolo pyridine systems self-assembling on the Au(1 1 1) surface, based on scanning tunnel microscopy and *ab initio* calculations [369].

4.3. ChB in catalysis and reactivity

The typical directionality and hydrophobic nature of ChB interactions make them particularly well-suited for homogeneous catalysis in apolar solvents [103,370,371]. Despite their numerous applications in this field, the theoretical analyses of ChB catalysts are relatively recent, and only a limited number of studies have investigated the nature of these interactions from a computational perspective. A survey of the few initial results obtained in this field was included in a 2021 review by Frontera and Bauzá [372].

In most cases, the ChB donor ability of the investigated compounds is studied in model adducts, especially with the Cl^- anion [103,212,219,373]. Most catalysts feature two ChB donor sites capable

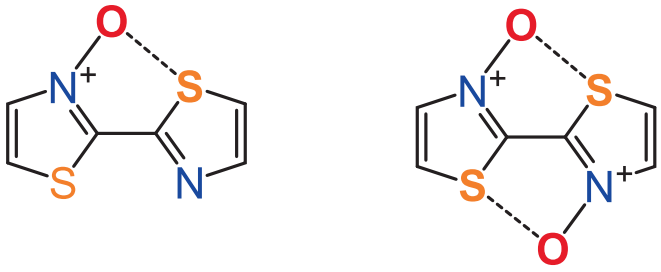

Scheme 57. Bithiazoles *N*-oxides featuring intramolecular O···S ChB interactions whose experimental absorption and emission properties were rationalized by means of TD-DFT calculations [356].

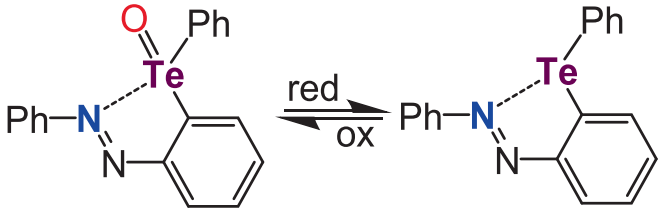

Scheme 58. Reduced and oxidized forms of a monosubstituted azobenzene, whose different photoswitching capabilities are due to the different strength of the intermolecular N···Te ChB [359].

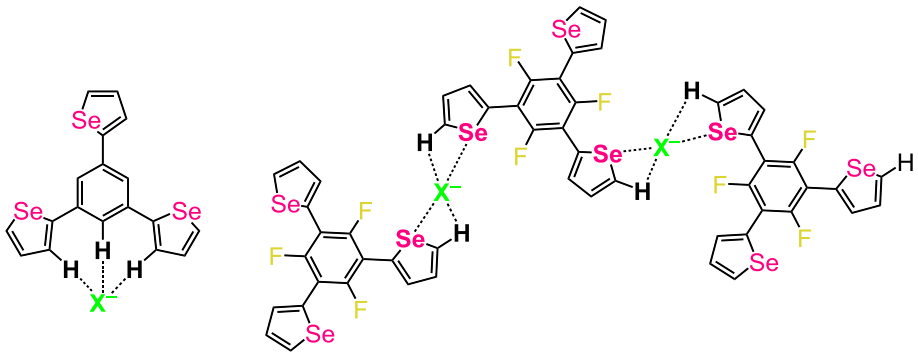

Scheme 59. 1:1 Halogen-bonded complex (left) and 1D polymers formed through a combination of ChB and HB interactions (right) through the anion recognition (X = Cl, Br) by two differently substituted tripodal sensors based on selenophene [363].

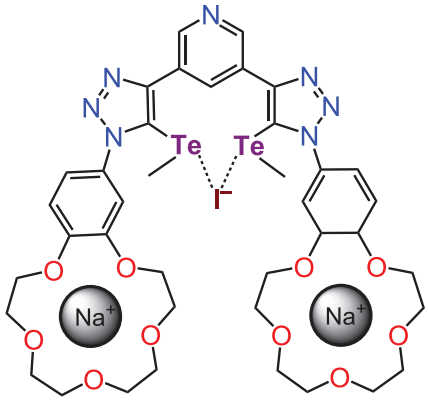

Scheme 60. Experimentally tested heteroditopic ion-pair receptors acting through the coordination of the cation by the macrocycles and a bidentate ChB between tellurium and the halide [364].

of simultaneously interacting with the substrates. Matile and coworkers reported [103] the catalytic activity of dithieno[3,2-*b*;2′,3′-*d*]thiophene (DDTs) derivatives, previously investigated for anion transport applications (E_{int} towards Cl^- up to –145 kJ mol^{-1}) [367], in the transfer hydrogenation of 2,3,6-substituted quinolines and diphenylmethanimine. Their work was supported by M06-2X/6-311G** optimization of the adduct formed by cyano-substituted DDT with formaldehyde and pyridine, yielding interaction energies (E_{int}) of –24.3 and –33.9 kJ mol^{-1}, respectively. This approach was also adopted to investigate benzo[1,2-*d*:4,3-*d*′]di([1,3]selenazole) (BDS) derivatives. Their rational design by DFT calculations enabled the identification of an optimal geometry for directional, noncovalent chloride binding (E_{int} values ranging from –109 to –222 kJ mol^{-1}, depending on the substituents) and ChB-based catalysts (Scheme 42a) [103].

The first application of selenium-based ChB in organocatalysis was reported by Huber and coworkers, who investigated the activation of C–Cl bonds of 1-chloroisochroman through a benchmark reaction with a series of cationic, bifunctional organoselenium compounds (N-alkyl-substituted 1,3-bis[2(3H)-alkylseleno-benzoimidazolium]benzene) [219]. Also in this case, the chloride 1:1 adduct was adopted as a model of ChB for QM calculations (Scheme 42d), carried out at the DFT level (M06-2X/TZVPP). Related dicationic Te-based compounds (4,4′-(1,3-phenylene)bis[5-(tellanyl)-1H-1,2,3-triazole]), which were experimentally investigated as Cl^- transporters [87], were found to be effective catalysts for the activation of C–C bonds in nitro-Michael reactions [374]: DFT calculations, including solvation methods, enabled a detailed mechanistic and kinetic analysis (Scheme 61) [375]. The same type of catalyst was also investigated for the activation of imines in Povarov [4+2] cycloaddition reactions, and the relevant intermediates and transition states were optimized at the DFT level, confirming the presence of Ch···N ChB interactions with the imine [376].

The activation mechanism of the substrate underlying the Ritter-like reaction of halogenated diphenylmethanes with diaryltelluronium cations as catalysts was investigated. The study revealed the formation of an adduct featuring Te···Br ChBs, in combination with HB and cation···π interactions, all playing a synergic role in the activation of the C–X bond (X = Cl, Br) [377]. Based on previous experimental work, a theoretical study was also conducted to investigate the role of ChB donor catalysts $Ch(R)_2$ and $CH_3Ch(R)_2^+$ (Ch = Se, Te; R = F, C_6F_5) in the intramolecular Rauhut-Currier (RC) reaction of bis(enones) [378]. Two mechanistic pathways were explored: one in which the catalyst acts on the thioalcohol anion promoter, and another in which it acts directly on the substrate through the formation of two Ch···O ChBs (Scheme 62 for R = F). The latter pathway was found to have a lower energy barrier. Moreover, it was shown that the σ-hole regions of the catalyst interact with the oxygen atoms, enhancing their polarization and thereby facilitating electron transfer processes in their vicinity [378].

The role of Ch···π ChBs was investigated in the hydrofunctionalization of alkenes catalyzed by 1,2-oxaselenonium salts [379]. Binding energies of about –36 to –49 kJ mol^{-1} were computed for the styrene-catalyst adducts, and the role of the counteranion was also investigated. This study concluded that ChBs serve as driving force in the activation of the π-system of the substrate through the formation of seleniranium intermediates [379].

The catalytic activity of arylated dibenzochacogenophenium cations in the Groebke-Blackburn-Bienaymè reaction between aldehydes and primary amines was investigated. The study revealed that the equatorial binding mode to the substrate (Scheme 63) is energetically more favorable than the axial one, and it suggested higher catalytic activity for the sulphur-based catalysts compared to their selenium analogoues [380]. A related computational study compared the catalytic performance of various halonium, chalconium, and pnictonium salts in

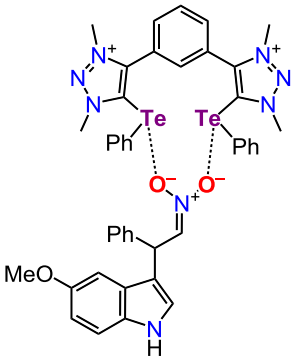

Scheme 61. Model complex between 4,4′-(1,3-phenylene)bis[5-(tellanyl)-1H-1,2,3-triazole] and the nitronate formed from 5-methoxyindole and *trans*-β-nitrostyrene [375].

reactions involving chloride elimination and electrophilic activation of a carbonyl group: among these, HX catalysts exhibited the highest activity, as reflected in the greater electrostatic potential at the σ-hole of the heteroatom compared to ChB and PnB systems [381].

Different halogen, chalcogen, and pnictogen bond donors of general formula C_6F_5Y (Y = Br, I, Se, Te, P, As, Sb) were computationally investigated as catalysts in the Reissert-type substitution of isoquinoline [382]. In this reaction, they form a Y···Cl interaction with the substrate, which weakens the C–Cl bond and activates chloride abstraction. For the ChB donor catalysts, the energy barrier was reduced from approximately 17 to 5–9 kJ mol^{-1}. The computed activity order of the catalysts is Pn > Ch > X, and an increase in catalytic activity was also observed when moving from the third row to the fourth row in the periodic table [382]. The potential of chalcogen bonding interactions for activating aziridines in their cycloaddition to alkenes was explored using various phosphonium selenide-based catalysts. Furthermore, adducts formed between some of these catalysts and 1-(phenylsulfonyl)aziridine were optimized, revealing the presence of cooperative Se···N and Se···O ChB interactions (Scheme 64), whose energy amounts approximately to 100 kJ mol^{-1} [383].

Another study demonstrated the ability of an alkynyl sulphonium salt to act as catalyst in a series of reactions, including transfer hydrogenation, bromination, bromoactonization, nitro-Michael addition reaction, and Ritter reaction. More importantly, the photocapability of ChB was first demonstrated in the synthesis of a variety of chalcogenoacetylenes starting from the same alkynyl sulphonium salt and dichalcogenides. Mechanistic studies on this reactivity confirmed the role of bifurcated S···Ch interactions between the sulphonium salt and the dichalcogenides (Ch = Se, Te; Scheme 65), leading to the subsequent formation of alkynyl radical intermediates [384].

In different publications, the role of intramolecular ChB interactions in the activity of various catalysts was also investigated. As an example, the S···O ChB in enantioselective isochalcogenourea catalysis was studied in a series of works, suggesting a significant orbital contribution for this interaction (Scheme 66) [385–387].

A series of tetravalent spiroselenuranes featuring an intramolecular Se···N chalcogen bond interaction were investigated as catalysts for the disproportionation of H_2O_2 and the activation of I_2 and N-bromosuccinimide (NBS). Mechanistic studies combining experimental measurements and DFT calculations (NBO, QTAIM) revealed that the highly electrophilic nature of Se depends on the presence of the intramolecular ChB [388]. The importance of the S···O intramolecular bond in sulfinylbenzaldehyde compounds for their regioselective monoesterification via chiral carbene-catalyzed oxidation processes was also demonstrated by DFT calculations [389]. Its presence induces a conformational locking effect, with the aldehyde moiety activated by the ChB selectively reacting with alcohols in the presence of the carbene catalyst to afford the corresponding chiral sulfoxide products with good optical purities [389].

Finally, the mechanisms of some reactions were investigated with respect to the potential role of chalcogen bonding. One example is the [3+2] cycloaddition reaction between 2-pyridiylselenyl halides or trifluoroacetates and isocyanates [390]. This reaction follows a concerted mechanism, as confirmed by DFT calculations: the adduct between the

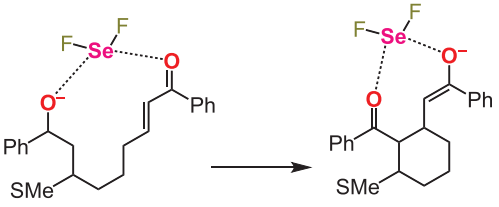

Scheme 62. Part of the reaction mechanism for the intramolecular asymmetric Rauhut-Currier reaction of bis(enones) through the formation of Ch···O ChBs with the SeF_2 catalyst [378].

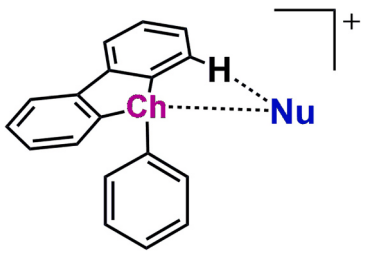

Scheme 63. Arylated dibenzochalcogenophenium cations and equatorial binding to the substrate Nu (Ch = S, Se) [381].

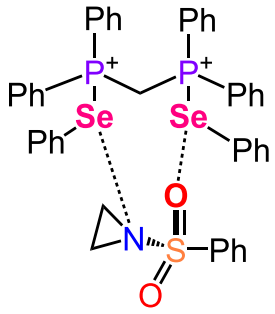

Scheme 64. Adduct between 1-(phenylsulfonyl)aziridine and the phosphonium selenide-based catalysts, showing cooperative Se···N and Se···O ChB interactions [383].

reagents features both a LP···π interaction between the nitrogen atom of the 2-pyridiylselenyl halides and the π system of the isocyanate, as well as a chalcogen bond between the selenium atom of the 2-pyridiylselenyl group and the nitrogen atom of the isocyanate (Scheme 67) [390]. Another example is a recent study on the photoreduction of the DNA nucleoside precursor thioanhydrouridine to 2'-deoxy-thiouridine with the hydrosulfide anion, which was modelled at the DFT level through the study of a chalcogen-bonded complex featuring S···S contacts [391].

5. Future perspectives

5.1.1. *Controversies and prospects*

As illustarted clearly form the literature discussed in this paper, a number of conceptual and methodological approaches has been shaping the research on chalcogen bonding. The main debate concerns the fundamental nature of the ChB interaction itself. While the predominant σ-hole model has traditionally considered ChBs as predominantly non-covalent, electrostatically driven contacts, increasing evidence indicates the limitations of this simplified description. Numerous studies suggest that ChBs frequently possess a non-negligible covalent or charge-transfer character, especially if heavier chalcogen atoms or strongly electron-withdrawing substituents are present. These contributions are reflected in features such as bond orders, bent geometries, and

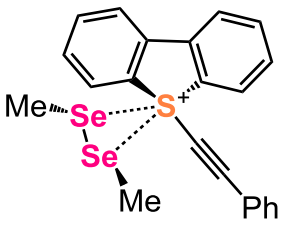

Scheme 65. Reaction intermediate between the alkynyl sulphonium cation and dimethyl diselenide, showing the bifurcated S···Se interactions [384].

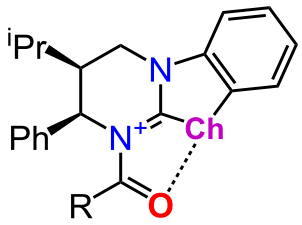

Scheme 66. N-acyl isochalcogenouronium intermediates in enantioselective isochalcogenourea catalysis, featuring intramolecular S···O ChB interactions (Ch = S, Se) [385,386].

substantial LP → σ* donation energies. As a consequence, some authors have questioned the description of ChBs as noncovalent interactions.

Another matter of debate relates to the uncertainty in classifying certain interactions as ChBs, i.e. how weak or heavily polarized a contact may be before it falls outside the domain of σ-hole bonding. These controversies are further complicated by methodological issues. For instance, DFT functionals vary widely in their ability to accurately reproduce ChB energies, and in some cases dispersion corrections exacerbate these errors, while energy decomposition schemes can emphasize or downplay some contributions. QTAIM may identify bond paths even in very weak or ambiguous interactions, whereas NBO analysis can overestimate orbital contributions in highly polarized systems. Consequently, there is still no universal agreement on the most reliable indicators for the classification or quantification of ChB interactions.

These unresolved issues raise several goals for future research, such as establishing clear criteria for quantifying the electrostatic and covalent contributions to ChBs, defining the lower boundary of interaction strength for these interactions, or determining the role of solvation, aggregation, and crystal packing. As experimental and theoretical tools continue to evolve, the study of ChBs will likely converge toward a unified vision, thereby facilitating the broader application of these interactions in supramolecular chemistry, catalysis, materials design, and molecular recognition.

5.1.2. Comparative analysis of research methods

As mentioned throughout this manuscript, a broad range of quantum-chemical methods have been employed to study ChB interactions, each offering specific advantages and limitations in terms of accuracy, computational cost, and suitability for different chemical systems. At the lowest level of theory, Hartree–Fock (HF) calculations provide an inexpensive description of electronic structures but completely neglect electron correlation and dispersion contributions; they remain useful for initial geometry optimizations or exploratory scans on very large systems. Post-Hartree–Fock methods offer higher accuracy but at greater computational expense. Second-order Møller–Plesset perturbation theory (MP2) and its resolution-of-identity variant (RI-MP2) explicitly capture dispersion and generally offer suitable descriptions of ChBs. Nevertheless, MP2 may overestimate binding energies in complexes featuring heavy chalcogens or strong polarization, and it exhibits pronounced basis-set dependence.

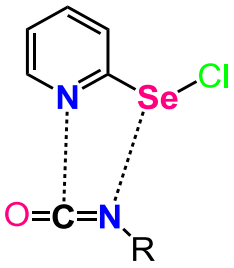

Scheme 67. Adduct between 2-pyridiylselenyl chloride and isocyanates preliminary to their [3+2] cycloaddition reaction, showing the concurrent presence of a LP···π and Se···N ChB interaction [390].

Density Functional Theory (DFT) offers a good compromise between feasibility and predictive power, although its performance is highly dependent on the chosen functional. Traditional and hybrid functionals often under- or over-estimate binding energies due to incorrect treatment of dispersion, while modern functionals such as M06-2X, ωB97M-V, PW6B95-D3(BJ), and carefully selected double-hybrids (e.g., revDSD-PBEP86-D3) provide more reliable geometries and energetics. Notably, several benchmark studies demonstrate that common empirical dispersion corrections (e.g., D3, D3(BJ), D4) can worsen accuracy in σ-hole systems.

Finally, coupled-cluster methods, especially CCSD and CCSD(T), probably represent the best option for accurately describing σ-hole interactions, reliably capturing the balance between electrostatics, induction, charge-transfer, and dispersion; nevertheless, the high computational cost restricts their application to small model systems; they remain a good source of reference data for benchmarking theoretical protocols. For cases involving significant static correlation, multireference methods such as CASSCF/CASPT2 can also be considered.

Beyond energy evaluation, the differences between the different methods in terms of interpretive tools should also be taken into account: MP2 and CCSD(T) provide reliable interaction energies but limited insights into bonding mechanisms, while DFT, being compatible with EDA, SAPT-DFT, NOCV-CD, and QTAIM, is ideal for mechanistic studies.

6. Conclusions

In this review, the widespread adoption of theoretical calculations as an invaluable tool to investigate, interpret, and predict chalcogen bond (ChB) interactions has been explored. While there is a general agreement in including ChB among noncovalent σ-hole interactions, it is indisputable that the subtle balance of various contributions to ChB interactions, such as charge-transfer, electrostatic, and dispersion effects, requires sophisticated calculations to accurately model these aspects.

Over the past two decades, several hundred papers have been published on the theoretical analysis of ChB interactions. Among them, a large number focus on modeling two, three, or even more extended simple interacting model molecules or ions, each featuring one or more ChB interactions involving a chalcogen atom Ch on the ChB-donor and a nucleophile (ChB-acceptor) with a halogen (Ch···X), pnictogen (Ch···Pn), or even a different chalcogen atom (Ch···Ch′). This analysis of model systems, summarized in this review, has provided valuable insights into the most promising computational methods for theoretically studying these systems. Significant efforts have also been made to investigate the competitive and/or cooperative effects between ChB and other non-covalent interactions.

Initially, the theoretical exploration of ChBs relied almost exclusively on post-Hartree-Fock (HF) perturbative methods, such as MP2, or multiconfigurational (CCSD) calculations. However, over the past decade, density functional theory (DFT) has gained increasing prominence, with a notable prevalence of functionals based on the meta-GGA approximation belonging to the Minnesota family, such as M06-2X. DFT calculations using the long-standing B3LYP hybrid functional, while not always providing the highest accuracy, have still frequently been reported.

Regardless of the theoretical approach, computational tools based on quantum theories such as QTAIM, NBO, and energy decomposition methods have been applied in the interpretation of ChB interactions, ultimately showing a continuum spectrum in the nature of the interactions, ranging from almost purely electrostatic to covalent, depending on the nature of the interacting ChB donor group and acceptor atoms, with a remarkable influence of the surrounding chemical environment.

Along with simpler models, QM calculations have also been

employed to study a larger range of specific and more complex compounds, with applications in catalysis, crystallography, spectroscopy, and biochemistry.

This body of research highlights the growing importance of theoretical calculations in interpreting the nature of ChB and related interactions, underscoring the continuing efforts of the computational chemistry community to model noncovalent interactions and shift focus from single molecules to increasingly complex supramolecular aggregates.

Declaration of competing interest

The authors declare the following financial interests/personal relationships which may be considered as potential competing interests: Anna Pintus reports financial support was provided by Sardegna Foundation. If there are other authors, they declare that they have no known competing financial interests or personal relationships that could have appeared to influence the work reported in this paper.

Data availability

No data was used for the research described in the article.

References

[1] C.B. Aakeroy, D.L. Bryce, G.R. Desiraju, A. Frontera, A.C. Legon, F. Nicotra, K. Rissanen, S. Scheiner, G. Terraneo, P. Metrangolo, G. Resnati, Definition of the chalcogen bond (IUPAC Recommendations 2019), Pure Appl. Chem. 91 (2019) 1889–1892, https://doi.org/10.1515/pac-2018-0713.

[2] I. Alkorta, J. Elguero, A. Frontera, Not only hydrogen bonds: other noncovalent interactions, Crystals 10 (2020) 180, https://doi.org/10.3390/cryst10030180.

[3] V. Oliveira, D. Cremer, E. Kraka, The many facets of chalcogen bonding: described by vibrational spectroscopy, J. Phys. Chem. A 121 (2017) 6845–6862, https://doi.org/10.1021/acs.jpca.7b06479.

[4] C.H. Suresh, G.S. Remya, P.K. Anjalikrishna, Molecular electrostatic potential analysis: a powerful tool to interpret and predict chemical reactivity, Wiley Interdiscip. Rev. Comput. Mol. Sci. 12 (2022) e1601, https://doi.org/10.1002/wcms.1601.

[5] P. Politzer, J.S. Murray, P. Lane, σ-Hole bonding and hydrogen bonding: competitive interactions, Int. J. Quantum Chem. 107 (2007) 3046–3052, https://doi.org/10.1002/qua.21419.

[6] P. Politzer, J.S. Murray, T. Clark, G. Resnati, The σ-hole revisited, Phys.Chem. Chem.Phys. 19 (2017) 32166–32174, https://doi.org/10.1039/C7CP06793C.

[7] P. Politzer, J.S. Murray, σ-Hole interactions: perspectives and misconceptions, Crystals 7 (2017) 212, https://doi.org/10.3390/cryst7070212.

[8] P. Politzer, J.S. Murray, M.C. Concha, σ-Hole bonding between like atoms; a fallacy of atomic charges, J. Mol. Model. 14 (2008) 659–665, https://doi.org/10.1007/s00894-008-0280-5.

[9] J.S. Murray, P. Lane, T. Clark, P. Politzer, σ-Hole bonding: molecules containing group VI atoms, J. Mol. Model. 13 (2007) 1033–1038, https://doi.org/10.1007/s00894-007-0225-4.

[10] P. Politzer, J.S. Murray, σ-Holes and π-holes: similarities and differences, J. Comput. Chem. 39 (2018) 464–471, https://doi.org/10.1002/jcc.24891.

[11] J.S. Murray, P. Lane, T. Clark, K.E. Riley, P. Politzer, σ-Holes, π-holes and electrostatically-driven interactions, J. Mol. Model. 18 (2012) 541–548, https://doi.org/10.1007/s00894-011-1089-1.

[12] L. Brammer, A. Peuronen, T.M. Roseveare, Halogen bonds, chalcogen bonds, pnictogen bonds, tetrel bonds and other σ-hole interactions: a snapshot of current progress, Acta Cryst. C 79 (2023) 204–216, https://doi.org/10.1107/s2053229623004072.

[13] N. Biot, D. Bonifazi, Chalcogen-bond driven molecular recognition at work, Coord. Chem. Rev. 413 (2020) 213243, https://doi.org/10.1016/j.ccr.2020.213243.

[14] K.T. Mahmudov, A.V. Gurbanov, V.A. Aliyeva, M.F.C. Guedes da Silva, G. Resnati, A.J.L. Pombeiro, Chalcogen bonding in coordination chemistry, Coord. Chem. Rev. 464 (2022) 214556, https://doi.org/10.1016/j.ccr.2022.214556.

[15] R. Hein, P.D. Beer, Halogen bonding and chalcogen bonding mediated sensing, Chem. Sci. 13 (2022) 7098–7125, https://doi.org/10.1039/d2sc01800d.

[16] E.R.T. Tiekink, Zero-, one-, two- and three-dimensional supramolecular architectures sustained by Se•••O chalcogen bonding: a crystallographic survey, Coord. Chem. Rev. 427 (2021) 213586, https://doi.org/10.1016/j.ccr.2020.213586.

[17] P.C. Ho, J.Z. Wang, F. Meloni, I. Vargas-Baca, Chalcogen bonding in materials chemistry, Coord. Chem. Rev. 422 (2020) 213464, https://doi.org/10.1016/j.ccr.2020.213464.

[18] K.T. Mahmudov, M.N. Kopylovich, M.F.C. Guedes Da Silva, A.J.L. Pombeiro, Chalcogen bonding in synthesis, catalysis and design of materials, Dalton Trans. 46 (2017) 10121–10138, https://doi.org/10.1039/c7dt01685a.

[19] P. Scilabra, G. Terraneo, G. Resnati, The chalcogen bond in crystalline solids: a world parallel to halogen bond, Acc. Chem. Res. 52 (2019) 1313–1324, https://doi.org/10.1021/acs.accounts.9b00037.

[20] M.S. Taylor, Anion recognition based on halogen, chalcogen, pnictogen and tetrel bonding, Coord. Chem. Rev. 413 (2020) 213270, https://doi.org/10.1016/j.ccr.2020.213270.

[21] L. Vogel, P. Wonner, S.M. Huber, Chalcogen bonding: an overview, Angew. Chem. Int. Ed. 58 (2019) 1880–1891, https://doi.org/10.1002/anie.201809432.

[22] S. Scheiner, M. Michalczyk, W. Zierkiewicz, Coordination of anions by noncovalently bonded σ-hole ligands, Coord. Chem. Rev. 405 (2020) 213136, https://doi.org/10.1016/j.ccr.2019.213136.

[23] M. Head-Gordon, J.A. Pople, M.J. Frisch, MP2 energy evaluation by direct methods, Chem. Phys. Lett. 153 (1998) 503–506, https://doi.org/10.1016/0009-2614(88)85250-3.

[24] W. Koch, M.C. Holthausen, A Chemist's Guide to Density Functional Theory, Wiley-VCH N. Y., 2001, https://doi.org/10.1002/3527600043.

[25] S. Sverrisdóttir, F.M. Faulstich, Exploring ground and excited states via single reference coupled-cluster theory and algebraic geometry, J. Chem. Theory Comput. 20 (2024) 8517–8528, https://doi.org/10.1021/acs.jctc.4c00644.

[26] P. E. M. Siegbahn, J. Almlöf, A. Heiberg, B. O. Roos, The complete active space SCF (CASSCF) method in a Newton–Raphson formulation with application to the HNO molecule. J. Chem. Phys. 74 (1981), 2384–2396. doi:https://doi.org/10.1063/1.441359.

[27] M.C. Aragoni, M. Arca, F.A. Devillanova, F. Isaia, V. Lippolis, Adducts of S/Se donors with dihalogens as a source of information for categorizing the halogen bonding, Cryst. Growth Des. 12 (2012) 2769–2779, https://doi.org/10.1021/cg201328y.

[28] F.S.S. Schneider, G.F. Caramori, R.L.T. Parreira, V. Lippolis, M. Arca, G. Ciancaleoni, Bond analysis in dihalogen–halide and dihalogen–dimethylchalcogenide systems, Eur. J. Inorg. Chem. 2018 (2018) 1007–1015, https://doi.org/10.1002/ejic.201701337.

[29] G. Ciancaleoni, M. Arca, G.F. Caramori, G. Frenking, F.S.S. Schneider, V. Lippolis, Bonding analysis in homo- and hetero-trihalide species: a charge displacement study, Eur. J. Inorg. Chem. 2016 (2016) 3804–3812, https://doi.org/10.1002/ejic.201600471.

[30] A. Das, E. Arunan, Unified classification of non-covalent bonds formed by main group elements: a bridge to chemical bonding, Phys. Chem. Chem. Phys. 25 (2023) 22583–22594, https://doi.org/10.1039/d3cp00370a.

[31] P. Politzer, J.S. Murray, Electrostatics and polarization in σ- and π-hole noncovalent interactions: an overview, ChemPhysChem 21 (2020) 579–588, https://doi.org/10.1002/cphc.201900968.

[32] P. Politzer, J.S. Murray, T. Clark, Explicit inclusion of polarizing electric fields in σ- and π-hole interactions, J. Phys. Chem. A 123 (2019) 10123–10130, https://doi.org/10.1021/acs.jpca.9b08750.

[33] P. Politzer, J.S. Murray, T. Clark, The π-hole revisited, Phys. Chem. Chem. Phys. 23 (2021) 16458–16468, https://doi.org/10.1039/d1cp02602j.

[34] L. de Azevedo Santos, S.C.C. van der Lubbe, T.A. Hamlin, T.C. Ramalho, F.A. M. Bickelhaupt, Quantitative molecular orbital perspective of the chalcogen bond, ChemistryOpen 10 (2021) 391–401, https://doi.org/10.1002/open.202000323.

[35] V. Oliveira, E. Kraka, D. Cremer, The intrinsic strength of the halogen bond: electrostatic and covalent contributions described by coupled cluster theory, Phys. Chem. Chem. Phys. 18 (2016) 33031–33046, https://doi.org/10.1039/c6cp06613e.

[36] N. Tarannam, R. Shukla, S. Kozuch, Yet another perspective on hole interactions, Phys. Chem. Chem. Phys. 23 (2021) 19948–19963, https://doi.org/10.1039/d1cp03533a.

[37] L. de Azevedo Santos, T.C. Ramalho, T.A. Hamlin, F.M. Bickelhaupt, Intermolecular covalent interactions: nature and directionality, Chem. Eur. J. 29 (2023) e202203791, https://doi.org/10.1002/chem.202203791.

[38] M. Savastano, Ye Olde supramolecular chemistry, its modern rebranding and overarching trends in chemistry, Dalton Trans. 53 (2024) 1373–1392, https://doi.org/10.1039/d3dt03686c.

[39] R. Taylor, Aerogen bond, halogen bond, chalcogen bond, pnictogen bond, tetrel bond, triel bond ... why so many names? Cryst. Growth Des. 24 (2024) 4003–4012, https://doi.org/10.1021/acs.cgd.4c00303.

[40] A.S. Novikov, Recent progress in theoretical studies and computer modeling of non-covalent interactions, Crystals 13 (2023) 361, https://doi.org/10.3390/cryst13020361.

[41] S. Scheiner, Participation of S and Se in hydrogen and chalcogen bonds, CrystEngComm 23 (2021) 6821–6837, https://doi.org/10.1039/d1ce01046h.

[42] W. Zierkiewicz, M. Michalczyk, S. Scheiner, Noncovalent bonds through sigma and pi-hole located on the same molecule. Guiding principles and comparisons, Molecules 26 (2021) 1740, https://doi.org/10.3390/molecules26061740.

[43] R. Shukla, D. Chopra, Chalcogen and pnictogen bonds: insights and relevance, Curr. Sci. 120 (2021) 1848–1853, https://doi.org/10.18520/cs/v120/i12/1848-1853.

[44] R. Gleiter, G. Haberhauer, D.B. Werz, F. Rominger, C. Bleiholder, From noncovalent chalcogen-chalcogen interactions to supramolecular aggregates: experiments and calculations, Chem. Rev. 118 (2018) 2010–2041, https://doi.org/10.1021/acs.chemrev.7b00449.

[45] H.S. Samuel, E.E. Etim, U. Nweke-Maraizu, Approaches for special characteristics of chalcogen bonding: a mini review, J. Appl. Organomet. Chem. 3 (2023) 199–212, https://doi.org/10.22034/jaoc.2023.405432.1089.

[46] A.C. Legon, Tetrel, pnictogen and chalcogen bonds identified in the gas phase before they had names: a systematic look at non-covalent interactions, Phys.

Chem. Chem. Phys. 19 (2017) 14884–14896, https://doi.org/10.1039/c7cp02518a.
[47] S. Kolb, G.A. Oliver, D.B. Werz, Chemistry evolves, terms evolve, but phenomena do not evolve: from chalcogen–chalcogen interactions to chalcogen bonding, Angew. Chem. Int. Ed. 59 (2020) 22306–22310, https://doi.org/10.1002/anie.202007314.
[48] G.A. DiLabio, A. Otero-de-la-Roza, Noncovalent Interactions in Density Functional Theory, Rev. Comput. Chem. 29 (2016) 1–97, https://doi.org/10.1002/9781119148739.ch1.
[49] S. Kristyán, P. Pulay, Can (semi)local Density Functional Theory account for the London dispersion forces? Chem. Phys. Lett. 229 (1994) 175–180, https://doi.org/10.1016/0009-2614(94)01027-7.
[50] N. Mehta, T. Fellowes, J.M. White, L. Goerigk, CHAL336 benchmark set: how Well do quantum-chemical methods describe chalcogen-bonding interactions? J. Chem. Theory Comput. 17 (2021) 2783–2806, https://doi.org/10.1021/acs.jctc.1c00006.
[51] K. Kříž, J. Řezáč, Non-covalent interactions atlas benchmark data sets 4: σ-hole interactions, Phys. Chem. Chem. Phys. 24 (2022) 14794–14804, https://doi.org/10.1039/d2cp01600a.
[52] Y. Zhao, D.G. Truhlar, The M06 suite of density functionals for main group thermochemistry, thermochemical kinetics, noncovalent interactions, excited states, and transition elements: two new functionals and systematic testing of four M06 functionals and 12 other functionals, Theor. Chem. Account 120 (2008) 215–241, https://doi.org/10.1007/s00214-007-0310-x.
[53] S. Kozuch, J.M.L. Martin, Halogen bonds: benchmarks and theoretical analysis, J. Chem. Theory Comput. 9 (2013) 1918–1931, https://doi.org/10.1021/ct301064t.
[54] A. Bauzá, I. Alkorta, A. Frontera, J. Elguero, On the reliability of pure and hybrid DFT methods for the evaluation of halogen, chalcogen, and pnicogen bonds involving anionic and neutral electron donors, J. Chem. Theory Comput. 9 (2013) 5201–5210, https://doi.org/10.1021/ct400818v.
[55] F. Weigend, M. Haser, H. Patzelt, R. Ahlrichs, RI-MP2: optimized auxiliary basis sets and demonstration of efficiency, Chem. Phys. Lett. 294 (1998) 143–152, https://doi.org/10.1016/s0009-2614(98)00862-8.
[56] C. Adamo, V. Barone, An accurate density functional method for the study of magnetic properties: the PBE0 model, J. Mol. Struct. THEOCHEM 493 (1999) 145–157, https://doi.org/10.1016/s0166-1280(99)00235-3.
[57] S. Grimme, A. Hansen, J.G. Brandenburg, C. Bannwarth, Dispersion-corrected mean-field electronic structure methods, Chem. Rev. 116 (2016) 5105–5154, https://doi.org/10.1021/acs.chemrev.5b00533.
[58] S. Grimme, S. Ehrlich, L. Goerigk, Effect of the damping function in dispersion corrected density functional theory, J. Comput. Chem. 32 (2011) 1456–1465, https://doi.org/10.1002/jcc.21759.
[59] G. Santra, N. Sylvetsky, J.M.L. Martin, Minimally empirical double-hybrid functionals trained against the GMTKN55 database: revDSD-PBEP86-D4, revDOD-PBE-D4, and DOD-SCAN-D4, J. Phys. Chem. A 123 (2019) 5129–5143, https://doi.org/10.1021/acs.jpca.9b03157.
[60] G. Santra, M. Cho, J.M.L. Martin, Exploring avenues beyond revised DSD functionals: I. range separation, with XDSD as a special case, J. Phys. Chem. A 125 (2021) 4614–4627, https://doi.org/10.1021/acs.jpca.1c01294.
[61] N. Mardirossian, M. Head-Gordon, ωB97M-V: a combinatorially optimized, range-separated hybrid, meta-GGA density functional with VV10 nonlocal correlation, J. Chem. Phys. 144 (2016) 214110, https://doi.org/10.1063/1.4952647.
[62] Y. Zhao, D.G. Truhlar, Design of density functionals that are broadly accurate for thermochemistry, thermochemical kinetics, and nonbonded interactions, J. Phys. Chem. A 109 (2005) 5656–5667, https://doi.org/10.1021/jp050536c.
[63] K.J. Daas, D.P. Kooi, N.C. Peters, E. Fabiano, F. Della Sala, P. Gori-Giorgi, S. Vuckovic, Regularized and opposite spin-scaled functionals from Møller-Plesset adiabatic connection–higher accuracy at lower cost, J. Phys. Chem. Lett. 14 (2023) 8448–8459, https://doi.org/10.1021/acs.jpclett.3c01832.
[64] A.V. Vidal, L.C. de Vicente Poutás, O. Nieto Faza, C.S. López, On the use of popular basis sets: impact of the intramolecular basis set superposition error, Molecules 24 (2019) 3810, https://doi.org/10.3390/molecules24203810.
[65] L. de Azevedo Santos, T.C. Ramalho, T.A. Hamlin, F.M. Bickelhaupt, Chalcogen bonds: hierarchical ab initio benchmark and Density Functional Theory performance study, J. Comput. Chem. 42 (2021) 688–698, https://doi.org/10.1002/jcc.26489.
[66] G.A. DiLabio, in: A.O. De La Roza, G.A. Dilabio (Eds.), Atom-centered potentials for noncovalent interactions and other applications in "non-covalent interactions in quantum chemistry and physics", Elsevier, 2017, pp. 221–240, https://doi.org/10.1016/b978-0-12-809835-6.00008-6.
[67] V.K. Prasad, A. Otero-De-La-Roza, G.A. DiLabio, Fast and accurate quantum mechanical modeling of large molecular systems using small basis set Hartree-Fock methods corrected with atom-centered potentials, J. Chem. Theory Comput. 18 (2022) 2208–2232, https://doi.org/10.1021/acs.jctc.1c01128.
[68] V.K. Prasad, A. Otero-De-La-Roza, G.A. DiLabio, Small-basis set Density-Functional Theory methods corrected with atom-centered potentials, J. Chem. Theory Comput. 18 (2022) 2913–2930, https://doi.org/10.1021/acs.jctc.2c00036.
[69] E. Caldeweyher, S. Ehlert, A. Hansen, H. Neugebauer, S. Spicher, C. Bannwarth, S. Grimme, A generally applicable atomic charge dependent London dispersion correction, J. Chem. Phys. 150 (2019) 154122, https://doi.org/10.1063/1.5090222.
[70] Y. Kim, S. Song, E. Sim, K. Burke, Halogen and chalcogen binding dominated by density-driven errors, J. Phys. Chem. Lett. 10 (2019) 295–301, https://doi.org/10.1021/acs.jpclett.8b03745.
[71] M.H. Kolář, P. Hobza, Computer modeling of halogen bonds and other σ-hole interactions, Chem. Rev. 116 (2016) 5155–5187, https://doi.org/10.1021/acs.chemrev.5b00560.
[72] P.V. Bijina, C.H. Suresh, Molecular electrostatic potential analysis of non-covalent complexes, J. Chem. Sci. 128 (2016) 1677–1686, https://doi.org/10.1007/s12039-016-1162-5.
[73] T. Brinck, A.N. Borrfors, Electrostatics and polarization determine the strength of the halogen bond: a red card for charge transfer, J. Mol. Model. 25 (2019) 1–9, https://doi.org/10.1007/s00894-019-4014-7.
[74] P. Politzer, J.S. Murray, T. Clark, Halogen bonding: an electrostatically-driven highly directional noncovalent interaction, Phys. Chem. Chem. Phys. 12 (2010) 7748–7757, https://doi.org/10.1039/c004189k.
[75] C.H. Suresh, S. Anila, Molecular electrostatic potential topology analysis of noncovalent interactions, Acc. Chem. Res. 56 (2023) 1884–1895, https://doi.org/10.1021/acs.accounts.3c00193.
[76] F. Weinhold, "Noncovalent interaction": a chemical misnomer that inhibits proper understanding of hydrogen bonding, rotation barriers, and other topics, Molecules 28 (2023) 3776, https://doi.org/10.3390/molecules28093776.
[77] P. Su, Z. Tang, W. Wu, Generalized Kohn-Sham energy decomposition analysis and its applications, WIREs Comput. Mol. Sci. 10 (2020) e1460, https://doi.org/10.1002/wcms.1460.
[78] K. Patkowski, Recent developments in symmetry-adapted perturbation theory, WIREs Comput. Mol. Sci. 10 (2020) e1452, https://doi.org/10.1002/wcms.1452.
[79] O.A. Stasyuk, R. Sedlak, C.F. Guerra, P. Hobza, Comparison of the DFT-SAPT and canonical EDA schemes for the energy decomposition of various types of noncovalent interactions, J. Chem. Theory Comput. 14 (2018) 3440–3450, https://doi.org/10.1021/acs.jctc.8b00034.
[80] F. De Vleeschouwer, M. Denayer, B. Pinter, P. Geerlings, F. De Proft, Characterization of chalcogen bonding interactions via an in-depth conceptual quantum chemical analysis, J. Comput. Chem. 39 (2018) 557–572, https://doi.org/10.1002/jcc.25099.
[81] C. Bleiholder, R. Gleiter, D.B. Werz, H. Köppel, Theoretical investigations on heteronuclear chalcogen-chalcogen interactions: on the nature of weak bonds between chalcogen centers, Inorg. Chem. 46 (2007) 2249–2260, https://doi.org/10.1021/ic062110y.
[82] W. Zierkiewicz, J. Fanfrlík, P. Hobza, D. Michalska, T. Zeegers-Huyskens, Ab initio and DFT studies of the interaction between carbonyl and thiocarbonyl groups: the role of S···O chalcogen bonds, Theor. Chem. Accounts 135 (2016) 1–11, https://doi.org/10.1007/s00214-016-1972-z.
[83] J. Fanfrlík, A. Přáda, Z. Padělková, A. Pecina, J. Macháček, M. Lepšík, J. Holub, A. Růžička, D. Hnyk, P. Hobza, The dominant role of chalcogen bonding in the crystal packing of 2D/3D aromatics, Angew. Chem. Int. Ed. 53 (2014) 10303–10306, https://doi.org/10.1002/anie.201405901.
[84] D.J. Pascoe, K.B. Ling, S.L. Cockroft, The origin of chalcogen-bonding interactions, J. Am. Chem. Soc. 139 (2017) 15160–15167, https://doi.org/10.1021/jacs.7b08511.
[85] R.F.W. Bader, Atoms in molecules, Acc. Chem. Res. 18 (1985) 9–15.
[86] C.F. Matta, R.J. Boyd (Eds.), The quantum theory of atoms in molecules: from solid state to DNA and drug design, Wiley-VCH, 2007, https://doi.org/10.1002/9783527610709.
[87] L.E. Bickerton, A. Docker, A.J. Sterling, H. Kuhn, F. Duarte, P.D. Beer, M. J. Langton, Highly active halogen bonding and chalcogen bonding chloride transporters with non-protonophoric activity, Chem. Eur. J. 27 (2021) 11738–11745, https://doi.org/10.1002/chem.202101681.
[88] M.D. Esrafili, F. Mohammadian-Sabet, M.A. Solimannejad, Theoretical evidence for mutual influence between S·· ·N(C) and hydrogen/lithium/halogen bonds: competition and interplay between π-hole and σ-hole interactions, Struct. Chem. 25 (2014) 1197–1205, https://doi.org/10.1007/s11224-014-0392-8.
[89] E. Alikhani, F. Fuster, B. Madebene, S.J. Grabowski, Topological reaction sites – very strong chalcogen bonds, Phys. Chem. Chem. Phys. 16 (2014) 2430–2442, https://doi.org/10.1039/c3cp54208d.
[90] L.M. Azofra, S. Scheiner, Substituent effects in the noncovalent bonding of SO_2 to molecules containing a carbonyl group. The dominating role of the chalcogen bond, J. Phys. Chem. A 118 (2014) 3835–3845, https://doi.org/10.1021/jp501932g.
[91] M.D. Esrafili, F. Mohammadian-Sabet, M.M. Baneshi, An ab initio investigation of chalcogen–hydride interactions involving HXeH as a chalcogen bond acceptor, Struct. Chem. 27 (2016) 785–792, https://doi.org/10.1007/s11224-015-0626-4.
[92] A. Bauzá, A. Frontera, Halogen and chalcogen bond energies evaluated using electron density properties, ChemPhysChem 21 (2020) 26–31, https://doi.org/10.1002/cphc.201901001.
[93] G. Ciancaleoni, F. Nunzi, L. Belpassi, Charge displacement analysis – a tool to theoretically characterize the charge transfer contribution of halogen bonds, Molecules 25 (2020) 300, https://doi.org/10.3390/molecules25020300.
[94] G. Ciancaleoni, C. Santi, M. Ragni, A.L. Braga, Charge-displacement analysis as a tool to study chalcogen bonded adducts and predict their association constants in solution, Dalton Trans. 44 (2015) 20168–20175, https://doi.org/10.1039/c5dt03388h.
[95] G. Ciancaleoni, Lewis base activation of Lewis acid: a detailed bond analysis, ACS Omega 3 (2018) 16292–16300, https://doi.org/10.1021/acsomega.8b02243.
[96] M. Mitoraj, A. Michalak, Donor–acceptor properties of ligands from the natural orbitals for chemical valence, Organometallics 26 (2007) 6576–6580, https://doi.org/10.1021/om700754n.
[97] Z. Konkoli, D. Cremer, A new way of analyzing vibrational spectra. I. Derivation of adiabatic internal modes, Int. J. Quantum Chem. 67 (1998) 1–9, https://doi.org/10.1002/(SICI)1097-461X(1998)67:1.

[98] D. Cremer, J.A. Larsson, E. Kraka, New developments in the analysis of vibrational spectra on the use of adiabatic internal vibrational modes, Theor. Comput. Chem. 5 (1998) 259–327, https://doi.org/10.1016/s1380-7323(98)80012-5.

[99] J. Alfuth, B. Zadykowicz, B. Wicher, K. Kazimierczuk, T. Połoński, T. Olszewska, Cooperativity of halogen- and chalcogen-bonding interactions in the self-assembly of 4-iodoethynyl- and 4,7-bis(iodoethynyl)benzo-2,1,3-chalcogenadiazoles: crystal structures, Hirshfeld surface analyses, and crystal lattice energy calculations, Cryst. Growth Des. 22 (2022) 1299–1311, https://doi.org/10.1021/acs.cgd.1c01266.

[100] E. Parisi, A. Carella, F. Borbone, F. Chiarella, F.S. Gentile, R. Centore, Effect of chalcogen bonding on the packing and coordination geometry in hybrid organic–inorganic Cu(II) networks, CrystEngComm 24 (2022) 2884–2890, https://doi.org/10.1039/d2ce00069e.

[101] Y.V. Torubaev, A.S. Samigullina, Long-range supramolecular synthon isomerism: insight from a case study of vinylic tellurium trihalides Cl(Ph)C=C(Ph)TeX$_3$ (X = Cl, I), Chem 4 (2022) 196–205, https://doi.org/10.3390/chemistry4010017/s1.

[102] V. Jurásková, F. Célerse, R. Laplaza, C. Corminboeuf, Assessing the persistence of chalcogen bonds in solution with neural network potentials, J. Chem. Phys. 156 (2022) 154112, https://doi.org/10.1063/5.0085153.

[103] S. Benz, J. Mareda, C. Besnard, N. Sakai, S. Matile, Catalysis with chalcogen bonds: neutral benzodiselenazole scaffolds with high-precision selenium donors of variable strength, Chem. Sci. 8 (2017) 8164–8169, https://doi.org/10.1039/c7sc03866f.

[104] B.R. Beno, K.S. Yeung, M.D. Bartberger, L.D. Pennington, N.A. Meanwell, A survey of the role of noncovalent sulfur interactions in drug design, J. Med. Chem. 58 (2015) 4383–4438, https://doi.org/10.1021/jm501853m.

[105] A. Bauzá, T.J. Mooibroek, A. Frontera, The bright future of unconventional σ/π-hole interactions, ChemPhysChem 16 (2015) 2496–2517, https://doi.org/10.1002/cphc.201500314.

[106] A.J. Mukherjee, S.S. Zade, H.B. Singh, R.B. Sunoj, Organoselenium chemistry: role of intramolecular interactions, Chem. Rev. 110 (2010) 4357–4416, https://doi.org/10.1021/cr900352j.

[107] H. Huang, L. Yang, A. Facchetti, T.J. Marks, Organic and polymeric semiconductors enhanced by noncovalent conformational locks, Chem. Rev. 117 (2017) 10291–10318, https://doi.org/10.1021/acs.chemrev.7b00084.

[108] S. Benz, J. López-Andarias, J. Mareda, N. Sakai, S. Matile, Catalysis with chalcogen bonds, Angew. Chem. Int. Ed. 56 (2017) 812–815, https://doi.org/10.1002/anie.201611019.

[109] P.R. Varadwaj, A. Varadwaj, H.M. Marques, P.J. MacDougall, The chalcogen bond: can it be formed by oxygen? Phys. Chem. Chem. Phys. 21 (2019) 19969–19986, https://doi.org/10.1039/c9cp03783g.

[110] P.R. Varadwaj, Does oxygen feature chalcogen bonding? Molecules 24 (2019) 3166, https://doi.org/10.3390/molecules24173166.

[111] M.A.A. Ibrahim, E.M.Z. Telb, σ-Hole and lone-pair hole interactions in chalcogen-containing complexes: a comparative study, ACS Omega 5 (2020) 21631–21640, https://doi.org/10.1021/acsomega.0c02362.

[112] A.N. Petelski, D.J.R. Duarte, N.M. Peruchena, Nature and strength of weak O···O interactions in nitryl halide dimers, ChemPhysChem 24 (2023) e202200768, https://doi.org/10.1002/cphc.202200768.

[113] T.M. Ismail, D. Patkar, P.K. Sajith, M.M. Deshmukh, Interplay of hydrogen, pnicogen, and chalcogen bonding in X(H$_2$O)$_{n=1-5}$ (X = NO, NO$^+$, and NO$^-$) complexes: energetics insights via a molecular tailoring approach, J. Phys. Chem. A 127 (2023) 10360–10374, https://doi.org/10.1021/acs.jpca.3c04181.

[114] M.J. Janicki, R. Szabla, J. Šponer, R.W. Góra, Photoinduced water–chromophore electron transfer causes formation of guanosine photodamage, Phys. Chem. Chem. Phys. 24 (2022) 8217–8224, https://doi.org/10.1039/d2cp00801g.

[115] M.D. Esrafili, F. Mohammadian-Sabet, Bifurcated chalcogen bonds: a theoretical study on the structure, strength and bonding properties, Chem. Phys. Lett. 634 (2015) 210–215, https://doi.org/10.1016/j.cplett.2015.06.034.

[116] S. Massahi, M. Ghobadi, M. Nikoorazm, Exceptional bifurcated chalcogen bonding interaction between Ph$_2$N$_2$O$_2$ and only one σ–hole on XCY (X = S, Se, Te and Y = O, S, Se, Te): a DFT study, Theor. Chem. Accounts 139 (2020) 162, https://doi.org/10.1007/s00214-020-02669-x.

[117] P. Ramasami, T.A. Ford, Chalcogen-bonded complexes. selenium-bound adducts of NH$_3$, H$_2$O, PH$_3$, and H$_2$S with OCSe, SCSe, and CSe$_2$, J. Mol. Model. 21 (2015) 35, https://doi.org/10.1007/s00894-014-2562-4.

[118] P. Ramasami, T.A. Ford, Chalcogen-bonded complexes of some carbon dioxide analogues, J. Mol. Struct. 1072 (2014) 28–31, https://doi.org/10.1016/j.molstruc.2014.03.055.

[119] F.T. Burling, B.M. Goldstein, Computational studies of nonbonded sulfur-oxygen and selenium-oxygen interactions in the thiazole and selenazole nucleosides, J. Am. Chem. Soc. 114 (1992) 2313–2320, https://doi.org/10.1021/ja00033a004.

[120] M.A.A. Ibrahim, M.N.I. Shehata, M.E.S. Soliman, M.F. Moustafa, H.R.A. El-Mageed, N.A.M. Moussa, Unusual chalcogen···chalcogen interactions in like···like and unlike YCY···YCY complexes (Y = O, S, and Se), Phys. Chem. Chem. Phys. 24 (2022) 3386–3399, https://doi.org/10.1039/d1cp02706a.

[121] F. Weigend, Accurate coulomb-fitting basis sets for H to Rn, Phys. Chem. Chem. Phys. 8 (2006) 1057–1065, https://doi.org/10.1039/b515623h.

[122] F. Weinhold, Natural bond orbital analysis: a critical overview of relationships to alternative bonding perspectives, J. Comput. Chem. 33 (2025) 2363–2379, https://doi.org/10.1002/jcc.23060.

[123] T. Ziegler, A. Rauk, A theoretical study of the ethylene-metal bond in complexes between Cu$^+$, Ag$^+$, Au$^+$, Pt^0 or Pt^{2+} and ethylene, based on the Hartree-Fock-Slater transition-state method, Inorg. Chem. 18 (1979) 1558–1565, https://doi.org/10.1021/ic50196a034.

[124] Q.Z. Li, R. Li, P. Guo, H. Li, W.Z. Li, J.B. Cheng, Competition of chalcogen bond, halogen bond, and hydrogen bond in SCSHOX and SeCSeHOX (X = Cl and Br) complexes, Comput. Theor. Chem. 980 (2012) 56–61, https://doi.org/10.1016/j.comptc.2011.11.019.

[125] J.E. Del Bene, I. Alkorta, J. Elguero, Exploring N···C tetrel and O···S chalcogen bonds in HN(CH)SX:OCS systems, for X = F, NC, Cl, CN, CCH, and H, Chem. Phys. Lett. 730 (2019) 466–471, https://doi.org/10.1016/j.cplett.2019.05.044.

[126] E. Del Bene, I. Alkorta, J. Elguero, N···C and S···S interactions in complexes, molecules, and transition structures HN(CH)SX:SCO, for X = F, Cl, NC, CCH, H, and CN, Molecules 24 (2019) 3232, https://doi.org/10.3390/molecules24183232.

[127] M.A.A. Ibrahim, R.R.A. Saeed, M.N.I. Shehata, E.E.B. Mohamed, M.E.S. Soliman, J.H. Al-Fahemi, H.R.A. El-Mageed, M.N. Ahmed, A.M. Shawky, N.A.M. Moussa, Unexplored σ-hole and π-hole interactions in (X$_2$CY)$_2$ complexes (X = F, Cl; Y = O, S), J. Mol. Struct. 1265 (2022) 133232, https://doi.org/10.1016/j.molstruc.2022.133232.

[128] X. Guo, Q. Li, B. Xiao, X. Yang, W. Li, J. Cheng, Influence of F and Se substitution on the structures, stabilities and nature of the complexes between F$_2$CSe and HOX (X = F, Cl, Br, and I), RSC Adv. 5 (2015) 52667–52675, https://doi.org/10.1039/c5ra08034g.

[129] F. Becke, Density-functional thermochemistry. III., The role of exact exchange, J. Chem. Phys. 98 (1993) 5648–5652, https://doi.org/10.1063/1.464913.

[130] C. Lee, W. Yang, R.G. Parr, Development of the Colle-Salvetti correlation-energy formula into a functional of the electron density, Phys. Rev. B 37 (1988) 785–789, https://doi.org/10.1103/physRevB.37.785.

[131] P. Sanz, M. Yáñez, O. Mó, Competition between X···H···Y intramolecular hydrogen bonds and X···Y (X = O, S, and Y = Se, Te) chalcogen-chalcogen interactions, J. Phys. Chem. A 106 (2002) 4661–4668, https://doi.org/10.1021/jp0143645.

[132] P. Sanz, O. Mó, M. Yáñez, Characterization of intramolecular hydrogen bonds and competitive chalcogen–chalcogen interactions on the basis of the topology of the charge density, Phys. Chem. Chem. Phys. 5 (2003) 2942–2947, https://doi.org/10.1039/b304699k.

[133] M.K. Si, R. Lo, B. Ganguly, The origin and magnitude of intramolecular quasi-cyclic S···O and S···S interactions revisited: a computational study, Chem. Phys. Lett. 631–632 (2015) 6–11, https://doi.org/10.1016/j.cplett.2015.04.036.

[134] P. Sanz, M. Yáñez, O. Mó, Resonance-assisted intramolecular chalcogen–chalcogen interactions? Chem. Eur. J. 9 (2003) 4548–4555, https://doi.org/10.1002/chem.200304891.

[135] F. Lei, Q. Liu, Y. Zhong, X. Cui, J. Yu, Z. Hu, G. Feng, Z. Zeng, T. Lu, Computational insight into the nature and strength of the π-hole type chalcogen•••chalcogen interactions in the XO$_2$•••CH$_3$YCH$_3$ complexes (X = S, Se, Te; Y = O, S, Se, Te), Int. J. Mol. Sci. 24 (2023) 16193, https://doi.org/10.3390/ijms242216193/s1.

[136] L. Mo, Y. Zeng, X. Li, X. Zhang, L. Meng, Chalcogen- and halogen-bonds involving SX$_2$ (X = F, Cl, and Br) with formaldehyde, J. Mol. Model. 22 (2016) 1–8, https://doi.org/10.1007/s00894-016-3037-6.

[137] C. Bleiholder, D.B. Werz, H. Köppel, R. Gleiter, Theoretical investigations on chalcogen-chalcogen interactions: what makes these nonbonded interactions bonding? J. Am. Chem. Soc. 128 (2006) 2666–2674, https://doi.org/10.1021/ja056827g.

[138] V. Previtali, G. Sánchez-Sanz, C. Trujillo, Theoretical investigation of cyano-chalcogen dimers and their importance in molecular recognition, ChemPhysChem 20 (2019) 3186–3194, https://doi.org/10.1002/cphc.201900899.

[139] G. Sánchez-Sanz, C. Trujillo, I. Alkorta, J. Elguero, Intermolecular weak interactions in HTeXH dimers (X = O, S, Se, Te): hydrogen bonds, chalcogen–chalcogen contacts and chiral discrimination, ChemPhysChem 13 (2012) 496–503, https://doi.org/10.1002/cphc.201100830.

[140] V.A. Adhav, B. Pananghat, K. Saikrishnan, Probing the directionality of S···O/N chalcogen bond and its interplay with weak C-H···O/N/S hydrogen bond using molecular electrostatic potential, J. Phys. Chem. B 126 (2022) 7818–7832, https://doi.org/10.1021/acs.jpcb.2c03745.

[141] M.A.A. Ibrahim, R.R.A. Saeed, M.N.I. Shehata, N.A.M. Moussa, M.-E.S. Soliman, S. Khan, M.A. El-Tayeb, T. Shoeib, On the versatility of the sp-, sp^2-, and sp^3-hybridized chalcogen-bearing molecules to engage in type I chalcogen···chalcogen interactions: a quantum mechanical investigation of like···like and unlike complexes, ACS Omega 9 (2024) 44448–44456, https://doi.org/10.1021/acsomega.4c05963.

[142] S. Scheiner, Comparison of CH···O, SH···O, chalcogen, and tetrel bonds formed by neutral and cationic sulfur-containing compounds, J. Phys. Chem. A 119 (2015) 9189–9199, https://doi.org/10.1021/acs.jpca.5b06831.

[143] M. Hoffman, S.S. Xantheas, Competition between hydrogen and chalcogen bonding in homodimers of chalcogen hydrides (H$_2$X)$_2$, X = O, S, Se, Te, J. Am. Chem. Soc. 147 (2025) 11152–11171, https://doi.org/10.1021/jacs.4c17428.

[144] B. Galmés, A. Juan-Bals, A. Frontera, G. Resnati, Charge-assisted chalcogen bonds: CSD and DFT analyses and biological implication in glucosidase inhibitors, Chem. Eur. J. 26 (2020) 4599–4606, https://doi.org/10.1002/chem.201905498.

[145] H.A. Samimi, M.D. Esrafili, F. Mohammadian-Sabet, H. Haddadi, Theoretical study on cooperative interplay between anion–π and chalcogen-bonding interactions, Mol. Phys. 113 (2015) 1442–1450, https://doi.org/10.1080/00268976.2014.1002551.

[146] S. Scheiner, Adjusting the balance between hydrogen and chalcogen bonds, Phys. Chem. Chem. Phys. 24 (2022) 28944–28955, https://doi.org/10.1039/d2cp04591e.

[147] Y. Zhang, W. Wang, The bifurcate chalcogen bond: some theoretical observations, J. Mol. Struct. THEOCHEM 916 (2009) 135–138, https://doi.org/10.1016/j.theochem.2009.09.021.

[148] K.D. Sharma, P. Kathuria, S.D. Wetmore, P. Sharma, Can modified DNA base pairs with chalcogen bonding expand the genetic alphabet? A combined quantum chemical and molecular dynamics simulation study, Phys. Chem. Chem. Phys. 22 (2020) 23754–23765, https://doi.org/10.1039/d0cp04921b.

[149] M.D. Esrafili, F. Mohammadian-Sabet, An ab initio study on chalcogen–chalcogen bond interactions in cyclic $(SHX)_3$ complexes (X = F, Cl, CN, NC, CCH, OH, OCH_3, NH_2), Chem. Phys. Lett. 628 (2015) 71–75, https://doi.org/10.1016/j.cplett.2015.04.013.

[150] L. Mo, Y. Zeng, X. Li, L. Meng, The enhancing effects of molecule X (X = PH_2Cl, SHCl, ClCl) on chalcogen–chalcogen interactions in cyclic trimers Y···Y···X (Y = SHCl, SeHCl), Int. J. Quantum Chem. 117 (2017) e25354, https://doi.org/10.1002/qua.25354.

[151] N. Liu, X. Xie, Q. Li, Chalcogen bond involving zinc(II)/cadmium(II) carbonate and its enhancement by spodium bond, Molecules 26 (2021) 6443, https://doi.org/10.3390/molecules26216443.

[152] Ciancaleoni, G.; Rocchigiani, L. Assessing the Orbital Contribution in the "Spodium Bond" by Natural Orbital for Chemical Valence–Charge Displacement Analysis. Inorg. Chem. 2021,60, 4683-4692. doi:https://doi.org/10.1021/acs.inorgchem.0c03650.

[153] Esrafili, M. D.; Mohammadian-Sabet, F. Homonuclear Chalcogen–Chalcogen Bond Interactions in Complexes Pairing YO_3 and YHX Molecules (Y = S, Se; X = H, Cl, Br, CCH, NC, OH, OCH_3): Influence of Substitution and Cooperativity. Int. J. Quantum Chem. 116 (2016), 529–536. doi:https://doi.org/10.1002/qua.25076.

[154] N.S. Venkataramanan, Electronic structure, stability, and cooperativity of chalcogen bonding in sulfur dioxide and hydrated sulfur dioxide clusters: a DFT study and wave functional analysis, Struct. Chem. 33 (2022) 179–193, https://doi.org/10.1007/s11224-021-01827-6.

[155] A. Suvitha, N.S. Venkataramanan, R. Sahara, Effect of water molecule in the structure, stability, and electronic properties of sulfur trioxide clusters: a computational analysis, Monatshefte fur Chemie 153 (2022) 347–357, https://doi.org/10.1007/s00706-022-02909-9.

[156] A. Suvitha, N.S. Venkataramanan, R. Sahara, The structure, stability, thermochemistry, and bonding in SO_3-$(H_2O)_n$ (n = 1–7) clusters: a computational analysis, Struct. Chem. 34 (2023) 225–237, https://doi.org/10.1007/s11224-022-02085-w.

[157] J. Langwald, R.M. Gomila, D. van Gerven, A. Frontera, M.S. Wickleder, Introducing (inter-)halogen polysulfates – a study on the influence of halogen bonding on weakly coordinating anions, Dalton Trans. 54 (2025) 16095–16105, https://doi.org/10.1039/D5DT02088C.

[158] M.D. Esrafili, F. Mohammadian-Sabet, Ab initio calculations of cooperativity effects on chalcogen bonding: linear clusters of $(OCS)_{2\text{-}8}$ and $(OCSe)_{2\text{-}8}$, Struct. Chem. 26 (2015) 199–206, https://doi.org/10.1007/s11224-014-0477-4.

[159] S. Scheiner, On the properties of X···N noncovalent interactions for first-, second-, and third-row X atoms, J. Chem. Phys. 134 (2011) 164313, https://doi.org/10.1063/1.3585611/189519.

[160] S. Adhikari, Scheiner, The S···N noncovalent interaction: comparison with hydrogen and halogen bonds, Chem. Phys. Lett. 514 (2011) 36–39, https://doi.org/10.1016/j.cplett.2011.08.029.

[161] U. Adhikari, S. Scheiner, Substituent effects on Cl···N, S···N, and P···N noncovalent bonds, J. Phys. Chem. A 116 (2012) 3487–3497, https://doi.org/10.1021/jp301288e.

[162] U. Adhikari, S. Scheiner, Sensitivity of pnicogen, chalcogen, halogen and H-bonds to angular distortions, Chem. Phys. Lett. 532 (2012) 31–35, https://doi.org/10.1016/j.cplett.2012.02.064.

[163] S. Scheiner, Sensitivity of noncovalent bonds to intermolecular separation: hydrogen, halogen, chalcogen, and pnicogen bonds, CrystEngComm 15 (2013) 3119–3124, https://doi.org/10.1039/c2ce26393a.

[164] S. Scheiner, Detailed comparison of the pnicogen bond with chalcogen, halogen, and hydrogen bonds, Int. J. Quantum Chem. 113 (2013) 1609–1620, https://doi.org/10.1002/qua.24357.

[165] R. Shukla, D. Chopra, Characterization of N···O non-covalent interactions involving σ-holes: "electrostatics" or "dispersion", Phys. Chem. Chem. Phys. 18 (2016) 29946–29954, https://doi.org/10.1039/c6cp05899j.

[166] M. D. Esrafili, A. Sadr-Mousavi, Chalcogen bonds tuned by an N–H···π or C–H···π interaction: investigation of substituent, cooperativity and solvent effects. Mol. Phys. 115 (2017), 1713–1723. doi:https://doi.org/10.1080/00268976.2017.1318227.

[167] M.D. Esrafili, F. Mohammadian-Sabet, An ab initio study on cationic chalcogen bond interactions between $F_{3\text{-}n}H_nS^+$ (n = 0–2) and nitrogen bases, Chem. Phys. Lett. 645 (2016) 32–37, https://doi.org/10.1016/j.cplett.2015.12.027.

[168] M.D. Esrafili, M. Vakili, Cooperativity effects between σ-hole interactions: a theoretical evidence for mutual influence between chalcogen bond and halogen bond interactions in F_2S···NCX···NCY Complexes (X = F, Cl, Br, I; Y = H, F, OH), Mol. Phys. 112 (2014) 2746–2752, https://doi.org/10.1080/00268976.2014.909057.

[169] Q. Zhao, Interplay between halogen and chalcogen bonding in the XCl●●●OCS●●●NH_3 (X = F, OH, NC, CN, and FCC) complex, J. Mol. Model. 20 (2014) 2458, https://doi.org/10.1007/s00894-014-2458-3.

[170] J. Yi, X. Qin, F. Chen, Theoretical studies on cationic chalcogen and pnicogen bonds in binary and ternary complexes, Chem. J. Chin. Univ. 40 (2019) 1439, https://doi.org/10.7503/cjcu20190101.

[171] B.M. Asiabar, M.D. Esrafili, F. Mohammadian-Sabet, H.R. Sobhi, M. Javaheri, An ab initio study on the concerted interaction between chalcogen and pnicogen bonds, J. Mol. Model. 20 (2014) 2545, https://doi.org/10.1007/s00894-014-2545-5.

[172] M.D. Esrafili, P. Mousavian, F. Mohammadian-Sabet, Tuning of pnicogen and chalcogen bonds by an aerogen-bonding interaction: a comparative ab initio study, Mol. Phys. 117 (2019) 58–66, https://doi.org/10.1080/00268976.2018.1492746.

[173] M. Otilia, M.M. Montero-Campillo, I. Alkorta, J. Elguero, M. Yáñez, Ternary complexes stabilized by chalcogen and alkaline-earth bonds: crucial role of cooperativity and secondary noncovalent interactions, Chem. Eur. J. 25 (2019) 11688–11695, https://doi.org/10.1002/chem.201901641.

[174] A. Soufi, S. Salehzadeh, The degree and origin of the cooperativity of the chalcogen (Ch···N) and dihydrogen (H···H) bonds in some triad systems, J. Comput. Chem. 46 (2025) e70022, https://doi.org/10.1002/jcc.70022.

[175] J. George, V.L. Deringer, R. Dronskowski, Cooperativity of halogen, chalcogen, and pnictogen bonds in infinite molecular chains by electronic structure theory, J. Phys. Chem. A 118 (2014) 3193–3200, https://doi.org/10.1021/jp5015302.

[176] M.D. Esrafili, N. Mohammadirad, An ab initio study on tunability of σ-hole interactions in $XHS:PH_2Y$ and $XH_2P:SHY$ complexes (X = F, Cl, Br; Y = H, OH, OCH_3, CH_3, C_2H_5, and NH_2), J. Mol. Model. 21 (2015) 1–8, https://doi.org/10.1007/s00894-015-2727-9.

[177] M.D. Esrafili, H. Akhgarpour, An ab initio study on competition between pnicogen and chalcogen bond interactions in binary $XHS:PH_0X$ complexes (X = F, Cl, CCH, COH, CH_3, OH, OCH_3 and NH_2), Mol. Phys. 114 (2016) 1847–1855, https://doi.org/10.1080/00268976.2016.1158421.

[178] R. Shukla, D. Chopra, "Pnicogen bonds" or "chalcogen bonds": exploiting the effect of substitution on the formation of P···Se noncovalent bonds, Phys. Chem. Chem. Phys. 18 (2016) 13820–13829, https://doi.org/10.1039/c6cp01703g.

[179] X. Li, A.Y. Li, Hemi bonds and noncovalent interactions in the cational systems $(XH_2P:SHY)^+$, Chem. Phys. Lett. 659 (2016) 126–132, https://doi.org/10.1016/j.cplett.2016.07.011.

[180] W. Zierkiewicz, J. Fanfrlík, M. Michalczyk, D. Michalska, P. Hobza, S···N chalcogen bonded complexes of carbon disulfide with diazines. theoretical study, Chem. Phys. 500 (2018) 37–44, https://doi.org/10.1016/j.chemphys.2017.11.014.

[181] X. Guo, Y.W. Liu, Q.Z. Li, W.Z. Li, J.B. Cheng, Competition and cooperativity between tetrel bond and chalcogen bond in complexes involving F_2CX (X = Se and Te), Chem. Phys. Lett. 620 (2015) 7–12, https://doi.org/10.1016/j.cplett.2014.12.015.

[182] M.D. Esrafili, F. Mohammadian-Sabet, σ-Hole bond tunability in YO_2X_2:NH_3 and YO_2X_2:H_2O complexes (X = F, Cl, Br; Y = S, Se): trends and theoretical aspects, Struct. Chem. 27 (2016) 617–625, https://doi.org/10.1007/s11224-015-0594-8.

[183] M.D. Esrafili, S. Asadollahi, Y. Dadban Shahamat, Competition between chalcogen bond and halogen bond interactions in YOX_4:NH_3 (Y = S, Se; X = F, Cl, Br) complexes: an ab initio investigation, Struct. Chem. 27 (2016) 1439–1447, https://doi.org/10.1007/s11224-016-0763-4.

[184] W. Dong, Q. Li, S. Scheiner, Comparative strengths of tetrel, pnicogen, chalcogen, and halogen bonds and contributing factors, Molecules 23 (2018) 1681, https://doi.org/10.3390/molecules23071681.

[185] C.T. Phan Dang, N.M. Tam, T.N. Huynh, N.T. Trung, Revisiting conventional noncovalent interactions towards a complete understanding: from tetrel to pnicogen, chalcogen, and halogen bond, RSC Adv. 13 (2023) 31507–31517, https://doi.org/10.1039/d3ra06078k.

[186] N. Liu, Q. Li, S.A.C. McDowell, Reliable comparison of pnicogen, chalcogen, and halogen bonds in complexes of 6-OXF_2-fulvene (X = As, Sb, Se, Te, Be, I) with three electron donors, Front. Chem. 8 (2020) 608486, https://doi.org/10.3389/fchem.2020.608486.

[187] M.D. Esrafili, R. Nurazar, Chalcogen bonds formed through π-holes: SO_3 complexes with nitrogen and phosphorus bases, Mol. Phys. 114 (2016) 276–282, https://doi.org/10.1080/00268976.2015.1098742.

[188] S. Scheiner, Dissection of the origin of π-holes and the noncovalent bonds in which they engage, J. Phys. Chem. A 125 (2021) 6514–6528, https://doi.org/10.1021/acs.jpca.1c05431.

[189] M.D. Esrafili, M. Vakili, M. Solimannejad, Cooperative interaction between π-hole and single-electron σ-hole interactions in O_2S···NCX···CH_3 and O_2Se···NCX···CH_3 complexes (X = F, Cl, Br and I), Mol. Phys. 112 (2014) 2078–2084, https://doi.org/10.1080/00268976.2014.884730.

[190] J. Zhang, W. Li, J. Cheng, Z. Liu, Q. Li, Cooperative effects between π-hole triel and π-hole chalcogen bonds, RSC Adv. 8 (2018) 26580–26588, https://doi.org/10.1039/c8ra04106g.

[191] I. Alkorta, J. Elguero, J.E. Del Bene, Complexes of O=C=S with nitrogen bases: chalcogen bonds, tetrel bonds, and other secondary interactions, ChemPhysChem 19 (2018) 1886–1894, https://doi.org/10.1002/cphc.201800217.

[192] X. Guo, X. An, Q. Li, Se···N chalcogen bond and Se···X halogen bond involving F_2C=Se: influence of hybridization, substitution, and cooperativity, J. Phys. Chem. A 119 (2015) 3518–3527, https://doi.org/10.1021/acs.jpca.5b00783.

[193] L.M. Azofra, I. Alkorta, S. Scheiner, Chalcogen bonds in complexes of SOXY (X, Y = F, Cl) with nitrogen bases, J. Phys. Chem. A 119 (2015) 535–541, https://doi.org/10.1021/jp511828h.

[194] A. Amonov, S. Scheiner, Comparison of the ability of N-bases to engage in noncovalent bonds, ChemPhysChem 24 (2023) e202300326, https://doi.org/10.1002/cphc.202300326.

[195] A. Amonov, S. Scheiner, Heavy pnicogen atoms as electron donors in sigma-hole bonds, Phys. Chem. Chem. Phys. 25 (2023) 23530–23537, https://doi.org/10.1039/d3cp03479h.

[196] G. Haberhauer, R. Gleiter, The Nature of strong chalcogen bonds involving chalcogen-containing heterocycles, Angew. Chem. Int. Ed. 59 (2020) 21236–21243, https://doi.org/10.1002/anie.202010309.

[197] C. Trujillo, I. Rozas, J. Elguero, I. Alkorta, G. Sánchez-Sanz, Modulating intramolecular chalcogen bonds in aromatic (thio)(seleno)phene-based derivatives, Phys. Chem. Chem. Phys. 21 (2019) 23645–23650, https://doi.org/10.1039/c9cp03694f.

[198] U. Adhikari, S. Scheiner, Effects of charge and substituent on the S···N chalcogen bond, J. Phys. Chem. A 118 (2014) 3183–3192, https://doi.org/10.1021/jp501449v.

[199] V.P.N. Nziko, S. Scheiner, Chalcogen bonding between tetravalent SF_4 and amines, J. Phys. Chem. A 118 (2014) 10849–10856, https://doi.org/10.1021/jp509212t.

[200] H. Zhou, X. Wang, X. An, Q. Li, A.C. McDowell, Methyl groups as unconventional Lewis bases in chalcogen bonding, CrystEngComm 27 (2025) 4516, https://doi.org/10.1039/d5ce00345h.

[201] W. Zierkiewicz, R. Wysokiński, M. Michalczyk, S. Scheiner, Chalcogen bonding of two ligands to hypervalent YF_4 (Y = S, Se, Te, Po), Phys. Chem. Chem. Phys. 21 (2019) 20829–20839, https://doi.org/10.1039/c9cp04006d.

[202] R. Shukla, D. Yu, T. Mu, S. Kozuch, Yet another perspective on hole interactions, part II: Lp-hole vs. Lp-hole interactions, Phys. Chem. Chem. Phys. 25 (2023) 12641–12649, https://doi.org/10.1039/d3cp00225j.

[203] M.A.A. Ibrahim, R.R.A. Saeed, M.N.I. Shehata, N.A.M. Moussa, A.M. Tawfeek, M. N. Ahmed, M.K. Abd El-Rahman, T. Shoeib, Sigma-hole and lone-pair-hole site-based interactions of seesaw tetravalent chalcogen-bearing molecules with Lewis bases. ACS, Omega 8 (2023) 32828–32837, https://doi.org/10.1021/acsomega.3c03981.

[204] S. Scheiner, Transition between the noncovalency and covalency of σ-hole bonds, J. Phys. Chem. A 127 (2023) 9760–9770, https://doi.org/10.1021/acs.jpca.3c06093.

[205] S. Scheiner, Competition between the two σ-holes in the formation of a chalcogen bond, ChemPhysChem 24 (2023) e202200936, https://doi.org/10.1002/cphc.202200936.

[206] M. Michalczyk, M. Malik, W. Zierkiewicz, S. Scheiner, Experimental and theoretical studies of dimers stabilized by two chalcogen bonds in the presence of a N···N pnicogen bond, J. Phys. Chem. A 125 (2021) 657–668, https://doi.org/10.1021/acs.jpca.0c10814.

[207] M. Ali Ben Aissa, S. Hassen, Y. Arfaoui, E. Manar, T. Youssef Arfaoui, Theoretical density functional theory insights into the nature of chalcogen bonding between CX_2 (X = S, Se, Te) and diazine from monomer to supramolecular complexes, Int. J. Quantum Chem. 119 (2019) e25837, https://doi.org/10.1002/qua.25837.

[208] E. Rahali, Z. Noori, Y. Arafoui, J. Poater, Chalcogen noncovalent interactions between diazines and sulfur oxides in supramolecular circular chains, J. Mol. Sci. 25 (2024) 7497, https://doi.org/10.3390/ijms25137497.

[209] E. Navarro-García, B. Galmés, M.D. Velasco, A. Frontera, A. Caballero, Anion recognition by neutral chalcogen bonding receptors: experimental and theoretical investigations, Chem. Eur. J. 26 (2020) 4706–4713, https://doi.org/10.1002/chem.201905786.

[210] A. Casula, P. Begines, A. Bettoschi, J.G. Fernandez-Bolaños, F. Isaia, V. Lippolis, Ó. López, G. Picci, A.M. Scorciapino, C. Caltagirone, Selenoureas for anion binding as molecular logic gates, Chem. Commun. 53 (2017) 11869–11872, https://doi.org/10.1039/c7cc07148e.

[211] A. Singh, A. Torres-Huerta, F. Meyer, H. Valkenier, Anion transporters based on halogen, chalcogen, and pnictogen bonds: towards biological applications, Chem. Sci. 15 (2024) 15006, https://doi.org/10.1039/d4sc04644g.

[212] L. Lu, Y. Lu, Z. Zhu, H. Liu, Pnictogen, chalcogen, and halogen bonds in catalytic systems: theoretical study and detailed comparison, J. Mol. Model. 26 (2020) 1–12, https://doi.org/10.1007/s00894-019-4275-1.

[213] W. Wang, B. Ji, Y. Zhang, Chalcogen bond: a sister noncovalent bond to halogen bond, J. Phys. Chem. A 113 (2009) 8132–8135, https://doi.org/10.1021/jp904128b.

[214] A.D. Becke, Density-functional exchange-energy approximation with correct asymptotic behavior, Phys. Rev. A 38 (1988) 3098–3100, https://doi.org/10.1103/physRevA.38.3098.

[215] A.D. Becke, Density-functional thermochemistry. V., Systematic optimization of exchange-correlation functionals, J. Chem. Phys. 107 (1997) 8554–8560, https://doi.org/10.1021/acs.chemrev.5b00533.

[216] D. Quiñonero, Anion recognition by pyrylium cations and thio-, seleno- and telluro- analogues: a combined theoretical and Cambridge Structural Database study, Molecules 20 (2015) 11632–11659, https://doi.org/10.3390/molecules200711632.

[217] S. Scheiner, Highly selective halide receptors based on chalcogen, pnicogen, and tetrel bonds, Chem. Eur. J. 22 (2016) 18850–18858, https://doi.org/10.1002/chem.201603891.

[218] G. Sánchez-Sanz, C. Trujillo, Improvement of anion transport systems by modulation of chalcogen interactions: the influence of solvent, J. Phys. Chem. A 122 (2018) 1369–1377, https://doi.org/10.1021/acs.jpca.7b10920.

[219] P. Wonner, L. Vogel, F. Kniep, S.M. Huber, Catalytic carbon–chlorine bond activation by selenium-based chalcogen bond donors, Chem. Eur. J. 23 (2017) 16972–16975, https://doi.org/10.1002/chem.201704502.

[220] S. Scheiner, Comparison of halide receptors based on H, halogen, chalcogen, pnicogen, and tetrel bonds, Faraday Discuss. 203 (2017) 213–226, https://doi.org/10.1039/c7fd00043j.

[221] M.A. Blanco, A. Martín Pendás, E. Francisco, Interacting quantum atoms: a correlated energy decomposition scheme based on the Quantum Theory of Atoms in Molecules, J. Chem. Theory Comput. 1 (2005) 1096–1109, https://doi.org/10.1021/ct0501093.

[222] P.L. Bora, M. Novák, J. Novotný, C. Foroutan-Nejad, R. Marek, Supramolecular covalence in bifurcated chalcogen bonding, Chem. Eur. J. 23 (2017) 7315–7323, https://doi.org/10.1002/chem.201700179.

[223] D. Fan, L. Chen, C. Wang, S. Yin, Y. Mo, Inter-anion chalcogen bonds: are they anti-electrostatic in nature? J. Chem. Phys. 155 (2021) 234302 https://doi.org/10.1063/5.0076872.

[224] S. Scheiner, Influence of internal noncovalent bonds on rotational dynamics, Inorg. Chem. 62 (2023) 13030–13037, https://doi.org/10.1021/acs.inorgchem.3c01837.

[225] M.D. Esrafili, F. Mohammadian-Sabet, Prediction and characterisation of a chalcogen···π interaction with acetylene as a potential electron donor in XHS···HCCH and XHSe···HCCH (X = F, Cl, Br, CN, OH, OCH_3, NH_2, CH_3) σ-hole complexes, Mol. Phys. 113 (2015) 3559–3566, https://doi.org/10.1080/00268976.2015.1039619.

[226] H. Su, H. Wu, H. Wang, H. Wang, Y. Ni, Y. Lu, Z. Zhu, A comparative study of S···π chalcogen bonds between SF_2 or SFH and C-C multiple bonds, J. Mol. Struct. 1188 (2019) 62–68, https://doi.org/10.1016/j.molstruc.2019.03.085.

[227] V.P.N. Nziko, S. Scheiner, S···π chalcogen bonds between SF_2 or SF_4 and C-C multiple bonds, J. Phys. Chem. A 119 (2015) 5889–5897, https://doi.org/10.1021/acs.jpca.5b03359.

[228] M. Saberinasab, S. Salehzadeh, Y. Maghsoud, M. Bayat, The significant effect of electron donating and electron withdrawing substituents on nature and strength of an intermolecular Se···π interaction. A theoretical study, Comput. Theor. Chem. 1078 (2016) 9–15, https://doi.org/10.1016/j.comptc.2015.12.009.

[229] M. Bortoli, S.M. Ahmad, T.A. Hamlin, F.M. Bickelhaupt, L. Orian, Nature and strength of chalcogen–π bonds, Phys. Chem. Chem. Phys. 20 (2018) 27592–27599, https://doi.org/10.1039/c8cp05922e.

[230] A. Bauzá, D. Quiñonero, P.M. Deyà, A. Frontera, Halogen bonding versus chalcogen and pnicogen bonding: a combined Cambridge Structural Database and theoretical study, CrystEngComm 15 (2013) 3137–3144, https://doi.org/10.1039/c2ce26741a.

[231] J.E. Del Bene, I. Alkorta, J. Elguero, Probing C···S chalcogen bonds in complexes SC:SHX, for X = NO_2, NC, F, Cl, CN, CCH, and NH_2, Chem. Phys. Lett. 721 (2019) 86–90, https://doi.org/10.1016/j.cplett.2019.02.016.

[232] Y. Zhang, W. Wang, Interplay between the N→C dative bond, intramolecular chalcogen bond and π conjugation in the complexes formed by cyclo[18]carbon and C_{14} polyyne with 1,2,5-chalcogenadiazoles, ChemPlusChem 90 (2025) e202400557, https://doi.org/10.1002/cplu.202400557.

[233] Y. Zhang, W. Wang, Chalcogen-bond-assisted formation of the N→C dative bonds in the complexes between chalcogenadiazoles/chalcogenatriazoles and fullerene C_{60}, Molecules 29 (2024) 2685, https://doi.org/10.3390/molecules29112685.

[234] M. Michalczyk, W. Zierkiewicz, S. Scheiner, Ability of strained C atoms to act as an electron donor, Chem. Sci. 16 (2025) 10572–10584, https://doi.org/10.1039/d5sc01632k.

[235] O. Loveday, J. Echeverría, Methyl groups as widespread Lewis bases in noncovalent interactions, Nat. Commun. 12 (2021) 1–9, https://doi.org/10.1038/s41467-021-25314-y.

[236] H. Zhou, S. Li, Q. Li, S. Scheiner, Revisiting the methyl group as a nonconventional electron donor in triel, tetrel, pnictogen, chalcogen, and halogen bonding, J. Phys. Chem. A 129 (2025) 7819–7831, https://doi.org/10.1021/acs.jpca.5c03722.

[237] M.D. Esrafili, F. Mohammadian-Sabet, Does single-electron chalcogen bond exist? Some theoretical insights, J. Mol. Model. 21 (2015) 65, https://doi.org/10.1007/s00894-015-2613-5.

[238] B. Galmés, J. Adrover, G. Terraneo, A. Frontera, G. Resnati, Radical···radical chalcogen bonds: CSD analysis and DFT calculations, Phys. Chem. Chem. Phys. 22 (2020) 12757–12765, https://doi.org/10.1039/d0cp01643h.

[239] N.A. Puskarevsky, A.I. Smolentsev, A.A. Dmitriev, I. Vargas-Baca, N.P. Gritsan, J. Beckmann, A.V. Zibarev, Bis(2,1,3-benzotelluradiazolidyl)2,1,3-benzotelluradiazole: a pair of radical anions coupled by Te···N chalcogen bonding, Chem. Commun. 56 (2020) 1113–1116, https://doi.org/10.1039/c9cc08110k.

[240] G. Saleh, C. Gatti, L. Lo Presti, Non-covalent interaction via the reduced density gradient: independent atom model vs experimental multipolar electron densities, Comput. Theor. Chem. 998 (2012) 148–163, https://doi.org/10.1016/j.comptc.2012.07.014.

[241] M.A.A. Ibrahim, Y.A.M. Mohamed, H.S.M. Abd Elhafez, M.N.I. Shehata, M.E. S. Soliman, M.N. Ahmed, H.R. Abd El-Mageed, N.A.M. Moussa, R•-hole interactions of group IV-VII radical-containing molecules: a comparative study, J. Mol. Graph. Model. 111 (2022) 108097, https://doi.org/10.1016/j.jmgm.2021.108097.

[242] J.M. Lehn, Supramolecular chemistry – scope and perspectives molecules, supermolecules, and molecular devices (Nobel Lecture), Angew. Chem. Int. Ed. 27 (1988) 89–112, https://doi.org/10.1002/anie.198800891.

[243] M.E. Brezgunova, J. Lieffrig, E. Aubert, S. Dahaoui, P. Fertey, S. Lebègue, J. G. Ángyán, M. Fourmigué, E. Espinosa, Chalcogen bonding: experimental and theoretical determinations from electron density analysis. Geometrical preferences driven by electrophilic-nucleophilic interactions, Cryst. Growth Des. 13 (2013) 3283–3289, https://doi.org/10.1021/cg400683u.

[244] M. Iwaoka, S. Takemoto, S. Tomoda, Statistical and theoretical investigations on the directionality of nonbonded S···O interactions. Implications for molecular design and protein engineering, J. Am. Chem. Soc. 124 (2002) 10613–10620, https://doi.org/10.1021/ja026472q.

[245] H. Wu, Y. Lu, C. Peng, Z. Xu, H. Liu, Theoretical study of the interplay between double chalcogen-bonding interactions and halogen bonds in ditopic molecular module systems, Comput. Theor. Chem. 1198 (2021) 113182, https://doi.org/10.1016/j.comptc.2021.113182.
[246] S. Scheiner, Quantum chemical analysis of noncovalent bonds within crystals. Concepts and concerns, CrystEngComm 25 (2023) 5060–5071, https://doi.org/10.1039/d3ce00708a.
[247] R. Shukla, D. Chopra, Crystallographic and theoretical investigation on the nature and characteristics of type I C=S···S=C interactions, Cryst. Growth Des. 16 (2016) 6734–6742, https://doi.org/10.1021/acs.cgd.6b01530.
[248] D.K. Miller, I.Y. Chernyshov, Y.V. Torubaev, S.V. Rosokha, From weak to strong interactions: structural and electron topology analysis of the continuum from the supramolecular chalcogen bonding to covalent bonds, Phys. Chem. Chem. Phys. 24 (2022) 8251–8259, https://doi.org/10.1039/d1cp05441d.
[249] A. Frontera, A. Bauza, Metal coordination enhances chalcogen bonds: CSD survey and theoretical calculations, Int. J. Mol. Sci. 23 (2022) 4188, https://doi.org/10.3390/ijms23084188/s1.
[250] M.C. Aragoni, M. Arca, V. Lippolis, A. Pintus, Y. Torubaev, E. Podda, A structural approach to the strength evaluation of linear chalcogen bonds, Molecules 28 (2023) 3133, https://doi.org/10.3390/molecules28073133/s1.
[251] A. V. Gurbanov, M.L. Kuznetsov, K.T. Mahmudov, A.J.L. Pombeiro, G. Resnati, Resonance assisted chalcogen bonding as a new synthon in the design of dyes. Chem. Eur. J. 26 (2020), 14833–14837. doi:https://doi.org/10.1002/chem.202002518.
[252] S. Jia, H. Ye, L. You, Interplay between chalcogen bonds and dynamic covalent bonds, Org. Chem. Front. 9 (2022) 3966–3975, https://doi.org/10.1039/d2qo00684g.
[253] T. Fellowes, B.L. Harris, J.M. White, Experimental evidence of chalcogen bonding at oxygen, Chem. Commun. 56 (2020) 3313–3316, https://doi.org/10.1039/c9cc09896h.
[254] M. Yokoyama, Y. Okayasu, Y. Kobayashi, H. Tanaka, Y. Haketa, H. Maeda, Ion-pairing assemblies of dithienylnitrophenol-based π-electronic anions stabilized by intramolecular interactions, Org. Lett. 25 (2023) 3676–3681, https://doi.org/10.1021/acs.orglett.3c01075.
[255] T. Inoue, N. Morita, Y. Amijima, R. Sakai, S. Hamada, S. Nakamura, Y. Kobayashi, T. Furuta, Formation of chalcogen-bonding interactions and their role in the trans–trans conformation of thiourea, Org. Biomol. Chem. 22 (2024) 5301–5305, https://doi.org/10.1039/d4ob00723a.
[256] P.X. Weng, J. Yan, Z. Cao, Y. Li, B. Jiang, Intramolecular chalcogen bonding to tune the molecular conformation of helical building blocks for a supramolecular helix, Chem. Commun. 58 (2022) 6461–6464, https://doi.org/10.1039/d2cc01615j.
[257] S. Mehrparvar, C. Wölper, R. Gleiter, G. Haberhauer, The carbonyl···tellurazole chalcogen bond as a molecular recognition unit: from model studies to supramolecular organic frameworks, Angew. Chem. Int. Ed. 59 (2020) 17154–17161, https://doi.org/10.1002/anie.202005374.
[258] P.C. Ho, P. Szydlowski, J. Sinclair, P.J.W. Elder, J. Kübel, C. Gendy, L.M. Lee, H. Jenkins, J.F. Britten, D.R. Morim, I. Vargas-Baca, Supramolecular macrocycles reversibly assembled by Te…O chalcogen bonding, Nat. Commun. 7 (2016) 11299, https://doi.org/10.1038/ncomms11299.
[259] P. Perdew, K. Burke, M. Ernzerhof, Generalized gradient approximation made simple, Phys. Rev. Lett. 77 (1996) 3865–3868, https://doi.org/10.1103/physRevLett.77.3865.
[260] P.C. Ho, V. Tomassetti, J.F. Britten, I. Vargas-Baca, Iso-tellurazolium -N-phenoxides: a family of Te···O chalcogen-bonding supramolecular building blocks, Inorg. Chem. 60 (2021) 16726–16733, https://doi.org/10.1021/acs.inorgchem.1c02585.
[261] P.C. Ho, J. Rafique, J. Lee, L.M. Lee, H.A. Jenkins, J.F. Britten, A.L. Braga, I. Vargas-Baca, Synthesis and structural characterisation of the aggregates of benzo-1, 2-chalcogenazole 2-oxides, Dalton Trans. 46 (2017) 6570–6579, https://doi.org/10.1039/c7dt00612h.
[262] E.A. Chulanova, E.A. Radiush, I.K. Shundrina, I.Y. Bagryanskaya, N.A. Semenov, J. Beckmann, N.P. Gritsan, A.V. Zibarev, Lewis ambiphilicity of 1,2,5-chalcogenadiazoles for crystal engineering: complexes with crown ethers, Cryst. Growth Des. 20 (2020) 5868–5879, https://doi.org/10.1021/acs.cgd.0c00536.
[263] Y.V. Torubaev, A.V. Rozhkov, I.V. Skabitsky, R.M. Gomila, A. Frontera, V. Y. Kukushkin, Heterovalent chalcogen bonding: supramolecular assembly driven by the occurrence of a tellurium(II)···Ch(I) (Ch = S, Se, Te) linkage, Inorg. Chem. Front. 9 (2022) 5635–5644, https://doi.org/10.1039/d2qi01420c.
[264] L. Groslambert, Y. Cornaton, P. Pale, M. Ditte, A. Tkatchenko, J.P. Djukic, V. Mamane, Chalcogen bonding with telluronium cations: toward selective population of tellurium σ-holes by Lewis bases, J. Org. Chem. 90 (2025) 8254–8268, https://doi.org/10.1021/acs.joc.5c00744.
[265] S. Mehrparvar, C. Wölper, G. Haberhauer, Chalcogen-bond-induced double helix based on self-assembly of a small planar building block, Angew. Chem. Int. Ed. 62 (2023) e202304202, https://doi.org/10.1002/anie.202304202.
[266] R. Weiss, E. Aubert, L. Groslambert, P. Pale, V. Mamane, Chalcogen bonding with diaryl ditellurides: evidence from solid state and solution studies, Chem. Eur. J. 28 (2022) e202200395, https://doi.org/10.1002/chem.202200395.
[267] H.S. Biswal, A.K. Sahu, B. Galmés, A. Frontera, D. Chopra, Se···O/S and S···O chalcogen bonds in small molecules and proteins: a combined CSD and PDB study, ChemBioChem 23 (2022) e202100498, https://doi.org/10.1002/cbic.202100498.
[268] K. Mandal, A. Hasija, R. Shukla, V.R. Hathwar, D. Chopra, Quantitative evaluation of the electronic features involving "nucleophilic–electrophilic" character in the chalcogen sulfur, Phys. Chem. Chem. Phys. 25 (2023) 19427–19434, https://doi.org/10.1039/d3cp02526h.
[269] R. Beccaria, A. Dhaka, M. Calabrese, A. Pizzi, A. Frontera, G. Resnati, Chalcogen and hydrogen bond team up in driving anion···anion self-assembly, Chem. Eur. J. 30 (2024) e202303641, https://doi.org/10.1002/chem.202303641.
[270] J. Liang, Y. Shi, Y. Lu, Z. Xu, H. Liu, Square tetravalent chalcogen bonds in dimeric aggregates: a joint crystallographic survey and theoretical study, CrystEngComm 24 (2022) 975–986, https://doi.org/10.1039/d1ce01364e.
[271] J.Q. Liu, Y. Zhang, W. Wang, Trifurcated chalcogen bond: design and synthesis, J. Phys. Chem. A 129 (2025) 7670–7678, https://doi.org/10.1021/acs.jpca.5c04400.
[272] S. Thakur, R.M. Gomila, A. Frontera, S. Chattopadhyay, A theoretical insight into the formation of chalcogen bonding (ChB) interactions involving coordinated DMSO molecules as σ-hole donors and benzoate groups as σ-hole acceptors in a dinuclear copper(II) complex, CrystEngComm 23 (2021) 5087–5096, https://doi.org/10.1039/d1ce00624j.
[273] M.N. Akhtar, M.A. AlDamen, W. Zierkiewicz, M. Michalczyk, A. Khan, K. Fouzia, T.A. Sheikh, M. Imran, Unusual oxygen···oxygen dichalcogen bond in an oxo-centered trinclear iron coordination cluster, J. Mol. Struct. 1274 (2023) 134318, https://doi.org/10.1016/j.molstruc.2022.134318.
[274] E.Y. Tupikina, M.P. Davydova, V.V. Mulloyarova, T.S. Sukhikh, D.G. Samsonenko, P.M. Tolstoy, A.V. Artem'ev, Remarkably short intermolecular Se···Se contacts in Ni(II) diselenophosphinates: interplay of electrostatic and dispersion forces, Inorg. Chem. Front. 12 (2025) 1568–1578, https://doi.org/10.1039/d4qi03204g.
[275] A. Tripathi, A. Daolio, A. Pizzi, Z. Guo, D.R. Turner, A. Baggioli, A. Famulari, G. B. Deacon, G. Resnati, H.B. Singh, Chalcogen bonds in selenocysteine seleninic acid, a functional GPx constituent, and in other seleninic or sulfinic acid derivatives, Chem. Asian J. 16 (2021) 2351–2360, https://doi.org/10.1002/asia.202100545.
[276] R.J. Fick, G.M. Kroner, B. Nepal, R. Magnani, S. Horowitz, R.L. Houtz, S. Scheiner, R.C. Trievel, Sulfur-oxygen chalcogen bonding mediates AdoMet recognition in the lysine methyltransferase SET7/9, ACS Chem. Biol. 11 (2016) 748–754, https://doi.org/10.1021/acschembio.5b00852.
[277] M.D.L.N. Piña, A. Frontera, A. Bauza, Charge assisted S/Se chalcogen bonds in SAM riboswitches: a combined PDB and ab initio study, ACS Chem. Biol. 16 (2021) 1701–1708, https://doi.org/10.1021/acschembio.1c00417.
[278] J.A. Fernández Riveras, A. Frontera, A. Bauzá, Selenium chalcogen bonds are involved in protein–carbohydrate recognition: a combined PDB and theoretical study, Phys. Chem. Chem. Phys. 23 (2021) 17656–17662, https://doi.org/10.1039/d1cp01929e.
[279] K. Kříž, J. Fanfrlík, M. Lepšík, Chalcogen bonding in protein−ligand complexes: PDB survey and quantum mechanical calculations, ChemPhysChem 19 (2018) 2540–2548, https://doi.org/10.1002/cphc.201800409.
[280] S.P. Thomas, K. Satheeshkumar, G. Mugesh, T.N. Gururow, Unusually short chalcogen bonds involving organoselenium: insights into the Se–N bond cleavage mechanism of the antioxidant Ebselen and analogues, Chem. Eur. J. 21 (2015) 6793–6800, https://doi.org/10.1002/chem.201405998.
[281] K. Alhameedi, G.S. Chandler, D. Jayatilaka, Results Chem. 2 (2020) 100053, https://doi.org/10.1016/j.rechem.2020.100053.
[282] S.P. Thomas, V. Kumar, K. Alhameedi, T.N. Guru Row, Non-classical synthons: supramolecular recognition by S···O chalcogen bonding in molecular complexes of riluzole, Chem. Eur. J. 25 (2019) 3591–3597, https://doi.org/10.1002/chem.201805131.
[283] M. Bai, S.P. Thomas, R. Kottokkaran, S.K. Nayak, P.C. Ramamurthy, T.N. Guru Row, A donor-acceptor-donor structured organic conductor with S···S chalcogen bonding, Cryst. Growth Des. 14 (2014) 459–466, https://doi.org/10.1021/cg401069y.
[284] A.D. Becke, K.E. Edgecombe, A simple measure of electron localization in atomic and molecular systems, J. Chem. Phys. 92 (1990) 5397–5403, https://doi.org/10.1063/1.458517.
[285] I.I. Fedorova, N.S. Soldatova, D.M. Ivanov, K. Nikiforova, I.S. Aliyarova, M. S. Yusubov, P.M. Tolstoy, R.M. Gomila, A. Frontera, V.Y. Kukushkin, P. S. Postnikov, G. Resnati, Benzothienoiodolium cations doubly bonded to anions via halogen-chalcogen and halogen-hydrogen supramolecular synthons, Cryst. Growth Des. 23 (2023) 2661–2674, https://doi.org/10.1021/acs.cgd.2c01485.
[286] A.S. Mikherdov, M.A. Kinzhalov, A.S. Novikov, V.P. Boyarskiy, I.A. Boyarskaya, D.V. Dar'In, G.L. Starova, V.Y. Kukushkin, Difference in energy between two distinct types of chalcogen bonds drives regioisomerization of binuclear (diaminocarbene)Pd^{II} complexes, J. Am. Chem. Soc. 138 (2016) 14129–14137, https://doi.org/10.1021/jacs.6b09133.
[287] Z. Alamiddine, S. Thany, J. Graton, J.Y. Le Questel, Conformations and binding properties of thiametoxam and clothianidin neonicotinoid insecticides to nicotinic acetylcholine receptors: the contribution of σ-hole interactions, ChemPhysChem 19 (2018) 3069–3083, https://doi.org/10.1002/cphc.201800656.
[288] T. Glodde, Y.V. Vishnevskiy, L. Zimmermann, H.G. Stammler, B. Neumann, N. W. Mitzel, The nature of chalcogen-bonding-type tellurium–nitrogen interactions: a first experimental structure from the gas phase, Angew. Chem. Int. Ed. 60 (2021) 1519–1523, https://doi.org/10.1002/anie.202013480.
[289] M. Bursch, L. Kunze, A.M. Vibhute, A. Hansen, K.M. Sureshan, P.G. Jones, S. Grimme, D.B. Werz, Quantification of noncovalent interactions in azide–pnictogen, –chalcogen, and –halogen contacts, Chem. Eur. J. 27 (2021) 4627–4639, https://doi.org/10.1002/chem.202004525.
[290] J.D. Chai, M. Head-Gordon, Long-range corrected hybrid density functionals with damped atom–atom dispersion corrections, Phys. Chem. Chem. Phys. 10 (2008) 6615–6620, https://doi.org/10.1039/b810189b.

[291] M. Kohout, A measure of electron localizability, Int. J. Quantum Chem. 987 (2004) 651–658, https://doi.org/10.1002/qua.10768.

[292] Y. Balmohammadi, S. Grabowsky, Arsenic-involving intermolecular interactions in crystal structures: the dualistic behavior of As(III) as electron-pair donor and acceptor, Cryst. Growth Des. 23 (2023) 1033–1048, https://doi.org/10.1021/acs.cgd.2c01195.

[293] R.M. Gomila, A. Frontera, Metalloid chalcogen–pnictogen σ-hole bonding competition in stibanyl telluranes, J. Organomet. Chem. 954–955 (2021) 122092, https://doi.org/10.1016/j.jorganchem.2021.122092.

[294] S. Heimann, A. Kuczkowski, D. Bläser, C. Wölper, R. Haack, G. Jansen, S. Schulz, Syntheses and solid-state structures of $Et_2SbTeEt$ and $Et_2BiTeEt$, Eur. J. Inorg. Chem. 28 (2014) 4858–4864, https://doi.org/10.1002/ejic.201402471.

[295] L.M. Lee, V.B. Corless, M. Tran, H. Jenkins, J.F. Britten, I. Vargas-Baca, Synthetic, structural, and computational investigations of N-alkyl benzo-2,1,3-selenadiazolium iodides and their supramolecular aggregates, Dalton Trans. 45 (2016) 3285–3293, https://doi.org/10.1039/c5dt04314j.

[296] V.N. Khrustalev, M.M. Grishina, Z.V. Matsulevich, J.M. Lukiyanova, G. N. Borisova, V.K. Osmanov, A.S. Novikov, A.A. Kirichuk, A.V. Borisov, E. Solari, A.G. Tskhovrebov, Novel cationic 1,2,4-selenadiazoles: synthesis via addition of 2-pyridylselenyl halides to unactivated nitriles, structures and four-center Se···N contacts, Dalton Trans. 50 (2021) 10689–10691, https://doi.org/10.1039/d1dt01322j.

[297] A.A. Artemjev, A.P. Novikov, G.M. Burkin, A.A. Sapronov, A.S. Kubasov, V. G. Nenajdenko, V.N. Khrustalev, A.V. Borisov, A.A. Kirichuk, A.S. Kritchenkov, R. M. Gomila, A. Frontera, A.G. Tskhovrebov, Towards anion recognition and precipitation with water-soluble 1,2,4-selenodiazolium salts: combined structural and theoretical study, Int. J. Mol. Sci. 23 (2022) 6372, https://doi.org/10.3390/ijms23126372.

[298] M.V. Grudova, V.N. Khrustalev, A.S. Kubasov, P.V. Strashnov, Z.V. Matsulevich, J.M. Lukiyanova, G.N. Borisova, A.S. Kritchenkov, M.M. Grishina, A.A. Artemjev, I.V. Buslov, V.K. Osmanov, V.G. Nenajdenko, N.Q. Trung, A.V. Borisov, A. G. Tskhovrebov, Adducts of 2-pyridylselenenyl halides and nitriles as novel supramolecular building blocks: four-center Se···N chalcogen bonding versus other weak interactions, Cryst. Growth Des. 22 (2022) 313–322, https://doi.org/10.1021/acs.cgd.1c00954.

[299] A.A. Artemjev, A.S. Kubasov, M.L. Kuznetsov, M.V. Grudova, V.N. Khrustalev, A. S. Kritchenkov, A.G. Tskhovrebov, Mechanistic investigation of 1,3-dipolar cycloaddition between bifunctional 2-pyridylselenyl reagents and nitriles including reactions with cyanamides, CrystEngComm 25 (2023) 3691–3701, https://doi.org/10.1039/d3ce00385j.

[300] J.D. Chai, M. Head-Gordon, Systematic optimization of long-range corrected hybrid density functionals, J. Chem. Phys. 128 (2008) 084106, https://doi.org/10.1063/1.2834918.

[301] C. Lefebvre, G. Rubez, H. Khartabil, J.C. Boisson, J. Contreras-García, E. Hénon, Accurately extracting the signature of intermolecular interactions present in the NCI plot of the reduced density gradient versus electron density, Phys. Chem. Chem. Phys. 19 (2017) 17928–17936, https://doi.org/10.1039/c7cp02110k.

[302] H. Wang, B. Li, X. Wang, F. Yin, Q. Wei, X. Wang, Y. Ni, H. Wang, First-principles study of square chalcogen bond interactions and its adsorption behavior on silver surface, Phys. Chem. Chem. Phys. 25 (2023) 10836–10844, https://doi.org/10.1039/d2cp05825a.

[303] V.A. Aliyeva, A.V. Gurbanov, M.F.C. Guedes da Silva, R.M. Gomila, A. Frontera, K.T. Mahmudov, A.J.L. Pombeiro, Substituent effect on chalcogen bonding in 5-substituted benzo[c][1,2,5]selenadiazoles and their copper(II) complexes: experimental and theoretical study, Cryst. Growth Des. 24 (2024) 781–791, https://doi.org/10.1021/acs.cgd.3c01209.

[304] V. Aliyeva, V. Andrè, L.M.D.R.S. Martins, A.V. Gurbanov, R.M. Gomila, A. Frontera, T.F.C. Cruz, K.T. Mahmudov, Chalcogen bonded metal–organic frameworks: insights from X-ray analysis and theoretical calculations, Chem. Commun. 61 (2025) 5962–5965, https://doi.org/10.1039/d5cc00548e.

[305] N. A. Pusharevsky, A. I. Smolentev, H. Wang, V. E. Shishova, E. A. Chulanova, Q. Wei, Y. Balmohammadi, E. A. Radiush, S. Grabowsky, J. Beckmann, J. D. Woollins, N. A. Semenov, A. Zibarev, Coordination polymers between 3,4-dicyano-1,2,5-telluradiazole and N,N,N′,N′-tetramethylethane-1,2-diamine: the decisive role of chalcogen bonding. Cryst. Growth Des. 24 (2024), 5236−5250. doi:https://doi.org/10.1021/acs.cgd.4c00475.

[306] Y. Lu, W. Li, W. Yang, Z. Zhu, Z. Xu, H. Liu, 2Ch–2N square and hexagon interactions: a combined crystallographic data analysis and computational study, Phys. Chem. Chem. Phys. 21 (2019) 21568–21576, https://doi.org/10.1039/c9cp04562g.

[307] F.U. Rahman, D. Tzeli, I.D. Petsalakis, G. Theodorakopoulos, P. Ballester, J. Rebek, Y. Yu, Chalcogen bonding and hydrophobic effects force molecules into small spaces, J. Am. Chem. Soc. 142 (2020) 5876–5883, https://doi.org/10.1021/jacs.0c01290.

[308] L.J. Riwar, N. Trapp, K. Root, R. Zenobi, F. Diederich, Supramolecular capsules: strong versus weak chalcogen bonding, Angew. Chem. Int. Ed. 57 (2018) 17259–17264, https://doi.org/10.1002/anie.201812095.

[309] T. Fellowes, E. Lee, J. Tran, R. Xu, A. Barber, S.C. Brydon, J.K. Clegg, J.M. White, Hammett structural relationships revealed in chalcogen-bonded co-crystals of electron-rich pyridines with 4′-substituted ebselen derivatives, Cryst. Growth Des. 23 (2023) 7179–7188, https://doi.org/10.1021/acs.cgd.3c00605.

[310] C. Adamo, V. Barone, Exchange functionals with improved long-range behavior and adiabatic connection methods without adjustable parameters: the mPW and mPW1PW models, J. Chem. Phys. 108 (1998) 664–675, https://doi.org/10.1063/1.475428.

[311] (a) W.R. Wadt, P.J. Hay, Ab initio effective core potentials for molecular calculations. Potentials for main group elements Na to Bi, J. Chem. Phys. 82 (1985) 284–298, https://doi.org/10.1063/1.448800;
(b) C.E. Check, T.O. Faust, J.M. Bailey, B.J. Wright, T.M. Gilbert, L.S. Sunderlin, Addition of polarization and diffuse functions to the LANL2DZ basis set for p-block elements, J. Phys. Chem. A 105 (2001) 8111–8116, https://doi.org/10.1021/JP011945L;
(c) L.E. Roy, P.J. Hay, R.L. Martin, Revised basis set for the LANL effective core potentials, J. Chem. Theory Comput. 4 (2008) 1029–1031, https://doi.org/10.1063/1.448800.

[312] M.C. Aragoni, M. Arca, C. Caltagirone, C. Castellano, F. Demartin, P.G. Jones, T. Pivetta, E. Podda, V. Lippolis, S. Murgia, G. Picci, Role of the solvent in the reactivity of bis-4-imidazoline-2-selone derivatives toward I_2: an experimental and theoretical approach, J. Org. Chem. 87 (2022) 15448–15465, https://doi.org/10.1021/acs.joc.2c01982.

[313] E.A. Radiush, E.A. Pritchina, E.A. Chulanova, A.A. Dmitriev, I.Y. Bagryanskaya, A. M.Z. Slawin, J.D. Woollins, N.P. Gritsan, A.V. Zibarev, N.A. Semenov, Chalcogen-bonded donor–acceptor complexes of 5,6-dicyano[1,2,5]selenadiazolo[3,4-b] pyrazine with halide ions, New J. Chem. 46 (2022) 14490–14501, https://doi.org/10.1039/d2nj02345h.

[314] M.J. Mayor-Lopez, J. Weber, K. Hegetschweiler, M.D. Meienberger, F. Joho, S. Leoni, R. Nesper, G.J. Reiss, W. Frank, B.A. Kolesov, V.P. Fedin, V. E., Fedorov Structure and reactivity of $[Mo_3\text{-}\mu_3S\text{-}(\mu S_2)_3]^{4+}$ complexes. Quantum chemical calculations, X-ray structural characterization, and Raman spectroscopic measurements, Inorg. Chem. 37 (1998) 2633–2644, https://doi.org/10.1021/ic971214t.

[315] A.V. Virovets, O. V. Volkov, Specific non-bonding contacts in the crystal structure of a solid solution $[Mo_3(\mu_3\text{-}S)(\mu\text{-}S_2)_3(S_2CNEt_2)_3]Cl_{0.53}Br_{0.47}$. J. Struct. Chem. 41 (2000), 713–716. doi:https://doi.org/10.1007/BF02683938.

[316] A.S. Novikov, A.L. Gushchin, Trinuclear molybdenum clusters with sulfide bridges as potential anionic receptors via chalcogen bonding, CrystEngComm 23 (2021) 4607–4614, https://doi.org/10.1039/d1ce00514f.

[317] A.F. Saifina, S.V. Kartashov, A.I. Stash, V.G. Tsirelson, R.R. Fayzullin, Unified picture of interatomic interactions, structures, and chemical reactions by means of electrostatic and kinetic force density fields: Appel's salt and its ion pairs, Cryst. Growth Des. 23 (2023) 3002–3018, https://doi.org/10.1021/acs.cgd.3c00088.

[318] L.H. Al-Wahaibi, B. Rahul, A.A.B. Mohamed, M.S.M. Abdelbaky, S. Garcia-Granda, A.A. El-Emam, M.J. Percino, S. Thamotharan, Supramolecular self-assembly built by weak hydrogen, chalcogen, and unorthodox nonbonded motifs in 4-(4-chlorophenyl)-3-[(4-fluorobenzyl)sulfanyl]-5-(thiophen-2-yl)-4H-1,2,4-triazole, a selective COX-2 inhibitor: insights from X-Ray and theoretical studi, ACS Omega 6 (2021) 6996–7007, https://doi.org/10.1021/acsomega.0c06287.

[319] F. Weigend, R. Ahlrichs, Balanced basis sets of split valence, triple zeta valence and quadruple zeta valence quality for H to Rn: design and assessment of accuracy, Phys. Chem. Chem. Phys. 7 (2005) 3297–3305, https://doi.org/10.1039/b508541a.

[320] E. Podda, M. Arca, M.C. Aragoni, C. Caltagirone, V. Lippolis, A. Pintus, D. B. Paixao, E.G.O. Soares, P.H. Schneider, Synergistic interplay between intermolecular halogen and chalcogen bonds in the dihalogen adducts of 2,5-bis (pyridine-2-yl)tellurophene: reactivity insights and structural trends, Inorg. Chem. 64 (2025) 10972–10988, https://doi.org/10.1021/acs.inorgchem.5c01084.

[321] R. Wysokiński, Anion···anion interaction within $Ch(CH_3)X_4^-$ (Ch = S, Se, Te; X = Cl, Br, I) dimers stabilized by chalcogen bonds, Phys. Chem. Chem. Phys. 24 (2022) 12860–12869, https://doi.org/10.1039/d2cp00271j.

[322] V. Matos, A. J. Zimmermann Londero, M. Roca Jungfer, U. Abram, E. Schulz Lang, The unique ambiphilicity of tellurium in the $[mesitylTe(I)(I_2)(I_3)]^-$ anion. Eur. J. Inorg. Chem. 26 (2023), e202300478. doi:https://doi.org/10.1002/ejic.202300478.

[323] A. Azhdari Tehrani, H. Ghasempour, A. Morsali, A. Bauzá, A. Frontera, P. Retailleau, Unraveling the dual character of sulfur atoms in a series of Hg(II) coordination polymers containing bis(4-pyridyl)disulfide, CrystEngComm 19 (2017) 1974–1981, https://doi.org/10.1039/c7ce00033b.

[324] E.S. Yandanova, D.M. Ivanov, M.L. Kuznetsov, A.G. Starikov, G.L. Starova, V. Y. Kukushkin, Recognition of S···Cl chalcogen bonding in metal-bound alkylthiocyanates, Cryst. Growth Des. 16 (2016) 2979–2987, https://doi.org/10.1021/acs.cgd.6b00346.

[325] R.M. Gomila, A. Bauzá, A. Frontera, Enhancing chalcogen bonding by metal coordination, Dalton Trans. 51 (2022) 5977–5982, https://doi.org/10.1039/d2dt00796g.

[326] S. Burguera, R.M. Gomila, A. Bauzá, A. Frontera, Selenoxides as excellent chalcogen bond donors: effect of metal coordination, Molecules 27 (2022) 8837, https://doi.org/10.3390/molecules27248837/s1.

[327] S.V. Baykov, D.M. Ivanov, I.I. Fedorova, S.O. Baykova, N.A. Bokach, Y. Z. Voloshin, V.Y. Kukushkin, Isomorphous structures of iron(II) clathrochelates featuring terminal σ-hole donor sites and exhibiting the Cl/Br/I/S quadruple heteroisostructural exchange, Cryst. Growth Des. 24 (2024) 4997–5006, https://doi.org/10.1021/acs.cgd.4c00204.

[328] A.A. Sapronov, A.A. Artemjev, G.M. Burkin, V.N. Khrustalev, A.S. Kubasov, V. G. Nenajdenko, R.M. Gomila, A. Frontera, A.S. Kritchenkov, A.G. Tskhovrebov, Robust supramolecular dimers derived from benzylic-substituted 1,2,4-selenodiazolium salts featuring selenium···π chalcogen bonding, Int. J. Mol. Sci. 23 (2022) 14973, https://doi.org/10.3390/ijms232314973/s1.

[329] J. Vrana, J. Holub, M.A. Samsonov, Z. Ruzickova, R. Bulanek, J. Fanfrlik, D. Hnyk, R.M. Gomila, A. Frontera, A. Ruzicka, Phenyl-substituted

thiaboranes−linked 2D and 3D aromatics as noncovalent organic framework materials, Inorg. Chem. 64 (2025) 7377–7387, https://doi.org/10.1021/acs.inorgchem.4c05457.
[330] S. Bhandary, A. Sirohiwal, R. Kadu, S. Kumar, D. Chopra, Dispersion stabilized Se/Te···π double chalcogen bonding synthons in in situ cryocrystallized divalent organochalcogen liquids, Cryst. Growth Des. 18 (2018) 3734–3739, https://doi.org/10.1021/acs.cgd.8b00585.
[331] S. Ghinato, A. Giordana, E. Diana, R.M. Gomila, E. Priola, A. Frontera, Synthesis, X-ray characterization and DFT analysis of dicyanidoaurate telluronium salts: on the importance of charge assisted chalcogen bonds, Dalton Trans. 52 (2023) 15688–15696, https://doi.org/10.1039/d3dt02787b.
[332] A.S. Smirnov, A.V. Rozhkov, M.A. Kryukova, V.V. Suslonov, A.Y. Ivanov, R. M. Gomila, A. Frontera, Y. Kukushkin, M.A. Bokach, Chalcogen bonding between tellurium(II) and the isocyanide carbon, Cryst. Growth Des. 24 (2024) 10393–10402, https://doi.org/10.1021/acs.cgd.4c01351.
[333] T. Lu, Q. Chen, Independent gradient model based on Hirshfeld partition: a new method for visual study of interactions in chemical systems, J. Comput. Chem. 43 (2022) 539–555, https://doi.org/10.1002/jcc.26812.
[334] T. Lu, F.W. Chen, Atomic dipole moment corrected Hirshfeld population method, J. Theor. Comput. Chem. 11 (2012) 163–183, https://doi.org/10.1142/s0219633612500113.
[335] A.V. Rozhkov, E.A. Katlenok, M.V. Zhmykhova, A.Y. Ivanov, M.L. Kuznetsov, N. A. Bokach, V.Y. Kukushkin, Metal-involving chalcogen bond., The case of platinum(II) interaction with Se/Te-based σ-hole donors, J. Am. Chem. Soc. 143 (2021) 15701–15710, https://doi.org/10.1021/jacs.1c06498.
[336] A.A. Busygina, A.A. Eliseeva, A.V. Rozhkov, D.M. Ivanov, R.M. Gomila, A. Frontera, N.A. Bokach, V.Y. Kukushkin, Synergistic σ/π-hole interactions directing supramolecular assembly: tellurium···platinum chalcogen bonding enhanced by π-stacking, Cryst. Growth Des. 24 (2024) 10235–10246, https://doi.org/10.1021/acs.cgd.4c01236.
[337] A.V. Rozhkov, S. Burguera, A. Frontera, V.Y. Kukushkin, Formal metal-dependent (M = Pt, Pd) switching between arene π-hole and σ-(Te)-hole in the arenetellurium(II) noncovalent binding, Cryst. Growth Des. 24 (2024) 9581–9589, https://doi.org/10.1021/acs.cgd.4c011.
[338] E.A. Katlenok, M.L. Kuznetsov, N.A. Semenov, N.A. Bokach, V.Y. Kukushkin, A new look at the chalcogen bond: π-hole-based chalcogen (Se, Te) bonding which does not include a σ-hole interaction, Inorg. Chem. Front. 10 (2023) 3065–3081, https://doi.org/10.1039/d3qi00087g.
[339] N. Kordts, S. Kunzler, S. Rathjen, T. Sieling, H. Groekappenberg, M. Schmidtmann, T. Muller, Silyl chalconium ions: synthesis, structure and application in hydrodefluorination reactions, Chem. Eur. J. 23 (2017) 10068–10079, https://doi.org/10.1002/chem.201700995.
[340] Q.Z. Li, H. Qi, R. Li, X.F. Liu, W.Z. Li, J.B. Cheng, Prediction and characterization of a chalcogen–hydride interaction with metal hybrids as an electron donor in F_2CS–HM and F_2CSe–HM (M = Li, Na, BeH, MgH, $MgCH_3$) complexes, Phys. Chem. Chem. Phys. 14 (2012) 3025–3030, https://doi.org/10.1039/c2cp23664h.
[341] H. Keil, R. Herbst-Irmer, S. Rathjen, C. Girschik, T. Müller, D. Stalke, Si-H···Se chalcogen-hydride bond quantified by diffraction and topological analyses, Inorg. Chem. 61 (2022) 6319–6325, https://doi.org/10.1021/acs.inorgchem.2c00629.
[342] J. Lu, S. Scheiner, Effects of halogen, chalcogen, pnicogen, and tetrel bonds on IR and NMR spectra, Molecules 24 (2019) 2822, https://doi.org/10.3390/molecules24152822.
[343] S. Scheiner, M. Michalczyk, W. Zierkiewicz, Correlation between noncovalent bond strength and spectroscopic perturbations within the Lewis base, J. Phys. Chem. A 128 (2024) 10875–10883, https://doi.org/10.1021/acs.jpca.4c07382.
[344] Michalczyk, M.; Zierkiewicz, W.; Scheiner, S. Ability of the Spectroscopic Properties of the P–Se Bond of a Base to Assess Noncovalent Bond Strength. J. Phys. Chem. A 129 (2025), 545−554. doi:https://doi.org/10.1021/acs.jpca.4c08283.
[345] J. Lu, S. Scheiner, Relationships between bond strength and spectroscopic quantities in H-bonds and related halogen, chalcogen, and pnicogen bonds, J. Phys. Chem. A 124 (2020) 7716–7725, https://doi.org/10.1021/acs.jpca.0c05936.
[346] K. Haupa, A. Bil, Z. Mielke, Donor-acceptor complexes between ammonia and sulfur trioxide: an FTIR and computational study, J. Phys. Chem. A 119 (2015) 10724–10734, https://doi.org/10.1021/acs.jpca.5b07936.
[347] Y. Geboes, F. De Vleeschouwer, F. De Proft, W.A. Herrebout, Exploiting the σ-hole concept: an infrared and Raman-based characterization of the S···O chalcogen bond between 2,2,4,4-tetrafluoro-1,3-dithiethane and dimethyl ether, Chem. Eur. J. 23 (2017) 17384–17392, https://doi.org/10.1002/chem.201704406.
[348] Y. Jin, X. Li, Q. Gou, G. Feng, J.U. Grabow, W. Caminati, Chalcogen bond and internal dynamics of the 2,2,4,4-tetrafluoro-1,3-dithietane···water complex, Phys. Chem. Chem. Phys. 21 (2019) 15656–15661, https://doi.org/10.1039/c9cp03301g.
[349] T. Lu, Y. Zheng, Q. Gou, G.L. Hou, G. Feng, Rotational characterization of S···F chalcogen bonds in the complex of 2,2,4,4-tetrafluoro-1,3-dithietane and difluoromethane, Phys. Chem. Chem. Phys. 21 (2019) 24659–24665, https://doi.org/10.1039/c9cp04628c.
[350] D.A. Obenchain, L. Spada, S. Alessandrini, S. Rampino, S. Herbers, N. Tasinato, M. Mendolicchio, P. Kraus, J. Gauss, C. Puzzarini, J.U. Grabow, V. Barone, Unveiling the sulfur–sulfur bridge: accurate structural and energetic characterization of a homochalcogen intermolecular bond, Angew. Chem. Int. Ed. 57 (2018) 15822–15826, https://doi.org/10.1002/anie.201810637.
[351] C.T. Haakansson, T.R. Corkish, P.D. Watson, H.T. Robinson, T. Tsui, A. J. McKinley, D.A. Wild, Spectroscopic investigation of chalcogen bonding: halide–carbon disulfide complexes, ChemPhysChem 22 (2021) 808–812, https://doi.org/10.1002/cphc.202100148.
[352] V. Kumar, Y. Xu, D.L. Bryce, Double chalcogen bonds: crystal engineering stratagems via diffraction and multinuclear solid-state magnetic resonance spectroscopy, Chem. Eur. J. 26 (2020) 3275–3286, https://doi.org/10.1002/chem.201904795.
[353] C. Almario, T. Nag, D.L. Bryce, Chemical shift tensors as probes of chalcogen bonds: solid-state NMR study of telluradiazole-XCN^- (X = O, S, Se) salt corystals, Facets 8 (2023) 1–14, https://doi.org/10.1139/facets-2023-0082.
[354] L. Groslambert, Y. Cornaton, M. Ditte, E. Aubert, P. Pale, A. Tkatchenko, J. P. Djukic, V. Mamane, Affinity of telluronium chalcogen bond donors for Lewis bases in solution: a critical experimental-theoretical joint study, Chem. Eur. J. 30 (2024) e202302933, https://doi.org/10.1002/chem.202302933.
[355] B. Lin, H. Liu, H.M. Scott, I. Karki, E.C. Vik, D.O. Madukwe, P.J. Pellechia, K. D. Shimizu, Transition state stabilizing effects of oxygen and sulfur chalcogen bond interactions, Chem. Eur. J. 30 (2024) e202402011, https://doi.org/10.1002/chem.202402011.
[356] G. S. Sinclair, R. C. M. Claridge, A. J. Kukor, W. S. Hopkins, D. J. Schipper, N-oxide S–O chalcogen bonding in conjugated materials. Chem. Sci. 12 (2021), 2304–2312. doi:https://doi.org/10.1039/d0sc06583h.
[357] G.E. Garrett, G.L. Gibson, R.N. Straus, D.S. Seferos, M.S. Taylor, Chalcogen bonding in solution: interactions of benzotelluradiazoles with anionic and uncharged Lewis bases, J. Am. Chem. Soc. 137 (2015) 4126–4133, https://doi.org/10.1021/ja512183e.
[358] H.J. Kim, I.S. Jung, S. Jung, D. Kim, D. Minami, S. Byun, T. Choi, J. Shin, S. Yun, C.J. Heo, K.B. Park, S.Y. Park, S.J. Lim, H.S. Lee, B. Choi, Harnessing intramolecular chalcogen-chalcogen bonding in merocyanines for utilization in high-efficiency photon-to-current conversion optoelectronics, ACS Appl. Mater. Interfaces 14 (2022) 4360–4370, https://doi.org/10.1021/acsami.1c16950.
[359] S. Mehrparvar, Z.N. Scheller, C. Wölper, G. Haberhauer, Design of azobenzene beyond simple on-off behavior, J. Am. Chem. Soc. 143 (2021) 19856–19864, https://doi.org/10.1021/jacs.1c09090.
[360] A.V. Marenich, C.J. Cramer, D.G. Truhlar, Universal solvation model based on solute electron density and on a continuum model of the solvent defined by the bulk dielectric constant and atomic surface tensions, J. Phys. Chem. B 113 (2009) 6378–6396, https://doi.org/10.1021/jp810292n.
[361] Z.N. Scheller, S. Mehrparvar, G. Haberhauer, Light-induced increase in bond strength from chalcogen bond to three-electron σ bond upon excitation, J. Am. Chem. Soc. 147 (2025) 6249–6258, https://doi.org/10.1021/jacs.4c18435.
[362] L. Cui, Y. Gong, X. Yu, C. Lv, X. Du, J. Zhao, Y. Che, Development of a fluorophore with enhanced unorthodox chalcogen bonding for highly sensitive detection of trimethyl arsine vapor, ACS Sens. 6 (2021) 2851–2857, https://doi.org/10.1021/acssensors.1c01185.
[363] E. Navarro-García, B. Galmés, J.L. Esquivel, M.D. Velasco, A. Bastida, F. Zapata, A. Caballero, A. Frontera, Host–guest complexes vs. supramolecular polymers in chalcogen bonding receptors: an experimental and theoretical study, Dalton Trans. 51 (2022) 1325–1332, https://doi.org/10.1039/D1DT03925C.
[364] T. Bunchuay, A. Docker, U. Eiamprasert, P. Surawatanawong, A. Brown, P. D. Beer, Chalcogen bond mediated enhancement of cooperative ion-pair recognition, Angew. Chem. Int. Ed. 59 (2020) 12007–12012, https://doi.org/10.1002/anie.202001125.
[365] A. Docker, I. Marques, H. Kuhn, Z. Zhang, V. Félix, P.D. Beer, Selective potassium chloride recognition, sensing, extraction, and transport using a chalcogen-bonding heteroditopic receptor, J. Am. Chem. Soc. 144 (2022) 14778–14789, https://doi.org/10.1021/jacs.2c05333.
[366] Y.C. Tse, A. Docker, I. Marques, V. Fèlix, P.D. Beer, Amphoteric chalcogen-bonding and halogen-bonding rotaxanes for anion or cation recognition, Nat. Chem. 17 (2025) 373–381, https://doi.org/10.1038/s41557-025-01742-x.
[367] J.Y.C. Lim, I. Marques, A.L. Thompson, K.E. Christensen, V. Félix, P.D. Beer, Chalcogen bonding macrocycles and [2]rotaxanes for anion recognition, J. Am. Chem. Soc. 139 (2017) 3122–3133, https://doi.org/10.1021/jacs.6b12745.
[368] Y. Xia, A. Hao, P. Xing, Chalcogen and pnictogen bonding-modulated multiple-constituent chiral self-assemblies, ACS Nano 17 (2023) 21993–22003, https://doi.org/10.1021/acsnano.3c08590.
[369] L. Camilli, C. Hogan, D. Romito, L. Persichetti, A. Caporale, M. Palummo, M. Di Giovannantonio, D. Bonifazi, On-surface molecular recognition driven by chalcogen bonding, JACS Au 4 (2024) 2115–2121, https://doi.org/10.1021/jacsau.4c00325.
[370] G. Sekar, V.V.J. Nair Zhu, Chalcogen bonding catalysis, Chem. Soc. Rev. 53 (2024) 586–605, https://doi.org/10.1039/d3cs00503h.
[371] G. Gao, D. Xie, P.P. Zhou, Chalcogen bonding catalysis in organic synthesis, Asian J. Org. Chem. 14 (2025) e202500098, https://doi.org/10.1002/ajoc.202500098.
[372] A. Frontera, A. Bauza, On the importance of pnictogen and chalcogen bonding interactions in supramolecular catalysis, Int. J. Mol. Sci. 22 (2021) 12550, https://doi.org/10.3390/ijms222212550.
[373] S. Benz, M. Macchione, Q. Verolet, J. Mareda, N. Sakai, S. Matile, Anion transport with chalcogen bonds, J. Am. Chem. Soc. 138 (2016) 9093–9096, https://doi.org/10.1021/jacs.6b05779.
[374] P. Wonner, A. Dreger, L. Vogel, E. Engelage, S.M. Huber, Chalcogen bonding catalysis of a nitro-Michael reaction, Angew. Chem. Int. Ed. 58 (2019) 16923–16927, https://doi.org/10.1002/anie.201910639.
[375] N. Tarannam, M.H.H. Voelkel, S.M. Huber, S. Kozuch, Chalcogen vs halogen bonding catalysis in a water-bridge-cocatalyzed nitro-Michael reaction, J. Org. Chem. 87 (2022) 1661–1668, https://doi.org/10.1021/acs.joc.1c00894.
[376] T. Steinke, P. Wonner, R.M. Gauld, S. Heinrich, S.M. Huber, Catalytic activation of imines by chalcogen bond donors in a Povarov [4+2] cycloaddition reaction,

Chem. Eur. J. 28 (2022) e202200917, https://doi.org/10.1002/chem.202200917.
[377] K. Takagi, N. Sakakibara, S. Kikkawa, S. Tsuzuki, Dicationic oligotelluroxane or mononuclear telluronium cation? Elucidation of the true catalytic species and activation mechanism of the benzylic carbon-halogen bond, Chem. Commun. 57 (2021) 13736–13739, https://doi.org/10.1039/d1cc06311a.
[378] Z. Wang, C. Zhao, X. Li, B. Shi, Y. Zeng, Neutral monodentate and hypervalent chalcogen bond catalysis on the intramolecular Rauhut-Currier reaction of bis (enones): a DFT study, Chem. Eur. J. 29 (2023) e202300171, https://doi.org/10.1002/chem.202300171.
[379] Q. Zhang, Y.Y. Chan, M. Zhang, Y.Y. Yeung, Z. Ke, Hypervalent chalcogenonium···π bonding catalysis, Angew. Chem. Int. Ed. 61 (2022) e202208009, https://doi.org/10.1002/anie.202208009.
[380] M.V. Il'In, A.S. Novikov, D.S. Bolotin, Sulfonium and selenonium salts as noncovalent organocatalysts for the multicomponent Groebke-Blackburn-Bienaymé reaction, J. Org. Chem. 87 (2022) 10199–10207, https://doi.org/10.1021/acs.joc.2c01141.
[381] A.S. Novikov, D.S. Bolotin, Halonium, chalconium, and pnictonium salts as noncovalent organocatalysts: a computational study on relative catalytic activity, Org. Biomol. Chem. 20 (2022) 7632–7639, https://doi.org/10.1039/d2ob01415g.
[382] Y. Li, L. Meng, C. Sun, Y. Zeng, Organocatalysis by halogen, chalcogen, and pnictogen bond donors in halide abstraction reactions: an alternative to hydrogen bond-based catalysis, J. Phys. Chem. A 124 (2020) 3815–3824, https://doi.org/10.1021/acs.jpca.0c01060.
[383] H. Zhu, P.P. Zhou, Y. Wang, Cooperative chalcogen bonding interactions in confined sites activate aziridines, Nat. Commun. 13 (2022) 3563, https://doi.org/10.1038/s41467-022-31293-5.
[384] Y. Lu, Q. Liu, Z.X. Wang, X.Y. Chen, Alkynyl sulfonium salts can be employed as chalcogen-bonding catalysts and generate alkynyl radicals under blue-light irradiation, Angew. Chem. Int. Ed. 61 (2022) e202116071, https://doi.org/10.1002/anie.202116071.
[385] E.R.T. Robinson, D.M. Walden, C. Fallan, M.D. Greenhalgh, P.H.Y. Cheong, A. D. Smith, Non-bonding 1,5-S···O interactions govern chemo- and enantioselectivity in isothiourea-catalyzed annulations of benzazoles, Chem. Sci. 7 (2016) 6919–6927, https://doi.org/10.1039/c6sc00940a.
[386] C.M. Young, A. Elmi, D.J. Pascoe, R.K. Morris, C. McLaughlin, A.M. Woods, A. B. Frost, A. de la Houpliere, K.B. Ling, T.K. Smith, A.M.Z. Slawin, P. H. Willoughby, S.L. Cockroft, A.D. Smith, The importance of 1,5-oxygen···chalcogen interactions in enantioselective isochalcogenourea catalysis, Angew. Chem. Int. Ed. 59 (2020) 3705–3710, https://doi.org/10.1002/anie.201914421.
[387] J. Wu, C. M. Young, A. A. Watts, A. M. Z. Slawin, G. R. Boyce, M. Bühl, A. D. Smith, Isothiourea-catalyzed enantioselective Michael addition of malonates to α,β-unsaturated aryl esters. Org. Lett. 24 (2022), 4040–4045. doi:https://doi.org/10.1021/acs.orglett.2c01486.
[388] M. Batabyal, A. Upadhyay, R. Kadu, N.C. Birudukota, D. Chopra, S. Kumar, Tetravalent spiroselenurane catalysts: intramolecular Se···N chalcogen bond-driven catalytic disproportionation of H_2O_2 to H_2O and O_2 and activation of I_2 and NBS, Inorg. Chem. 61 (2022) 8729–8745, https://doi.org/10.1021/acs.inorgchem.2c00651.
[389] J. Liu, M. Zhou, R. Deng, P. Zheng, Y.R. Chi, Chalcogen bond-guided conformational isomerization enables catalytic dynamic kinetic resolution of sulfoxides, Nat. Commun. 13 (2022) 4793, https://doi.org/10.1038/s41467-022-32428-4.
[390] A.A. Artemjev, A.S. Kubasov, V.P. Zaytsev, A.V. Borisov, A.S. Kritchenkov, V. G. Nenajdenko, R.M. Gomila, A. Frontera, A.G. Tskhovrebov, Novel chalcogen bond donors derived from [3+2] cycloaddition reaction between 2-pyridylselenyl reagents and isocyanates: synthesis, structures and theoretical studies, Cryst. Growth Des. 23 (2023) 2018–2023, https://doi.org/10.1021/acs.cgd.3c00101.
[391] M.J. Janicki, R. Szabla, Chalcogen bonds enable efficient photoreduction of sulfur-containing heterocycles, Angew. Chem. Int. Ed. 64 (2025) e202413498, https://doi.org/10.1002/anie.202413498.